YRKESHÖGSKOLAN NOVIA

Design and Development of an Integrated Renewable Energy Centre in Cervià de les Garrigues, Catalonia

Pol Mestrich Palau

Maria Teresa Sellart Garcia

Bachelor Thesis for Bachelor of Engineering

Degree Programme in Energy Technology

Vaasa, Finland, 2022

ACKNOWLEDGEMENTS

We would like to express our gratitude to everyone who helped and supported us with the development of the thesis. Our parents and siblings deserve special appreciation for their unwavering support and guidance. Especially since they have always encouraged us to do our best and advance despite the challenges we face throughout our lives.

We want to appreciate the teachers who have laboured tirelessly to impart their wisdom and knowledge. The completion of this thesis could not have been accomplished without our two supervisors. We are delighted to have cooperated with them and, correspondingly, for the support and dedication they have offered us. Our warmest thanks to Dr. Antonio Palau for guiding us and proposing this interesting topic, and to Philip Hollins for all the necessary support and feedback provided. Collaboration has been crucial in providing advice and assisting us in finding solutions to our problems.

On the other hand, a debt of gratitude to the University of Lleida and NOVIA University of Applied Sciences for this superb double degree programme. Katja Bonäs and Roger Mäntylä, in particular, for making us feel at home and for guiding us during this wonderful stay in Finland. Much obliged to our classmates with whom we have shared this stage of our lives in order to make it more pleasant and unwind.

Finally, to acknowledge the City Council of Cervià de les Garrigues and, specifically, its mayor, Mrs. Mercè Rubió Tarré, for this unimaginable opportunity and the information provided. We hope that this theoretical study will be materialised to mitigate the critical environmental situation that is causing human-induced climate change. To achieve a society with net-zero greenhouse gas emissions, it is vital to implement projects that encourage renewable energy and use it to the best advantage of natural resources. Sustainable energy production is essential to nourishing our ecosystem.

DEGREE THESIS

Author: Pol Mestrich Palau and Maria Teresa Sellart Garcia

Degree Programme: Electrical Engineering and Automation

Specialisation: Energy Technology

Supervisors: Philip Hollins and Dr. Antoni Palau

Title: Design and development of an integrated renewable energy centre in Cervià de les Garrigues, Catalonia.

Date:	Number of pages:	Appendices:
17th May 2022	77	7

Abstract

This theoretical project has been accomplished in cooperation with Novia University of Applied Sciences and the City Council of Cervià de les Garrigues. The purpose was to design an integrated renewable energy centre capable of supplying the public electricity demand of the village, using agricultural waste and offering socio-cultural services to the area.

Literature research was undertaken to obtain background information about the municipality. Furthermore, with the meteorological and biomass data estimated, the viability of different green technologies was analysed. According to the availability of usable natural resources, it is feasible to install photovoltaic panels and a combined heat and power biofuel boiler.

Power simulations were performed with SAM software to estimate electricity generation, obtaining an environmentally-safe installed capacity of 394 kW that provides a net output of 1,466 MWh/year. Additionally, a financial analysis was conducted, determining that the estimated initial investment of €503,524 would be amortized over a minimum period of 14.6 years. To conclude, several limitations and enhancements were identified to be able to apply the methodology to forthcoming studies of these characteristics.

Language: English

Key Words: Renewable Energies, Research-Based Energy Design, Solar Energy, Biomass, System Advisor Model (SAM)

Table of Contents

List of Figures

List of Tables

Glossary

Acronyms

AC	Alternating Current
a.s.l.	Height above sea level
CHP	Combined Heat and Power
COE	Cost of Energy
Csa	Hot-summer Mediterranean climate
DC	Direct Current
DHI	Diffuse horizontal irradiance
DNI	Direct normal irradiance
GHI	Global horizontal irradiance
IDESCAT	Institute of Statistics of Catalonia
IDW	Inverse Distance Weighted
INE	National Electoral Institute of Spain
IRR	Internal Rate of Return
NASA	National Aeronautics and Space Administration
NOAA	National Oceanic and Atmospheric Administration
NREL	National Renewable Energy Laboratory
NSRDB	United States National Solar Radiation Database
METEOCAT	Meteorological Service of Catalonia
POA	Plan of Array
PV	Photovoltaic
SAM	System Advisor Model (SAM)
SE	South East

Units

ºC	Degree Celsius
$	Dollar
€	Euro
Btu	British Thermal Unit
CV	Horsepower
g	Gram
h	Hour
ha	Hectarea
J	Joule
m	Metre
Pa	Pascal
s	Second
t	Tonne
W	Watt
yr	Year

1 Introduction

Global society is undergoing a critical period of climate emergency caused principally by the use of limited fossil fuels. According to Abas, Kalair and Khan (2015), given current conditions, it is expected that oil will last 50 years, natural gas 60 years, uranium 100 years, and coal 110 years. The abusive usage of these energy sources has occasioned concerning concentrations of greenhouse gases in the atmosphere, leading to serious global warming. (Olah, Alain Goeppert & Surya, 2018).

To mitigate human-induced climate change, humanity needs to conduct an energy transition from a carbon-based to a non-carbon-based society (Wuebbles & Jain, 2001). For this reason, the European Union has defined several objectives and incentives to progressively decarbonise society by 2030 and achieve an economy with net-zero greenhouse gas emissions by 2050 (Europa.eu, 2021). The fundamental factor is to install low-impact renewable energy sources, such as solar, wind, hydraulic, tidal, geothermal, or bioenergy. In addition, green energy reduces production costs, creates new jobs and relieves countries' dependence on fossil fuel reserves (petroleum, coal and natural gas) (Bogdanov *et al.*, 2021).

In particular, the town of Cervià de les Garrigues (located in the North-East of Spain) desires to profit from the recent European and state initiatives that promote the development of sustainable energy solutions to revitalise local socio-economic activities. Basically, Cervià is involved in an active farming community; and as in many countryside regions, it has suffered a substantial rural exodus that has reduced the vitality of the population and deteriorated the financial system of the area. Consequently, the city council is analysing proposals to design an integrated renewable energy centre that will favour sustainable power production with low environmental impact and the development of social, cultural and economic activities. (A. Palau Ibars 2021, personal communication, 17 December).

Implementing two or more renewable energies, an integrated renewable energy centre will be created to supply the public power needs of the village (Yang *et al.*, 2017). The electricity consumed by Cervià arrives from various distant origins, partly renewable (hydroelectric and wind) and partly non-renewable (nuclear, gas, and diesel). A significant amount of this power is used for heating (with gas or diesel boilers) during the cold seasons. Therefore, a stand-alone system will be designed to offer local energy autonomy.

The centre will reduce the regional carbon footprint and the levels of air pollution by sulphur oxide, carbon dioxide, and nitrogen oxides to significantly enhance the lives of the inhabitants and the environment. Consequently, it will lead the municipality's progress towards decarbonisation through the generation of green energy. (A. Palau Ibars 2021, personal communication, 12 December).

On the other hand, from a socio-cultural point of view, this project can contribute to stabilising and even increasing the resident population by improving local public infrastructure, where different cultural and leisure activities attractive to the population will be accomplished. The infrastructure will enable significant energy savings for the local administration in the short term, while it will be financially cost-effective in the long term. Moreover, it will promote the local circular economy with the use of a significant part of the waste generated by its main primary activity, the rainfed agriculture and the manufacture of the purest, high-quality olive oil. (A. Palau Ibars 2021, personal communication, 15 December).

1.1 Aims and objectives

The aim of this thesis is to engineer an integrated renewable energy centre in three out-of-service industrial buildings of the village. As a consequence, an environment capable of offering services to the municipality and prompting pursuits for the socio-cultural development of the local population will be created.

To achieve the purpose of this thesis, the following objectives are defined:

- Design an infrastructure to generate and supply renewable energy to the village.
- Determine the availability of agricultural waste generated in the area for bioenergy production.
- Redevelopment of outbuildings for boiler installation, biomass storage, as well as a community multi-use space.
- Analyse the economic viability of the project, determining if it is profitable or not.

1.2 Project purpose

The thesis has been commissioned by Dr. Antonio Palau Ibars, Assistant Professor at the University of Lleida who works in the environmental management of natural systems. The results of this study are intended to determine the feasibility of a sustainable energy project in Cervià, adapted to the availability of local renewable energy sources. Furthermore, this theoretical study will provide a global vision to the mayor of the municipality, Mrs. Mercè Rubió Carré, of the constructive and economic feasibility of the project. If favourable, the environmentally-safe proposal will be examined in detail. Consequently, the academic analysis will be utilised as a basis, and eventually, a specialised company will be contracted for its future development.

1.3 Document structure

Section 2 provides a description and a theoretical study of the necessary previous concepts that encompass the thesis (location, demography, economy, legal framework, etc.). Section 3 justifies the selection of software used to model viable energies and explains the process of prior inputs required. Subsequently, in section 4, the energy simulation of the infrastructure is performed, while in section 5, the economic viability is studied. Section 6 summarises the results of the SAM simulations, which are discussed in section 7. Finally, the conclusions are drawn in section 8.

2 Study background

This section justifies the development of the thesis by explaining its context, standards, and principal concepts. The area is described in section 2.1 and the unfavourable demographic trend of the village in section 2.2. Subsequently, section 2.3 provides an overview of the main economic activities of the municipality. The description of the infrastructure is detailed in section 2.4. Moreover, the study of the selection of renewable energy sources is presented in section 2.5, and the uses that the customer wants to give to the installation are in section 2.6. Finally, section 2.7 focuses on the legislation and legal framework that influence the project, and the public grants that may be used to finance it are detailed in section 2.8.

2.1 Description of the area

The geographic work area is located in the central sector of the region of les Garrigues, in the province of Lleida, Catalonia, north-eastern Spain, and its total area is 34.5 km^2 (Figure 1) (Ajuntament de Cervià de les Garrigues, 2022). Regarding the geomorphology of the terrain, Cervià (444 m a.s.l.) is located in a mountainous territory integrated into the mountain range called Serra de la Llena. The highest altitude of the municipality is the acme named Punta dels Marquesos (655 m a.s.l.). (Catalunya.com, 2013).

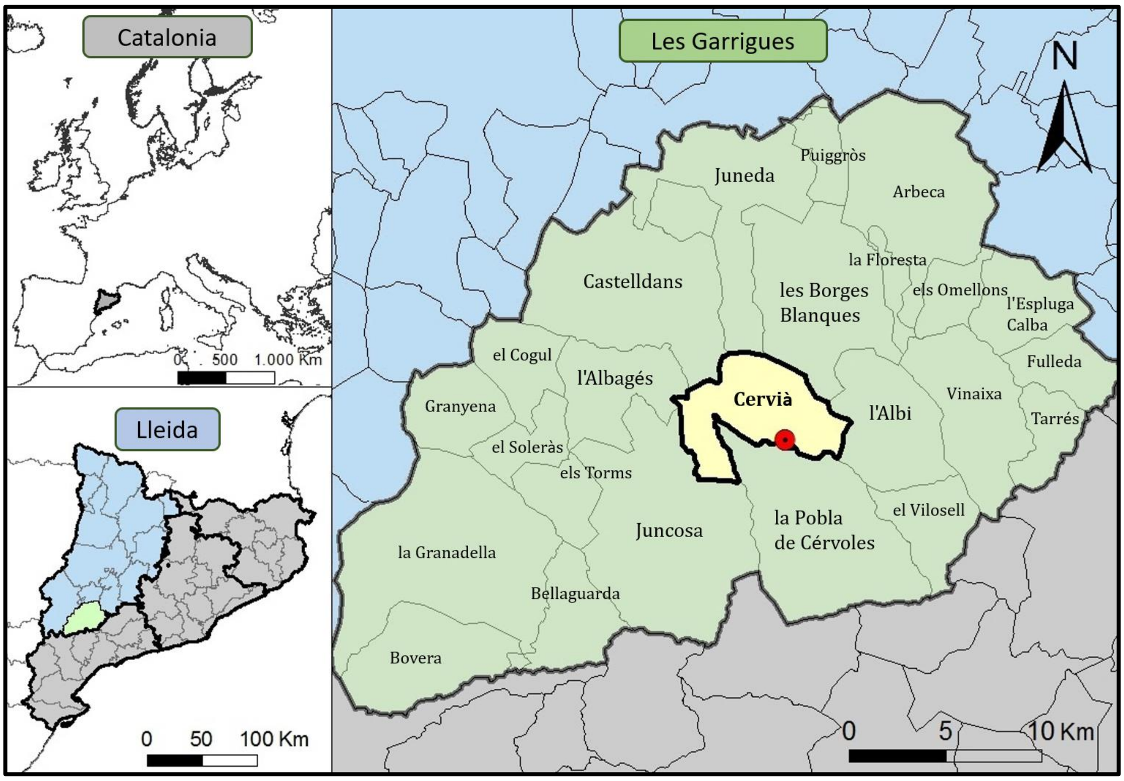

Figure 1. Location of Cervià de les Garrigues. (Author's own, adapted with ArcGis).

The town can be accessed by the conventional road LV-7031, which connects with the capital of the region, les Borges Blanques. It is also communicated by the LP-7032 which conducts to the AP-2 motorway. Moreover, four tarred rural roads contribute to local and regional accessibility, connecting la Pobla de Cérvoles, l'Albí, Castelldans, and l'Albagés. (Turisme de les Garrigues, 2021).

The meteorological characteristics of les Garrigues region are known as the Dry Continentalized Mediterranean climate (De, 2020). According to the Köppen classification, this is formally categorised as Csa (Britannica, 2022). As can be perceived in Figure 2, it is characterised by relatively cold winters, averaging 4° C and occasional fog. Summers are hot, with a mean of 25 ºC (Martin-Vide *et al.*, 2016; Meteo.cat, 2019). Accordingly, these climate conditions will have a direct influence on electricity generation and biomass production.

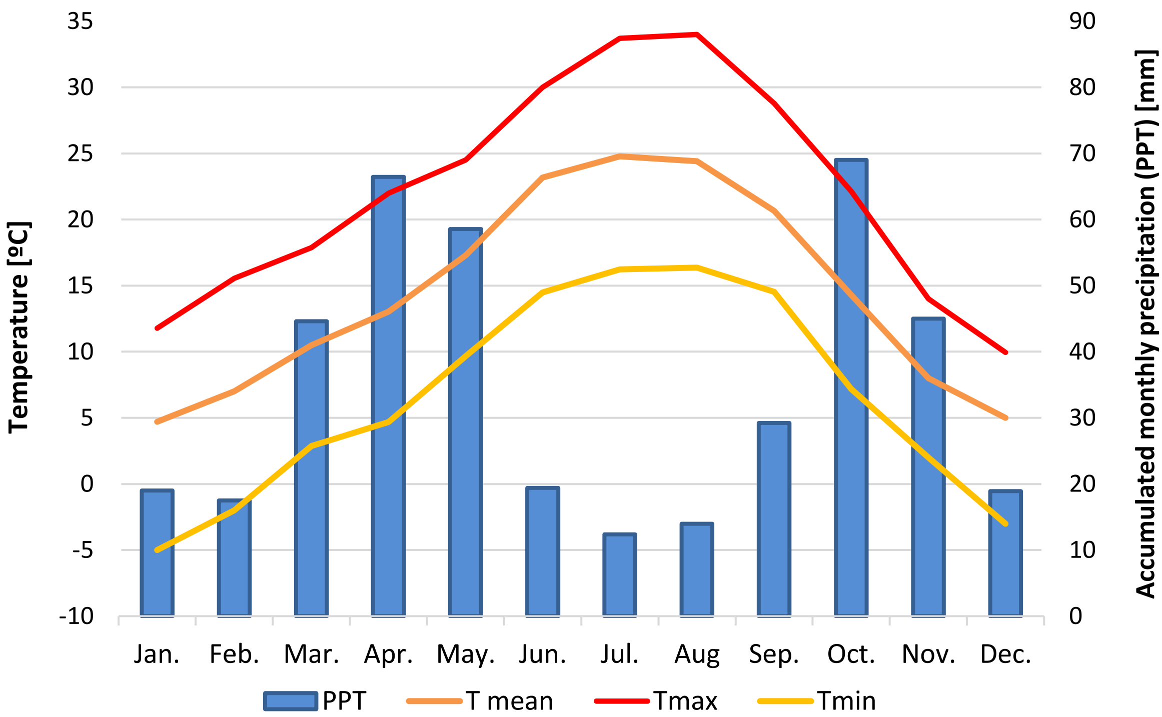

Figure 2. Climograph of les Garrigues. (Adapted from Meteo.cat, 2019).

A major peculiarity of this area is the annual and daily thermal amplitude. The main cause of sudden temperature fluctuations is continentality. There is a natural geographical barrier that prevents the influence of the sea from reaching it, which increases the oscillations (Alonso *et al.*, 2004). Additionally, as can be observed in Figure 2, there is light and irregular rainfall. The annual precipitation is between 400 mm and 450 mm, with maximums in spring and autumn. In section 3.6, the different relevant meteorological parameters obtained from the weather station are analysed in detail.

2.2 Demographics of Cervià de les Garrigues

According to data published in January of 2021 by the National Electoral Institute of Statistics Spain (INE, 2016), the municipality of Cervià de les Garrigues had 665 inhabitants. Consequently, the population density stands at 19 inhabitants per km^2. Figure 3 illustrates the number of residents since 1900.

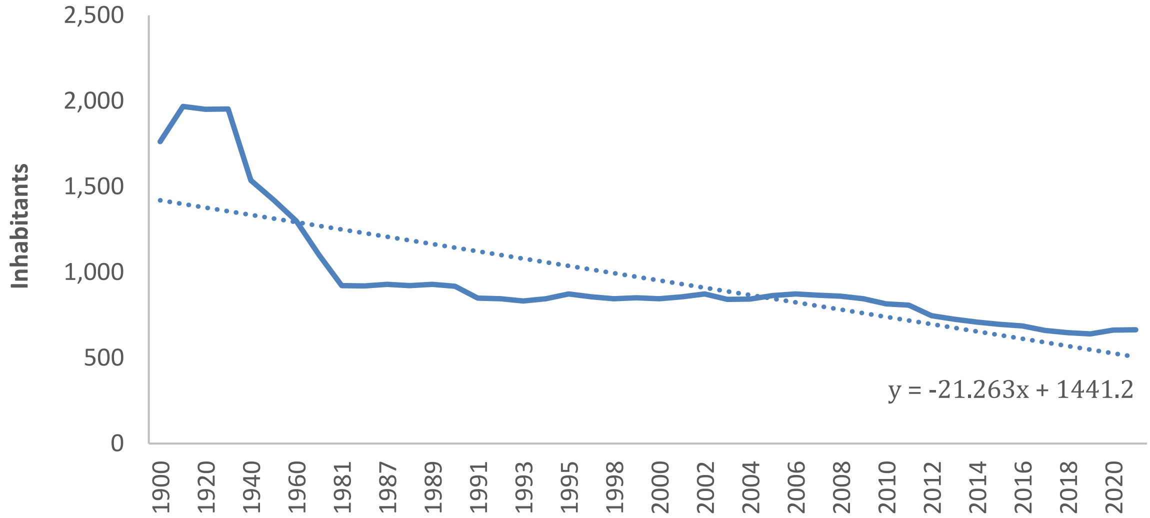

Figure 3. Temporal evolution of Cervià's demography. (Adapted from Idescat.cat, 2022).

The population increased until 1910, when it remained constant. Afterwards, in the mid-1930s, it decreased drastically as a result of the Spanish Civil War (Menacho *et al.*, 2002). This negative trend has continued until nowadays. To comprehend this negative tendency, deaths must be contrasted with births (Figure 4).

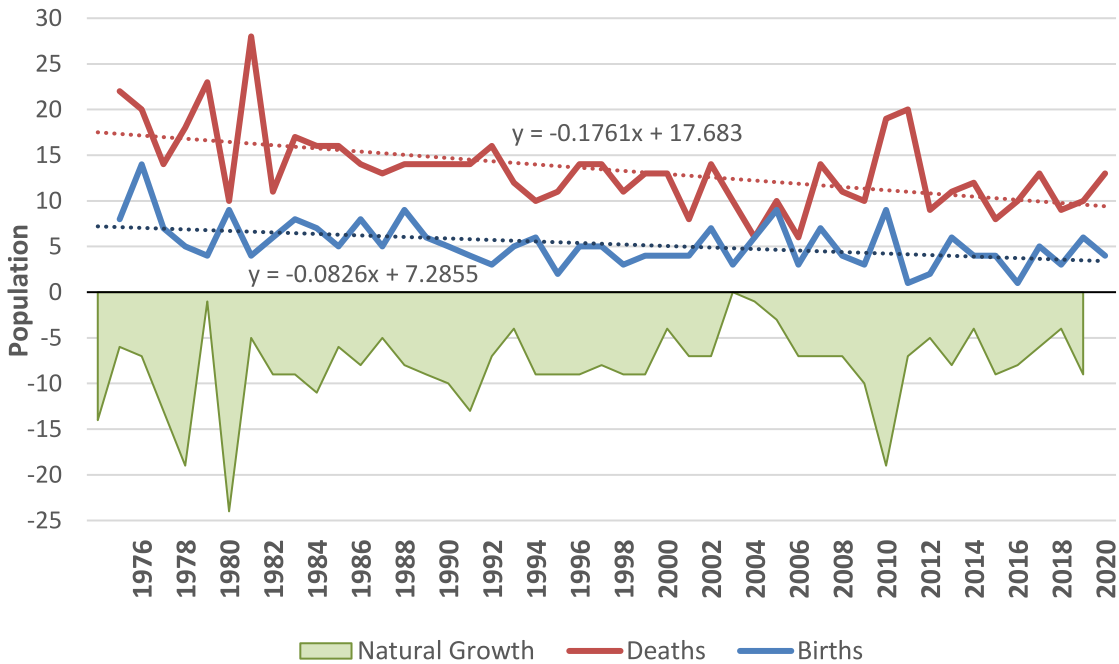

Figure 4. Natural growth of Cervià's population. (Adapted from Idescat.cat, 2022).

For example, according to the latest data published by the INE (INE, 2016), there were only 4 births compared to 14 deaths. The villagers have an increasingly noticeable tendency to decrease due to population ageing. Likewise, the population pyramid for the year 2021 is attached (Figure 5).

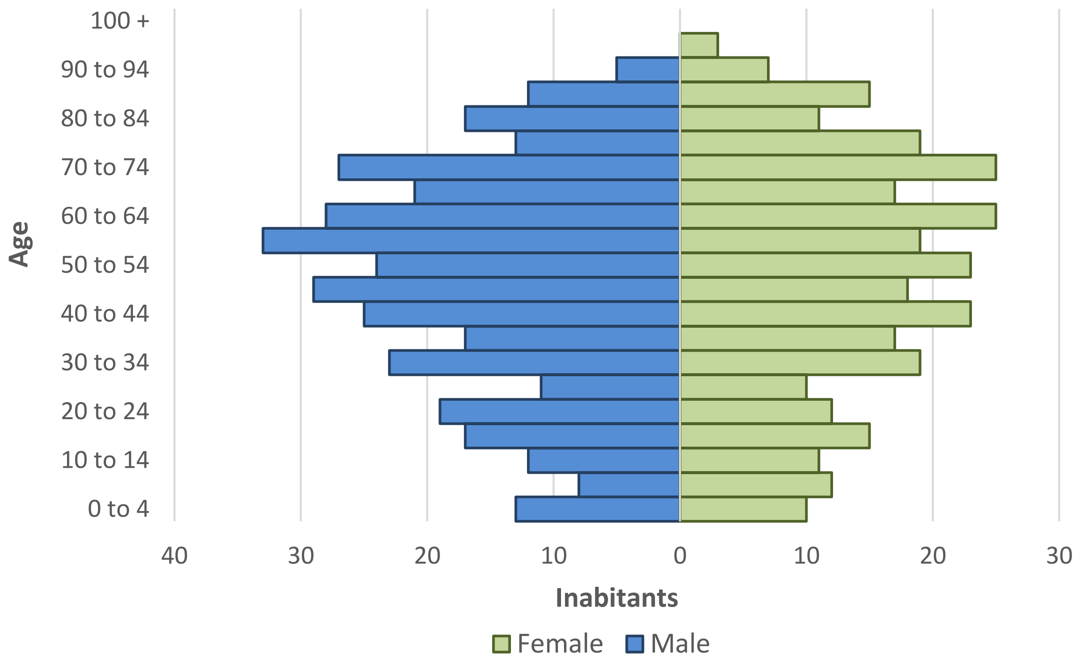

Figure 5. Cervià's population pyramid (2021). (Adapted from Idescat.cat, 2022).

As can be observed in Figure 5, the population pyramid of Cervià is completely regressive. Residents of legal age (18 years) represent the majority with 87.2%. The low birth and mortality rates cause progressive population senescence, resulting in the average age of the inhabitants being 49 years. The demographic trend of a depleted and ageing rural population mirror closely the trend found in many areas of Spain in the last century. Young adults are forced to leave their native rural areas and migrate to urban zones to search for employment, due to the lack of interest in agriculture (low profitability), and the lower local opportunities (Quelart, 2013). This has had a negative impact on the economy of the region. It should be noted that, currently, there is a growing trend of reoccupying these small population centres by urban youth, who aspire to a better quality of life, lower housing costs and can accomplish their professional activity without alterations. Consequently, it has a direct influence on the electricity demand and the vitality of the population. (Vega, 2022).

2.3 Economic activities of the village

The economic sectors and activities of the municipality of Cervià are fundamentally based on agriculture and livestock. The latest data collected in 2009 by INE (2016), indicates that the total exploitation of the utilised agricultural area of the village was 2431 hectares (ha). 2333 ha belonged to cultivated land and the remaining 98 ha to permanent pasture. In Figure 6, the distribution of agriculture is specified.

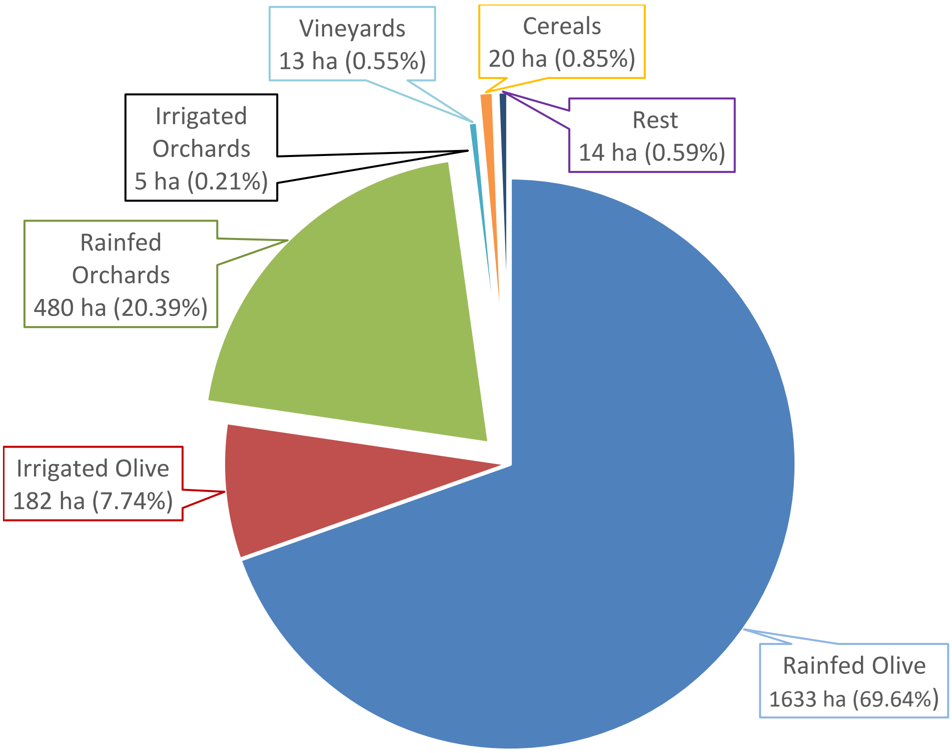

Figure 6. Distribution of the 2,333 hectares of agricultural land in Cervià. (Adapted from Uab.cat, 2022; Idescat.cat, 2022).

From Figure 6, it can be perceived that most crops are rainfed, representing 92%. However, it is predicted that the percentage will decrease significantly with the installation of the Segarra-Garrigues irrigation canal. In addition, it should be noted that olive cultivation is the most common, specifically the type of arbequina olive, from which high-quality oil is made (María Paz Aguilera *et al.*, 2004). Since its foundation in 1914, the Camp Cooperative of Cervià (the association of local olive oil producers) mainly produces oil with the les Garrigues denomination (quality mark) of origin, recognised internationally by experts. It is the only major industry in the town and is considered the main business and economic driver. In addition, of the 485 ha of orchards, the majority belong to almond trees. (Campdecervia.com, 2022).

On the other hand, livestock complements the local economy. According to the latest data recorded by the Institute of Statistics of Catalonia (IDESCAT) (2022), poultry farming stands out, accounting for a total of 69,000 heads. In addition, the farmers of the town also have pig-type farms (408 heads) and goat-type farms (52 heads). Finally, about the forest area, it is occupied by 721 ha of Aleppo pine (*Pinus halepensis*) and oak (*Quercus ilex*) forests, and 505 ha of Mediterranean scrubland. (Idescat.cat, 2022).

2.4 Characterization of the infrastructure and ownership

The three buildings, which are the object of study in this project, are a former textile industrial facility owned by STOCKFIL S.L., built-in 1972. The occupied land is classified as urban and located on the outskirts of the village, on Av. Sardana 2, 25460. The exact location and the plan view can be appreciated in Figure 7.

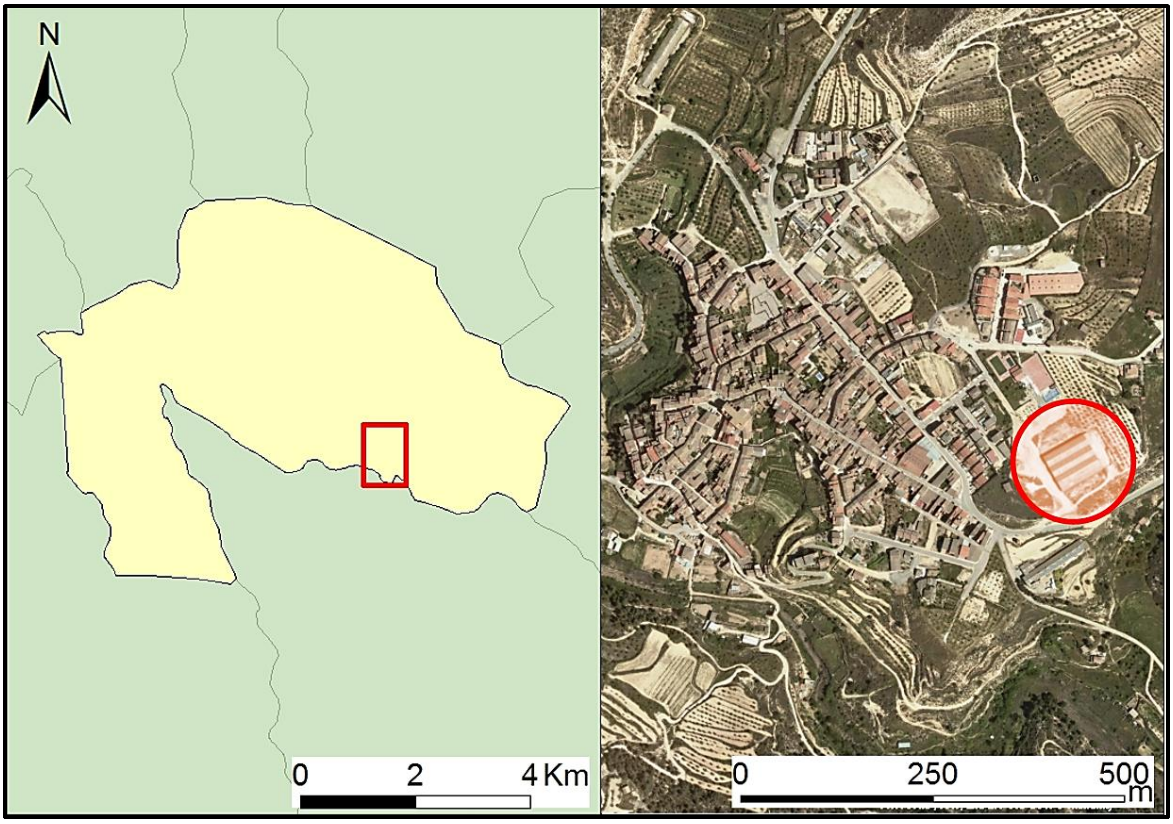

Figure 7. Location of the three industrial buildings. (Author's own, adapted with ArcGis).

The installation is located at the most elevated geographical point of the town and has a total area of 3200 m^2, of which 3118 m^2 are useful and 3090 m^2 of floor plan. It is a four-wind construction with approximately 8000 m^2 of adjoining plots of ground unbuilt. The cadastral reference and geographical coordinates are seen in Table 1. Additionally, in Appendix I.1.1, the cadastral map of the area is attached.

Table 1. Location of the three industrial buildings

Latitude [º]	Longitude [º]	Altitude [m]	Cadastral reference
41.424637	0.864385	470	1683008CF2818S0001AI

(Sedecatastro.gob.es, 2022).

The industrial buildings have a regulatory low voltage installation. The electrical power of the machines was 57 CV and 7 kW, equivalent to a total electrical power of 48 kW. However, the infrastructure was calculated for a maximum power of 74 kW (100CV). The three-phase and neutral power supply a voltage of 380/220V. In addition, there are unified active and reactive power meters, general protection panels, and relevant grounding, as reflected in detail in Appendix I.2.3 plans. Furthermore, in Appendix I.2.2, it is seen the distribution and the exact measures of the construction.

Additionally, the construction has an adequate condition of the walls, ceilings, accesses and stairs, as well as a sufficient height of roofs. There are toilets and a mezzanine with offices. The wastewater produced in the toilets is conveniently conducted by driving masons to the general sewerage system. Furthermore, it fulfils the Fire Prevention Regulations NB-CPI-91, with fire extinguishers placed in such a way that there is no distance greater than 25 metres between any point of the premises and them.

However, there is a serious construction problem as the roof is made of asbestos. Asbestos fibre is considered a toxic material. Installation and sale throughout Europe, and in particular in Spain, have been prohibited since December 2002 (Ccoo.es, 2015). With the Spanish weather conditions, it is estimated that this material has a lifespan of 30-35 years. When it is fragmented or deteriorated, its fibres can be released into the environment and can be inhaled into the lungs, potentially causing illness over time. Logically, the risk depends on factors such as the concentration, quantity, duration, and frequency of inhalation. It can cause respiratory problems such as asbestosis, lung cancer, or other illnesses (Craighead & Gibbs, 2009). For its removal, the services of a specialised and approved company must be contracted. In Spain, the removal and management conditions are included in the Royal Decree (396/2006) of March 31st.

2.5 Types of renewable energies sources

Renewable energies are those that are obtained from inexhaustible natural processes or that have the capacity to be renewed (National Geographic Society, 2019). As defined in 2022 by the International Energy Agency (IEA), these are considered to renew themselves more rapidly at the rate at which they are consumed. They have the quality of not being contaminated or producing a low environmental impact as they generate almost insignificant or non-existent pollution (OECD, 2022). In Figure 8, a classification is performed, indicating the source of origin and its different types.

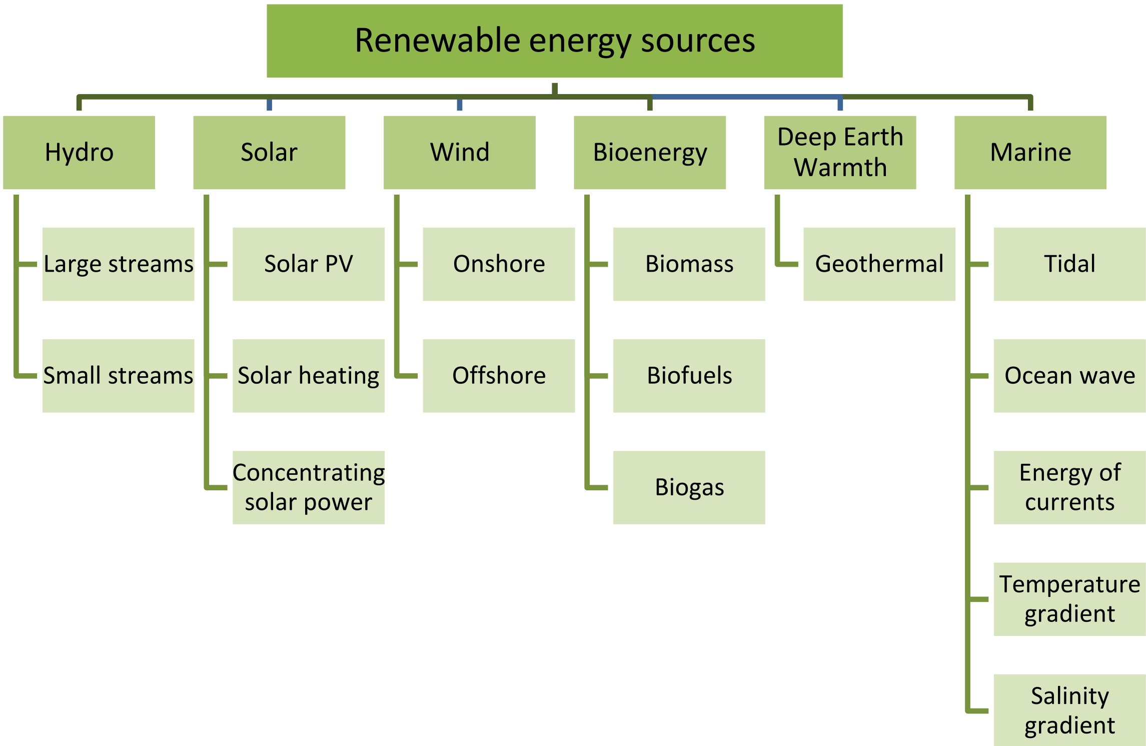

Figure 8. Renewable energy sources classification. (Adapted from Eia.gov, 2022).

Accordingly, in the sections (2.5.1, 2.5.2, 2.5.3 and 2.5.4), their source of origin and their availability in the location of the installation are analysed. Consequently, it will be discerned which are the most appropriate to install in the present project.

2.5.1 Marine, Hydropower and geothermal sources feasibility

Marine and hydropower are doubtlessly discarded as there is no river, reservoir or sea nearby. Furthermore, to use geothermal energy to transform it into electricity, medium and high-temperature geothermal deposits are required to generate steam. Consequently, a turbine connected to a generator is rotated. Observing the geothermal map of Spain (Figure 9), it can be decided that it is not the proper place to install this type of technology.

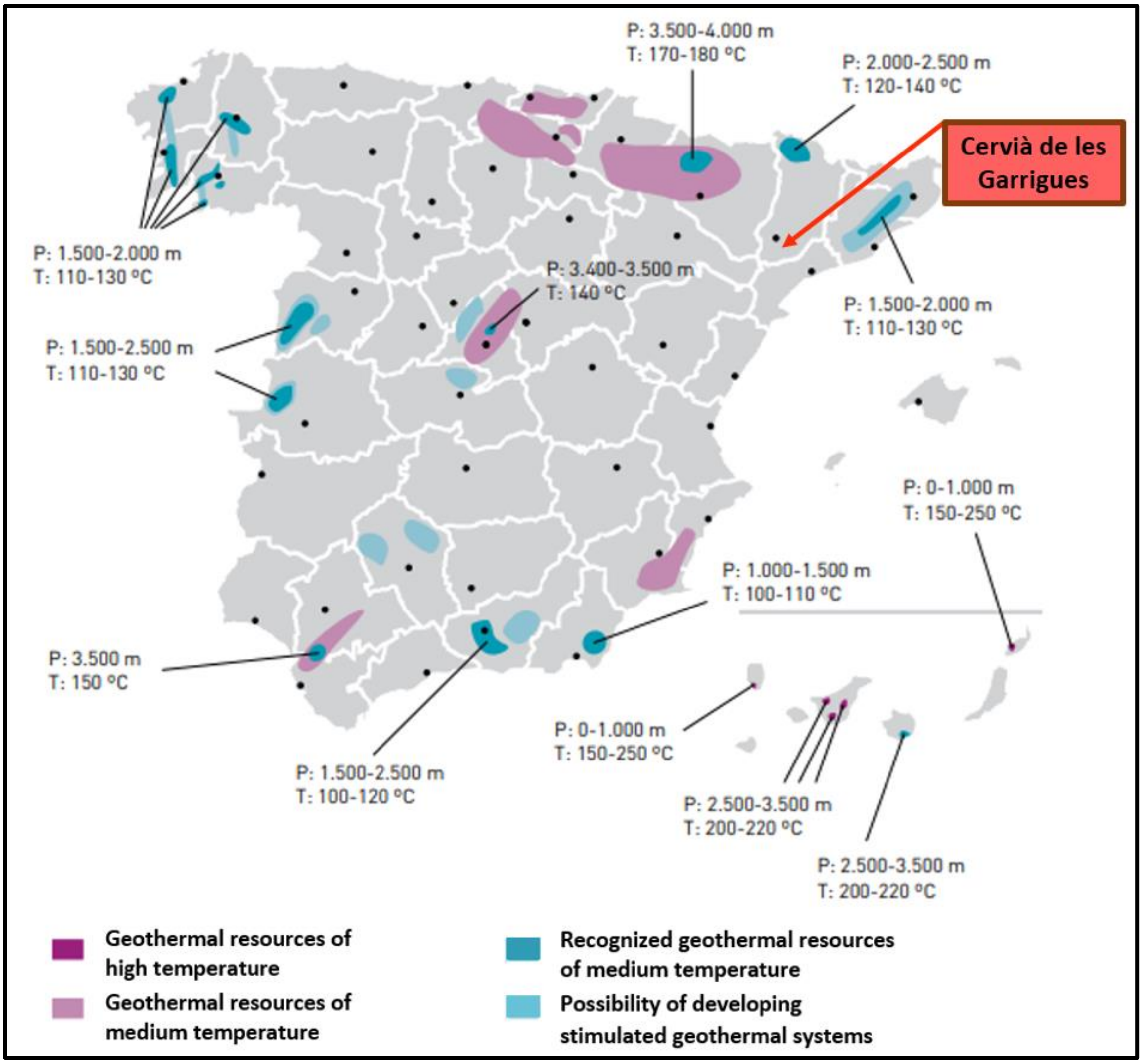

Figure 9. Spanish map of medium and high-temperature geothermal resources. (Idae.es, 2021).

2.5.2 Solar source feasibility

Spain has excellent climatic conditions for this type of technology as it is one of the countries in Europe with the highest total number of hours of daylight (Prieto, 2017). Observing the map of the Technical Building Code of Spain (CTE), it can be realised that the location is totally favourable (Figure 10). Moreover, it is important to contrast it with the characteristics of the infrastructure, as it has 3200 m^2 of roof facing South East (SE) for the installation of Photovoltaic (PV) panels (Appendix I.2.1).

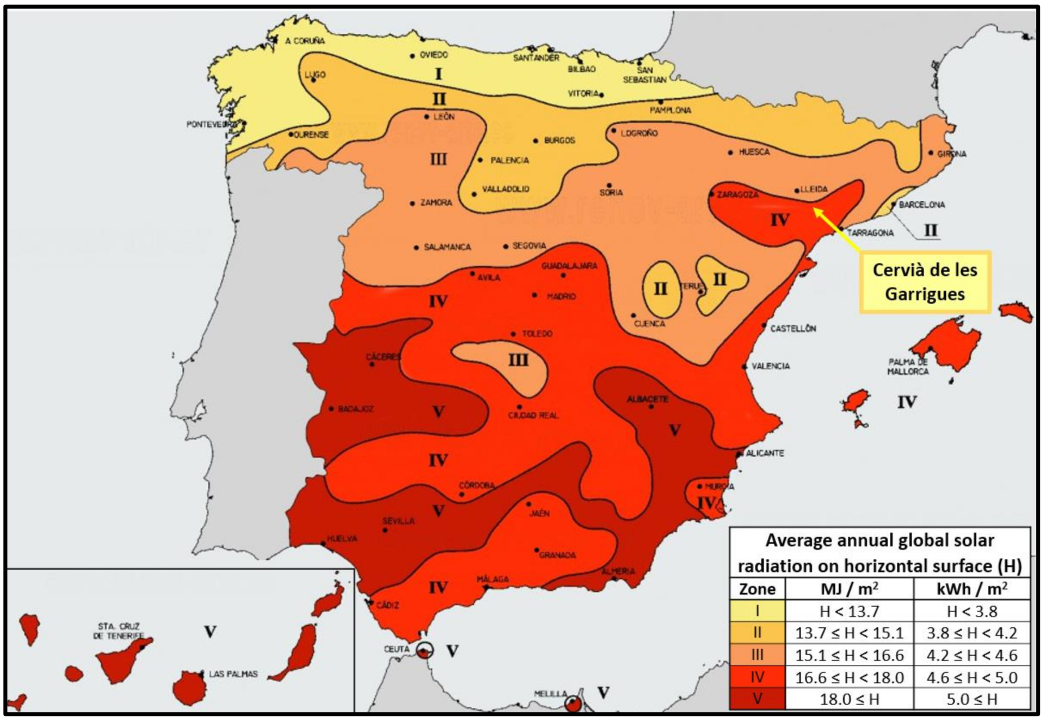

Figure 10. Average annual solar radiation map on the horizontal surface of Spain. (CTE, 2021).

2.5.3 Wind source feasibility

Spain ranks fifth in the world with the highest installed wind power (Statista, 2022). Currently, in terms of installed power, this is the country's main source of energy, avoiding the emission of about 29 million tonnes of CO_2 per year (Energia.gob.es, 2021). Figure 11 contextualises the availability of the resource in the Iberian Peninsula.

Figure 11. Spanish map of the average annual wind speed (at 80 m.). (Diego, 2019).

Although Cervià is not one of the most satisfactory locations for its installation, wind energy has the advantage that it can be exploited by different types of turbines, with completely different powers and functionalities, depending on the weather characteristics. It is not necessary to have large gusts of wind for the correct generation of electricity (Wagner, 2017). By observing the turbine power curve and wind speed, the most cost-effective wind turbine can be determined (Benmedjahed *et al.*, 2017). Due to the location of the project site, a domestic wind turbine must be used. Despite it being located at the highest point of the town, it is within the village. Consequently, it must have a friendly design that operates quietly, without producing vibrations. Section 3.6.2 discusses the availability of this natural resource, determining whether the technology is feasible.

2.5.4 Bioenergy source usability

Contrasting the economic activities of the village, it is determined that of the different types of bioenergy, it is only viable to use biomass. According to the Spanish Association for Standardization and Certification (AENOR), biomass is defined as all biological material with the exception of those that have been formed in the geological mineralization process (www.boe.es, 2012). This type emphasizes because it maintains its energy until the time of use and can be transformed at any time without depending on its state (Santamarta & Jarabo, 2013). Consequently, it provides an adjustable supply, contrasting the intermittent production of wind and solar energy.

Biomass has an expansive range of sources, such as agriculture, forestry, municipal waste, industries, etc. (Institut Català d'Energia, 2019). However, discerning the land map (Appendix I.1.2) and the economic activities of the village, only those of agricultural, forestry, and agro-industrial origin will be considered.

Most of the raw materials obtainable are from the farm; pruning, uprooting, and harvesting crops. In addition, there is the agro-industrial waste generated by the Camp Cooperative of Cervià after the elaboration of the different products (oil press and almond shell, basically). Finally, some hectares belong to meadows and unproductive land that farmers usually use to leave the animals grazing. Accordingly, Table 2 indicates the estimation of the functional amount of agricultural waste that could be obtained.

Table 2. Types and properties of biomass available in Cervià

Biomass type	Crop type	Hectares [ha]	Calorific Values [MJ /kg]	Wet optimum production [t/ha yr]	Dry optimum production [t/ha yr]	Biomass Harvest Time (4)	Drying Time (4,5) [months]
Forestry	-	1,342 (1)	12.00	166.00	116.2	Apr – May	6
Agriculture (Herbaceous)	Grain	20	17.00	0.61	0.43	Jun-Sep	2
Agriculture (Woody)	Vineyards	13	12.00	1.43	1.00	Sep-Oct	4
	Olive	1,815	12.00	0.56	0.39	Nov – Jan	5
	Orchards	485	12.00	0.81	0.57	Sep – Oct	8
Agro-industrial	Olive Pit	-	19.68	- (2)	-	Nov – Jan	3
	Almond Shell	-	18.83	- (3)	-	Sep – Oct	3
Totals	-	3,675	-	-	-	-	-

1. Only 28% of the total forest area is available for exploitation (General Forest Policy Plan of Catalonia, 2014).
2. 1500 tones/year (15% moisture). Data provided by the city council (personal communication, 10.01.2022).
3. 100 tones/year (15% moisture). Data provided by the city council (personal communication, 10.01.2022).
4. Data provided by an interview with a local farmer (personal communication, 4.01.2022).
5. Drying time at ambient temperature without any specific process.

(Adapted from Estudi de disponibilitat de biomassa i demanda energètica, 2020).

The values documented in Table 2 are the optimal values that can be obtained if the land resources are used efficiently. By multiplying the production per hectare by the surface, approximately 158,000 tonnes of dry agricultural waste are supposed to be acquired. Notwithstanding, this value is not realistic as it considers that the farmers would be working and collecting all the possible agricultural waste. For this reason, in section 3.6.3, the estimated production is calculated by applying percentages of obtainability.

The biomass obtained should be transformed to adapt and optimise the process. Moreover, it should be splintered and dried for its efficient storage (Cantero, 2021). Although pellet stoves are emerging significantly, the splintering should be preferred due to the pellets requiring additional pre-preparation, implicating an additional cost and the use of more machinery (Malik *et al.*, 2015). The main purpose of the biomass boiler is to use agricultural waste to generate electricity during the hours when there is no availability of other renewable energy. Nevertheless, in the current market, Combined Heat and Power (CHP) boilers predominate as they generate electricity and profit from the heat generated during the process, with elevated efficiencies of around 90%. The heat obtained could be used for drying biomass, production of hot water, and even heating during the winter months. (Liu, 2011).

2.6 Use to be given to the infrastructure

Beforehand, the necessities of the installation of renewable energies should be examined. Inside, it is required to reserve significant space for the biomass boiler. It must have a strategic position for the exit of gases and the supply of raw materials. Consequently, a diaphanous warehouse must be built to store biomass. It should be located with direct access to the outside with a large door for its uncomplicated use. Moreover, all the materials, equipment, and control systems associated with the installed renewable energy must be distributed. The simulation planning will be performed in section 6.3 and in Appendix I.2.2, where the infrastructure plans are attached.

On the other hand, in order to be able to plan the integral centre efficiently, the uses and characteristics that the city council wants to offer in the infrastructure must be considered. Along with the biomass repository, there will be another municipal storage with the same characteristics. An event hall with access to the warehouse is also designed so that local socio-cultural activities (the auditorium) could take place there. Furthermore, there will be a coffee bar to offer food and drinks. It will also have access to the outside due to being able to place a terrace during the months when the weather is suitable. Likewise, as mentioned in the previous section 2.4, there used to be a mezzanine with offices. This space will be used to relocate new municipal offices. Additionally, two rooms for different local associations, such as the young or the elderly, could be located on this upper floor.

Similarly, it is necessary to consider the number of toilets and what would be their correct location to satisfy the needs of future users. Considering that in each group of toilets there is one for gentlemen, one for ladies, and one for the disabled, it is estimated that a minimum of 3 sets are indispensable. They will be strategically located, one next to the auditorium, one in the bar and one upstairs. Finally, if there is still unutilised interior space, a multipurpose room will be left without a specified use.

Finally, outdoors, it is convenient to have a parking area for at least 25 cars and 10 motorcycles. Moreover, it would be appropriate to plant trees to create a green area and to be able to shade the different vehicles that can be parked there. A part could also be paved next to the bar terrace. It would be a versatile use for various outdoor local activities and festivities, such as summer festivals, summer popular dinners, the oil fair, etc.

2.7 Legislation affecting the project

The significant prosperity in the renewable energy sector is marked by stable and vanguard regulation. The legislation for the development of the project is divided into three geopolitical levels, differentiating between the continental (European Union), state (Spain) and autonomous community (Catalonia) perspectives (Energia.gob.es, 2019). European legislation establishes explicit targets focused on the abandonment of fossil fuels and energy efficiency in all economic sectors. For example, by 2030 it is intended to ensure environmental sustainability by reducing greenhouse gases by 40% (comparing 1990 data as reference) or achieving 32% renewable energy (Miteco.gob.es, 2012). On the contrary, each autonomous community controls the authorities granted by the state. Notwithstanding, there are no relevant restrictions that affect the project directly (Informe del sector de l'energia, 2009).

In Table 3, a selection of the legal framework that was considered most applicable to the project is made. Additionally, in Appendix I.3, there is a table with a concise description of each.

Table 3. Classification of the relevant legal regulations for the project

	European Legislation	**Spanish Legislation**	**Catalan Legislation**
Energy efficiency and savings	European Directive 2006/32/CE of 5th April 2006 Community Program SAVE	Royal Decree 56/2016 of 12th February Energy Saving and Efficiency Action Plan Royal Decree 900/2015 of 9th October	Energy Sector Plan
Renewable energies use	Directive 2009/28/CE of 23th April 2009 European Directive 2018/2001 of 11th December 2018	Royal Decree 413/2014 of 6th June Renewable Energy Plan Royal Decree 436/2004 of 12th March Climate Change and Energy Transition	Energy Sector Plan
Efficiency certifications	European Green Deal	Royal Decree 235/2013 of 5th April Royal Decree 244/2019 of 5th April Law 24/2013 of 26th December	Since 1/6/2013 Law 16/2017 of 1st August
Solar energy	Clean Energy for All Europeans	Royal Decree 14/2010 of 23rd December Royal Decree 1003/2010 of 5th August Royal Decree 1663/2000 of 29th September	Decree 352/2001 of 18th December
Wind energy	EU Biodiversity Strategy to 2030	Royal Decree 947/2015 of 16th October	Decree 174/2002 of 11th June
Biomass energy	Renewable Energy Directive 2018/2001 of 11th December 2018	Royal Decree 178/2021 of 23rd March	Law 22/2011 of 28th June

(Adapted from Energy, 2022; BOE, 2022; GENCAT, 2009).

Spanish specific laws for solar energy, wind energy, and biomass legislation are organised, of which the last two are noteworthy. In the case of wind power, because domestic technology is selected, the Royal Decree (1367/2007) of October 19th states that authorization for their site is needed as well as proof that it is sufficiently distant from houses, thus avoiding noise pollution. Notably, for biomass, the Royal Decree (178/2021) of March 23rd applies the UNE 303-5 standard, which establishes minimum requirements for energy efficiency and emission values depending on the characteristics of the boiler (Idae.es, 2020).

On the other hand, in Spain, there are multiple laws in force that regulate the use of renewable energy. Remarkably, according to the Royal Decree (436/2004) of March 12th, the owner of the installation can vend the electricity generated to the distribution company at an agreed regulated rate or sell it directly to the common market. Supporting this, there is the Royal Decree (244/2019) of 5th April and a Law (24/2013) of 26th December, which define the two different forms of self-consumption. The first type, without surpluses, does not authorise energy to be discharged to the distribution grid, and surpluses do. Within the second mode, there is the possibility that the remaining electricity is marketed at the agreed price. The standard selling price ranges from 0.05 €/kWh to 0.06 €/kWh (Es, 2020).

2.8 Public grants applicable to the project

Although the project contributes to significant socio-economic progress by promoting a sustainable energy supply, it must be economically practicable and competitive. An integrated centre of this magnitude requires a strong initial capital investment that will be amortized in long term, reducing electricity costs and monetizing the surplus. Considering that the total economic budget for 2021 of the Cervia's townhall was approximately €1,440,000 (BOP, 2021; CIDO, 2020), it is necessary to examine alternatives to finance it. Moreover, subsidies and public funds that promote this type of environmentally friendly investment should be used. Favourably, nowadays there are a wide variety of possibilities for obeying European Directives to achieve an economy with net-zero greenhouse gas emissions by 2050 (Climate Action, 2018).

Applying for financial assistance and attaining the requirements does not guarantee its grant. Additionally, the time to receive monetary support can be considerably extended (Figure 12). For this reason, only those that are considered most important to exemplify and demonstrate that there are viable options are discussed. Accordingly, a thorough study should be conducted to contrast more possibilities and evaluate the possible benefits that could be received. If the project is finally developed, the public funding should be exhaustively analysed, determining its conditions and usefulness.

Figure 12. General procedure for public awarding grants. (Adapted from Ajuts a l'autoconsum, 2021).

Probably the most relevant state programme is the US5000-ICAEN. It is an assent regulated by the Royal Decree (692/2021) of August 3rd to promote investments in clean energy projects for sustainable advancement in municipalities with demographic challenges. The financial support covers completely the necessary processes for the execution of infrastructure with the characteristics of this project, such as the assembly, equipment, materials, reports, processing of grants, etc. The amount of basic assets is 85% of the investment, which increases to 100% if it is considered an "integrated project".

Catalan fundings, such as subvention for self-consumption with renewable energy sources and renewable thermal systems, are also available and are regulated by the Royal Decree (477/2021) of 29th June. These subsidise a percentage of the total cost or price per kilowatt installed, depending on the technology, power, and capacity. The foremost requirement is to justify that the electricity consumed is equal to 80% (or greater) of the renewable energy generated.

Finally, as aforementioned in section 2.4, it should be noted that the asbestos roof should be removed. Nevertheless, the 2022 incentives (TES / 1068/2022) of 18th May are not yet published since they are posted every year in summer. It is estimated that the value will be the same as in previous years, which financed 100% of the cost. Expenses considered eligible are the removal, transport, and treatment of residues as long as the asbestos subtraction is executed by companies registered in the General Register of Waste Managers of Catalonia (RGPGRC). However, the expenditures to replace the function performed by the removed asbestos are not covered (the reconstruction of the roof).

3 Software selection and obtaining the meteorological required data

Firstly, section 3.1 justifies the choice of software that is used to model the system. In section 3.2, the weather variables required by the selected software are specified, while section 3.3 explains how Cervià variables are obtained, and section 3.4 explains the interpolation method used. Subsequently, the interpolated data must be adapted so that it can be entered into the program (section 3.5). Section 3.6 discusses the availability of natural resources (sun, wind, and biomass) at the project's site, determining the types of technology that are viable to install. Finally, the public energy demand to satisfy the public of the municipality is studied (section 3.7).

3.1 System Advisor Model (SAM) software selection

The modelling of the three types of energy to be installed in the project will be performed using a single simulation tool called System Advisor Model (SAM). This free software was developed by the United States Department of Energy and the National Renewable Energy Laboratory (NREL). SAM was released in August 2007 and is vigorously updated and supported formally online at https://sam.nrel.gov and informally on internet channels which are actively updated and supported. (Nrel.gov, 2021a). It is widely used in the research community with publications related to renewable energy modelling such as DiOrio *et al.*, 2015; Gilman *et al*., 2018; and Freeman *et al*., 2019. Note that the simulations have been accomplished with the most up-to-date version to date (2021.12.02).

SAM software empowers the user to parametrically evaluate the energy production and economic performance of different types of renewable energy, such as solar, wind, biomass, tidal, or geothermal (Clean Energy, 2012). To analyse them, a single case must be created for each type of energy. Subsequently, the program permits the creation of a generic case where the data from each case is automatically collected to obtain a combined result (Figure 13).

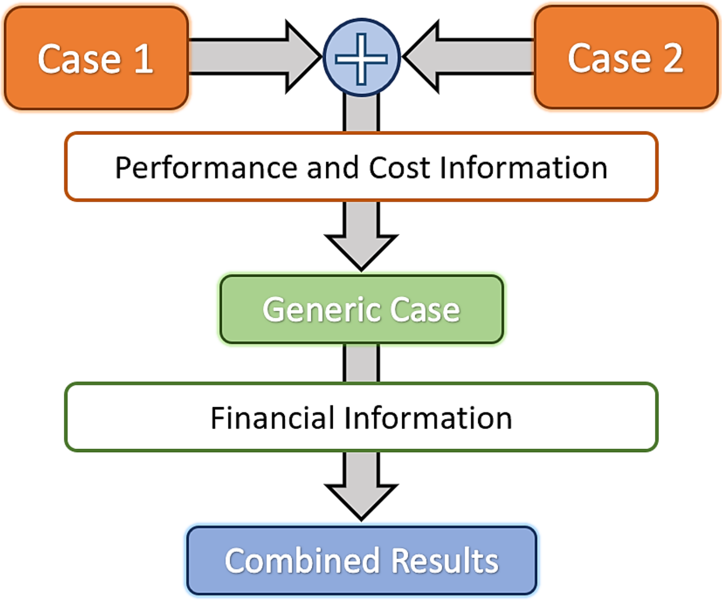

Figure 13. Outline of generic case methodology used by SAM. (Adapted from SAM Help's System, 2022).

The SAM platform offers feature data libraries that permit the simulation of commercial components of energy systems or manually entering the desired characteristics. Likewise, it offers weather data sets from different locations or lets the user enter their own (Nrel.gov, 2021c). If the location to be studied is not in the library, the application offers to download it by entering the coordinates or location name data from the NREL United States National Solar Radiation Database (NSRDB).

Apart from the United States, the NREL provides meteorological data for different nations in the world, including Spain, calculated by the SUNY Semi-Empirical Model. Nevertheless, this method estimates the rest of the values from the cloud index obtained via satellite, which may in some cases be inaccurate (Nrel.gov, 2014). As a result, efforts are undertaken to acquire local data in order to create a more precise and realistic analysis.

3.2 Summary of important climatological specifications of SAM files

As can be perused from SAM's Help System document (SAM Help’s System, 2022), a weather file is an annual hourly or sub-hourly data file. The values can be from a single specific year or a typical multi-year representing historical data. The software used supports various types of weather file formats. Due to its comfort in management, the comma-separated text (*CSV*) format is utilised as it can be edited in any spreadsheet program or text editor. For wind energy data, it admits comma-delimited text with the *.srw* extension.

In both cases, in order to determine the timestep without error, the data must be an integer multiple of 8760 h/yr. For example, if there are 35040 rows, it is considered to be data every 15 min. Note that the program does not permit leap years, and it is recommended to delete them. However, if it is not removed, it should not have a discernible effect because it would use the data for February 29 for March 1 and discard the data for December 31.

According to SAM's General Description manual (Blair *et al.*, 2018), it is advisable to input data from a single year when the simulation of the system is studied without the financial model. In addition, it provides accurate data for that period by applying electricity prices and specific energy consumption. On the other hand, the typical year file contains long-term data, for example, the first 10 days of January 2021, the remaining 21 days of January 2014, February 2018, etc. This type is ideal for simulating solar, biomass, and geothermal energy systems but should be avoided in the case of wind energy. In addition, it is recommended to use it in the case of the economic analysis function.

Table 4 specifies the minimum variables necessary to simulate the three renewable energies that are desired to be installed. The program requires a valid value of each variable for each time pass since it is not capable of executing if any is missing. Furthermore, the speed and direction of the wind must be measured at 10 metres above the ground.

Table 4. Variables required by SAM to model different types of renewable energy

Parameter	**Unit**	**Detailed PV model**	**Biomass Power**	**Wind Power**
Latitude	[dec. degrees]	x		
Longitude	[dec. degrees]	x		
Elevation above sea level	[m]	x		x
Hour of the day	[-]	x	x	
Diffuse horizontal irradiance	[W/m²]	x (1)		
Direct normal irradiance	[W/m²]	x (1)		
Global horizontal irradiance	[W/m²]	x (1)		
Albedo	[-]	x (2)		
Atmospheric pressure	[mbar]		x	x
Dry bulb temperature	[°C]	x	x	x
Wet-bulb temperature	[°C]		x (4)	
Relative humidity	[%]		x	
Wind velocity	[m/s]	x	x	x
Wind direction	[degrees]			x
Snow depth	[cm]	x (3)		

1. The weather file may include two of these irradiance components and estimate the third.
2. If there are no values, the monthly values determined manually in the program is used.
3. It is not necessary. The snow losses can be calculated if the value is in the file.
4. When this value is missing, it is calculated using the method of A. T. Martinez, 1994.
(Adapted from SAM file format description from Help, 2020).

Consequently, two files will be created. A specific one for wind energy will only be from the previous year, 2021. It will include the variables mentioned in Table 4 and will be formatted with the mandated specifications. Otherwise, a typical year's weather file will be created for biomass and solar energy that will contain the other values needed. The historical dates used will depend on the availability of the weather stations. Finally, specify that all the information required by the files can be found in chapter 6. *Weather Data* and 7. *Weather File Document Formats* of the *SAM's Help System document*.

3.3 Cervia's meteorological data

The Meteorological Service of Catalonia (SMC or METEOCAT) has a network of 186 automatic stations distributed throughout Catalonia (XEMA) to be able to predict and analyse the weather conditions (Gencat.cat, 2013). With the corresponding sensors, a secondary sampling of the main meteorological variables is taken for the calculation of minute average data (Table 5). Subsequently, the half-hourly or hourly period data is generated with the minute averages.

All stations have been storing period data in the Meteorological Database of Catalonia since January 2009. Additionally, under the supervision of qualified technical personnel, all the data recorded by XEMA is passed through quality control that consists of several hierarchical and semi-automatic processes. (De, 2020).

Table 5. Variables obtained from METEOCAT's weather stations

Variable	**Acronym**	**Unit**	**Range (min/max)**
Maxim temperature	TX	ºC	-30/46
Average temperature	TM	ºC	-30/46
Minimum temperature	TN	ºC	-30/46
Relative humidity	HRM	%	0/100
Precipitation	PPT	mm	0/100
Maximum wind speed	VVX	km/h	0/55
Wind speed	VVM	km/h	0/55
Wind direction	DVM	degree	0/360
Global horizontal irradiance	RS	W/m^2	0/1400
Atmospheric pressure	PM	hPa	700/1060
Snow thickness on the ground	SD	mm	0/4660

(Adapted from Meteo.cat, 2022).

Unfortunately, Cervià de les Garrigues does not have a public weather station (Meteo.cat, 2012). Therefore, at least two nearby stations must be selected and the data interpolated. Logically, the more nearby points available, the more accurate the estimation (Kalina et al., 2018). The data can be requested from METEOCAT via an online form but has an economic cost proportional to the time required for the preparation of the files (67€/h) (De, 2021). As there is no budget for the development of this thesis, it is decided that the data will be extracted and copied manually from the website. The process involves going to the website, selecting the desired day where the daily table of values is displayed, and copying it to an Excel spreadsheet for subsequent management. It takes about 30 minutes to extract a complete month.

Consequently, it is necessary to find an equilibrium to obtain the most realistic and approximate data possible without consuming unnecessary time. Table 6 lists the seven closest operating stations. The distance to the location of the renewable energy center is calculated using the Haversine formula in Appendix II.1. Its implementation is performed using MATLAB, executing the code of Appendix III.1.

Table 6. Closest public weather stations to Cervià

County	Municipality	Operating date [dd.mm.yyyy]	Latitude [º]	Longitude [º]	Altitude [m]	Distance to Cervià [km]
Priorat	Ulldemolins	17.04.2008	41.32000	0.88570	687	11.7832
Baix Camp	Prades	31.01.2013	41.31481	0.98161	926	15.6642
Conca de Barberà	L'Espluga de Francolí	23.02.1996	41.39241	1.09894	446	19.9087
Conca de Barberà	Blancafort	18.01.2000	41.44237	1.15998	438	24.7483
Garrigues	La Granadella	30.01.1992	41.35991	0.66789	505	17.9215
Garrigues	Les Borges Blanques	25.01.2017	41.51135	0.85617	283	9.6769
Priorat	Margalef	14.01.1996	41.28521	0.75383	404	18.0617

(Adapted from Meteo.cat, 2012).

Finally, it is decided to select the three closest stations so that they form a triangle with Cervià inside (Figure 14). The locations of La Granadella, Borges Blanques, and Ulldemolins are considered to be sufficiently close and well distributed to obtain reliable and realistic data.

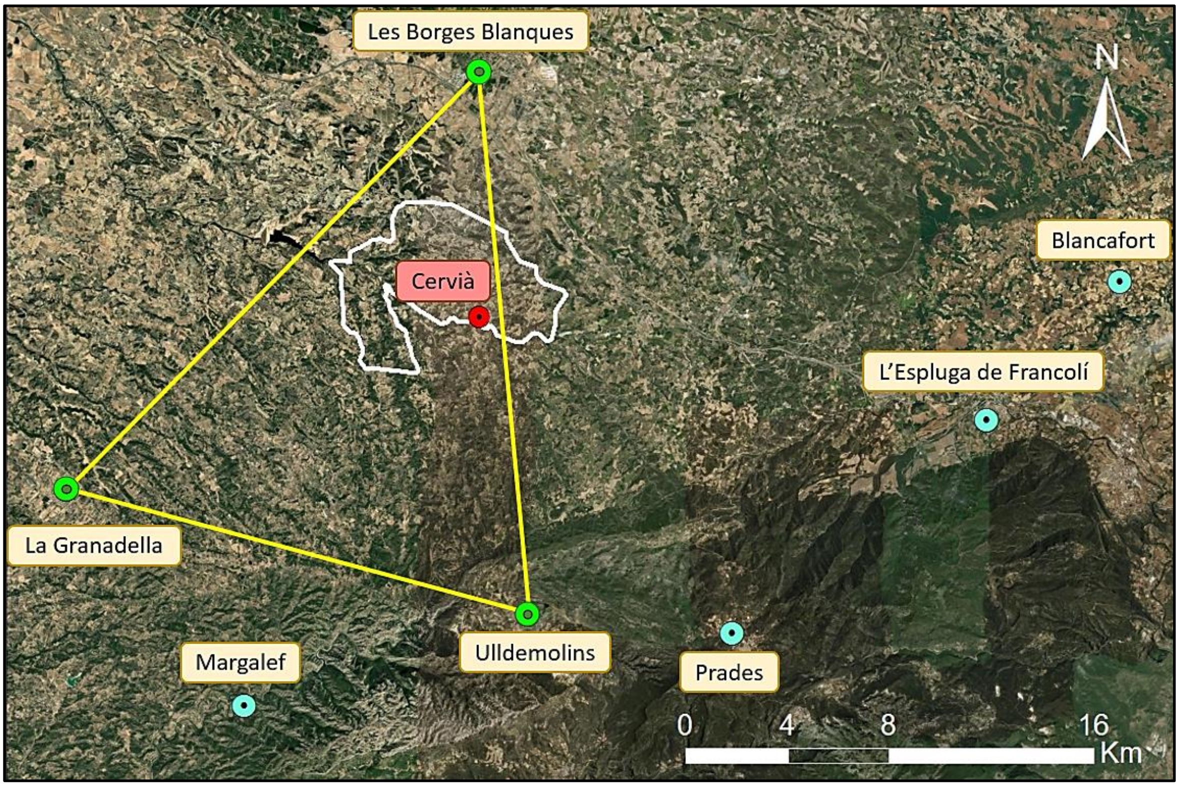

Figure 14. Location of the closest public weather stations to Cervià (Author's own, adapted with ArcGis).

Only three are selected because adding one significantly increases the data extraction time because it is a time-consuming process. Regrettably, the snow depth variable is not present in any of the three seasons, but this is not a problem because it rarely snows. Moreover, observing the dates on which the weather stations were inaugurated, it is confirmed that the data for the year 2021 can be used for the wind file. Semi-randomly distributed temporal data will be used between 25/01/2017 and 28/02/2022 for the weather file. The correspondence of the selected dates is described in Appendix II.4 and performed using the MATLAB code in Appendix III.2. Finally, different data for 2020 will be exported consciously to perform the comparison between two consecutive years and to be able to analyse and contrast it.

3.4 Interpolation of the atmospheric data

In numerical analysis, interpolation is the estimation of the values of a variable in unknown positions from known values at a set of nearby sampling points. There are many different interpolation methods of varying complexity (Florinsky, 2016). In the context of geospatial information, surface interpolation is performed by estimating the values of defined points with two-dimensional functions defined by two coordinates (Kumari *et al.*, 2018).

Additionally, it focuses on the analysis and modelling of the variables associated with spatial information including climatological data. Several studies, such as Rossi *et al.* (1994); Bárdossy and Li (2008), (Sluiter, 2009) and Adhikary *et al.* (2017), demonstrate that in many cases the Kringing and CoKringing method is the most appropriate for interpolating meteorological data. Nevertheless, having three relatively near points, it is decided to use a more uncomplicated method to interpolate it. As the study by Fung *et al.*, 2022 evidences, climate variables can be considered uniform within a section of these characteristics. Furthermore, it should be noted that there is no significant natural barrier between the sampling data that could alter the calculations.

The inverse distance weighted (IDW) method is used as it is appropriate for spatially unevenly distributed sampling points (Halit Apaydin *et al.*, 2004). This exact deterministic interpolation calculates the values based on the weighted average of the known values, applying the inverse distance between the position of the sampling point and the unknown point. Therefore, the nearest points have a more significant influence. Formula 1 is the mathematical expression for IDW:

$$z_j = \frac{\sum_{i=0}^{n} \frac{z_i}{d_{ij}^P}}{\sum_{i=0}^{n} \frac{1}{d_{ij}^P}} \qquad \begin{aligned} z_j &= \text{Known point value} \\ z_i &= \text{Interpolated point value} \\ d_{ij}^P &= \text{Distance between the two points} \end{aligned} \tag{1}$$

Note that to calculate the distance between two points in the plane ($\mathbb{R}^2$) the Pythagorean theorem applies. In formula 2, the module of the vector formed by two points (A, B) is calculated:

$$\mathrm{A}(x_1, y_1) \qquad \mathrm{B}(x_2, y_2)$$

$$d(\mathrm{A}, \mathrm{B}) = d(\mathrm{A}(x_1, y_1), \mathrm{B}(x_2, y_2)) = \sqrt{(x_2 - x_1)^2 + (y_2 - y_1)^2} \tag{2}$$

If the procedure is applied to the situation created by the selected weather stations, a plan is described as shown in Figure 15. This method controls the influence of available samples based on the distance to the point to be interpolated (formula 1). By defining a higher value of power at distance (*P*), more emphasis is given to the nearest points. A power of two is most commonly used in IDW. (Berthet, 2009; Velasquez *et al.*, 2011).

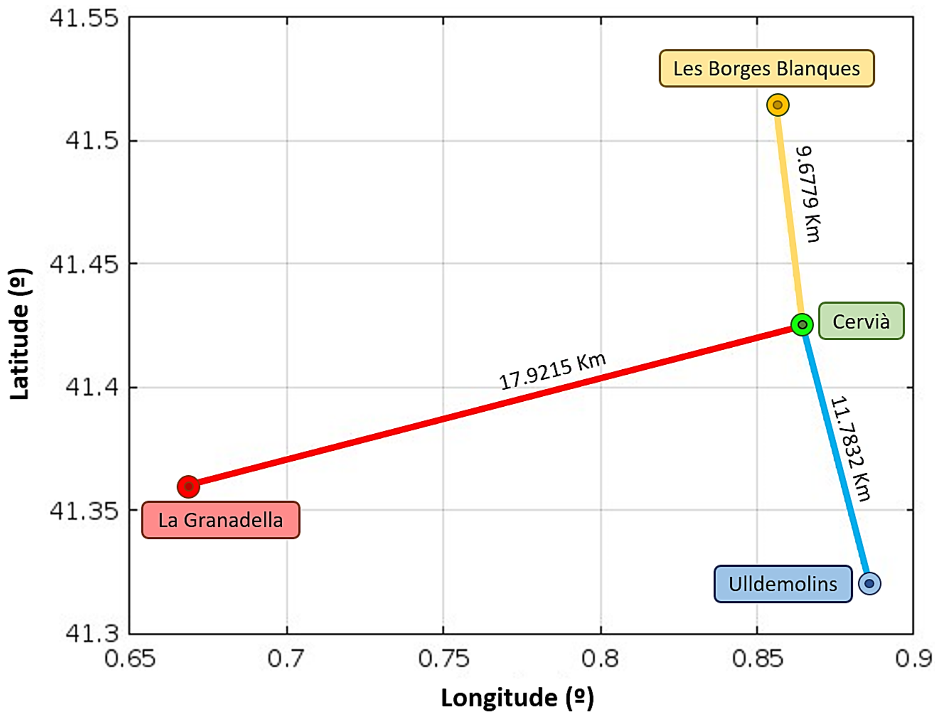

Figure 15. Representative plan of the IDW method applied to Cervià. (Autor's Own, adapted with MATLAB).

3.5 SAM files preparation

Considerable considerations, processes, and modifications have been made to create the two SAM files. Once the manually copied data is available on an Excel sheet, a quality assessment is applied to it to find out if there is any erroneous data. The METEOCAT website labels it with the text *"(s/d)"*, denoting that the sensor has not been able to read and transmit the value. Excel's "Find and Select" function is used to locate it. Subsequently, it is interpolated with the two adjacent values using a linear function using the "Series" tool. Observing the data obtained and the correction process, it is concluded that it is not frequent and mostly occurs in the sensors of precipitation and solar radiation when there are countable values followed equal to zero.

Once the values have been verified in all boxes, the variables are manually exported to MATLAB. This platform for programming and numerical calculation agilely processes data matrices and represents functions. Finally, after creating the *.txt* files, the first lines containing the file information (location, altitude, coordinates, etc.) are added with Excel, and the Wind file is exported in the *.srw* format. Reflect that it is necessary to interpolate 17520 annual values for each variable. To accelerate and reduce the workload, only one code is programmed for the creation of files, attached in Appendix III.3. Raw and interpolated data have been archived and can be found in MS OneDrive folder.

Contrasting the variables that measure the weather stations and the conditions of SAM (Table 5), it can be detected that five inputs are missing to be able to run the simulation correctly. Snow depth and albedo are no problem as they are not necessary. In addition, the software is able to calculate the wet-bulb temperature when simulating biomass. Nonetheless, only one of the three irradiance values is available (Global Horizontal Irradiance) and at least two are needed. The process used to calculate one of the two remaining irradiances is developed in section 3.5.1.

In addition, distinguishing the technical characteristics of the weather stations, it is observed that Ulldemolins and Les Borges Blanques are tested at ten metres above ground level. Inversely, La Granadella is only two metres sampled. Therefore, this data will need to be corrected to the appropriate height for proper interpolation. Section 3.5.2 explains the procedure used.

3.5.1 DIRINT model to calculate direct normal irradiance (DNI)

As examined in section 3.2, SAM software needs at least two of the irradiance components. The weather station only provides global horizontal irradiance (GHI). Consequently, diffuse horizontal irradiance (DHI) or direct normal irradiance (DNI) must be calculated. This relationship is expressed by formula 3:

$$GHI = DNI \cdot \cos(\theta_s) + DHI \qquad (3)$$

$GHI =$ Global Horizontal Irradiance [W/m^2]
$DNI =$ Direct Normal Irradiance [W/m^2]
$DHI =$ Diffused Horizontal Irradiance [W/m^2]
$\theta_s =$ Solar zenith angle [DD]

A priori, three of the four variables are unspecified. For this reason, an alternative decomposition model should be pursued that estimates one of the irradiances. There are several methods of different application complexities that require different input values, such as Reindl, Posadillo, or Boland (Gueymard, 2010). In contrast to the data available from the weather stations, it was decided to use the DIRINT method. This procedure is an improved version of the DISC method developed by Pérez *et al*. (1988, 1990, 1991) by the American Society of Heating, Refrigerating and Air-Conditioning Engineers (ASHRAE). This method is used and supported by other institutions such as the National Aeronautics and Space Administration (NASA) and the National Oceanic and Atmospheric Administration (NOAA). In addition, SAM software recommends using it in case there is only the GHI.

Its implementation is realised with MATLAB in interpolation code (Appendix III.3). The function used to execute the DIRINT method is from Sandia National Laboratories (SandiLabs), a laboratory conducted by the U.S. Department of Energy's National Nuclear Safety Administration (Sandialabs, 2016; GitHub, 2022). Note that the code has been reviewed and verified by comparing it with their extensive mathematical development (Maxwell, 1987). As can be extrapolated in the implemented code, a supplementary problem arises since the DIRINT model needs the solar zenith angle. NOAA proposes a method for estimating the solar zenith angle based on geographic coordinates and time of day (NOAA, 2022; US, 2022). Its development is integrated into the MATLAB code and the function that executes the model is also attached to the MS One Drive folder.

3.5.2 Granadella wind speed at 10 metres

In the Earth's crust, the wind speed increases as the altitude rises, as the surface causes friction. The wind direction is considered to be constant. The mathematical representation of this natural phenomenon is the vertical profile of the wind and can be modelled by a variety of mathematical formulas of different complexities, such as Monin-Obukhov (1954), Sathe *et al.* (2010), etc. The exponential profile is used (formula 4) since it is one of the most frequently used methods in the problems related to the production of renewable energy (Díaz & Manuel, 2013). The logarithmic method is also commonly used, but it is not as conservative due to significantly higher values being obtained.

$$V_z = V_{ref} \cdot \left(\frac{Z}{Z_{ref}}\right)^{\alpha} \tag{4}$$

V_{ref} = Known speed value [m/s]
Z_{ref} = Sampling height [m]
V_z = Calculated speed value [m/s]
α = Wind shear exponent [-]

Generally, it is recommended to use this formula when two samples are available from the same point at different heights at the same instant of time (Diego, 2013). Consequently, the wind shear exponent can be estimated. This value parameterizes the roughness of the sampling terrain. The most irregular surfaces will have a greater influence on the wind speed, attributing a higher value of α (Bratton & Womeldorf, 2011; Sciencing, 2020). However, the measurement is only available at a single height of 2 m. For this reason, in Appendix II.2, the coefficient is calculated from empirical tables that assign a value based on the characteristics of the surrounding area.

3.6 Analysis of the natural resources available with the Cervià data obtained

With the data consolidated, the feasibility of the three previously chosen types of renewable energy is studied. The natural resources and relevant conditions presented at the location are meticulously studied with the previously interpolated data. Furthermore, depending on the assessment obtained, it is determined whether the installation is attainable to exploit the relevant energy resources.

3.6.1 Solar resource availability

Photovoltaic panels are responsible for capturing solar radiation and transforming it to direct current (DC). Figure 16 represents the grid configuration of the components of a PV installation. The DC is transferred directly to the inverter where it is converted to alternate current (AC). Among the grid and these elements, there is the metre to control the production, electricity consumption, and the amount of energy that would be injected into the grid in the case of surplus. (Altas & Sharaf, 2014).

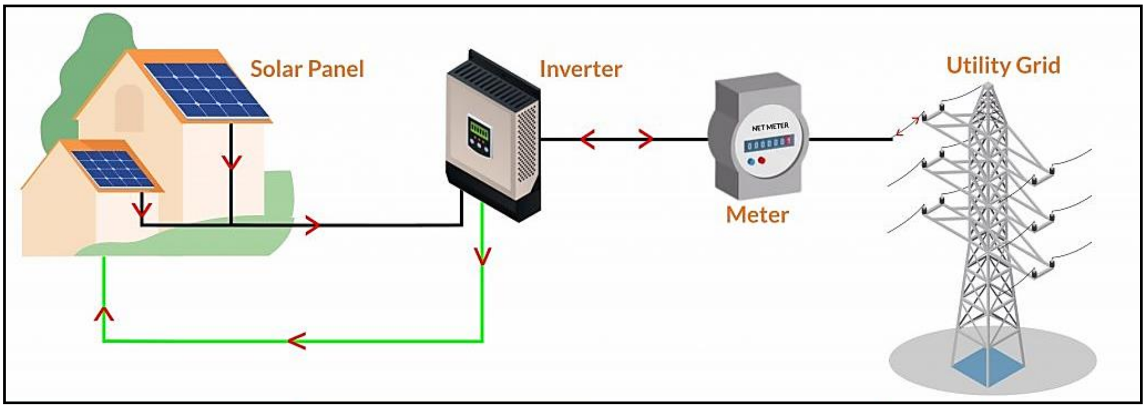

Figure 16. Simplified connection diagram of a typical photovoltaic installation. (Solar Power, 2021).

There are various factors to evaluate when choosing the right module model. Logically, the main climatic factor that will determine the production is solar irradiation. With the data for 2020 and 2021, it is calculated that over a year (8760 h), there are 4603 hours of sunshine. Figure 17 describes the temporal distribution of the variable during 2020 and 2021, using daily averages and the maximum value. The MATLAB code used is attached in Appendix III.4 and in MS OneDrive folder.

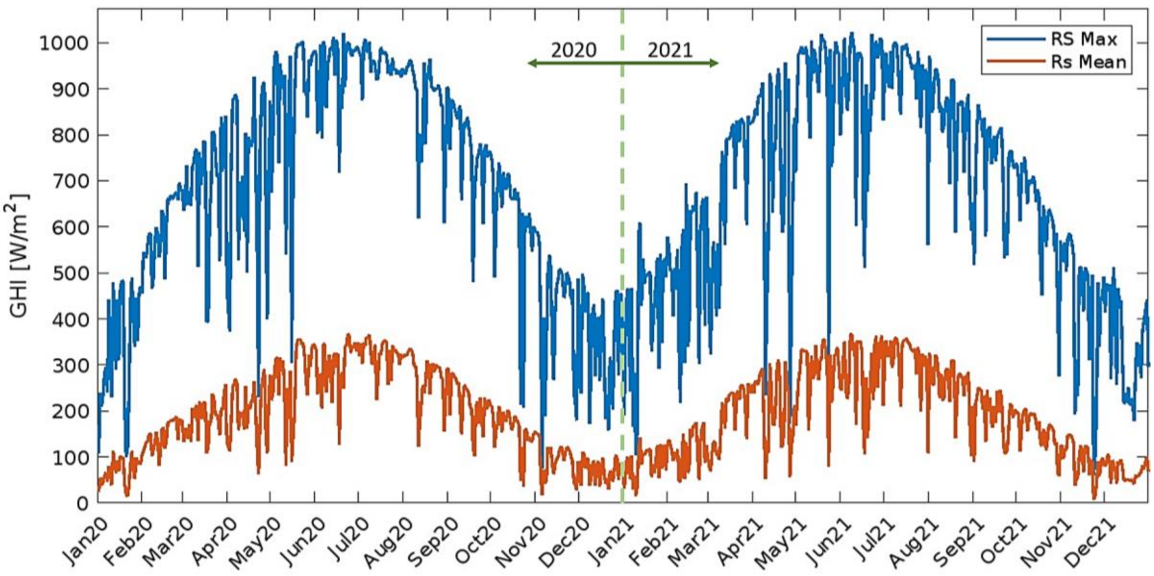

Figure 17. Daily GHI measurements in Cervià (2020-2021). (Author's own, adapted with MATLAB).

The annual average could be considered low, but it should be noted that the total calculation also assumes the night hours. Logically, due to the location of Cervià, the variable increases during the three months of summer and gradually decreases until it reaches its minimum in the middle of winter. There are several sharp fluctuations, mainly in the spring and afternoon. They probably represent cloudy and rainy days. For a more comprehensive analysis of the values obtained, simple statistical calculations are performed, comparing values such as the median, standard deviation, or coefficient of variation (Table 7).

Table 7. Annual solar radiation statistics for Cervià

	2020	**2021**
Average [W/m^2]	193.23	188.92
Median [W/m^2]	5.19	5.14
Maximum value [W/m^2]	1021.60	1023.20
Average of Daily Maximum [W/m^2]	680.26	675.69
Standard deviation [W/m^2]	276.30	273.23
Coefficient of variation [%]	142.99	144.62

(Author's own, adapted with MATLAB).

Firstly, from Table 7 it can be extracted that the variability between two consecutive years is numerically negligible. The median is positive, reaffirming that there are more hours of sunlight than darkness. In addition, the average obtained is approximately 190 W/m^2. According to the solar irradiation map of Spain (Figure 10), for its location, Cervià offers a range of [4.6 - 5.0] kWh/m^2. Performing the correct conversion factors, the value with the interpolated Cervià average is 4.59 kWh/m^2. The value is out of range but could be considered numerically sufficient close, validating and approving it.

The irradiance is approximately 1,675 kWh/m^{2}yr, which with the characteristics of the roof has a potential of 5,026 MWh/yr. Applying a common efficiency of solar panels (20%; adapted from SunPower Residential, 2021) and calculating that 1/3 of the roof was covered, an estimated production of 335 MWh/yr is obtained.

On the other hand, the other variable that characterises the operation and performance of PV panels is temperature. The Cervià region is relatively hot, and the optimal conditions for the operation of the modules are 25ºC or lower. The datasheets specify coefficients as a function of temperature. For example, a typical efficiency value would be -0.3%/ºC (adapted from Europe-solarstore.com, 2015). Figure 18 offers the daily averages and their maximum values during 2020 and 2021, representing only the hours when there was solar irradiance.

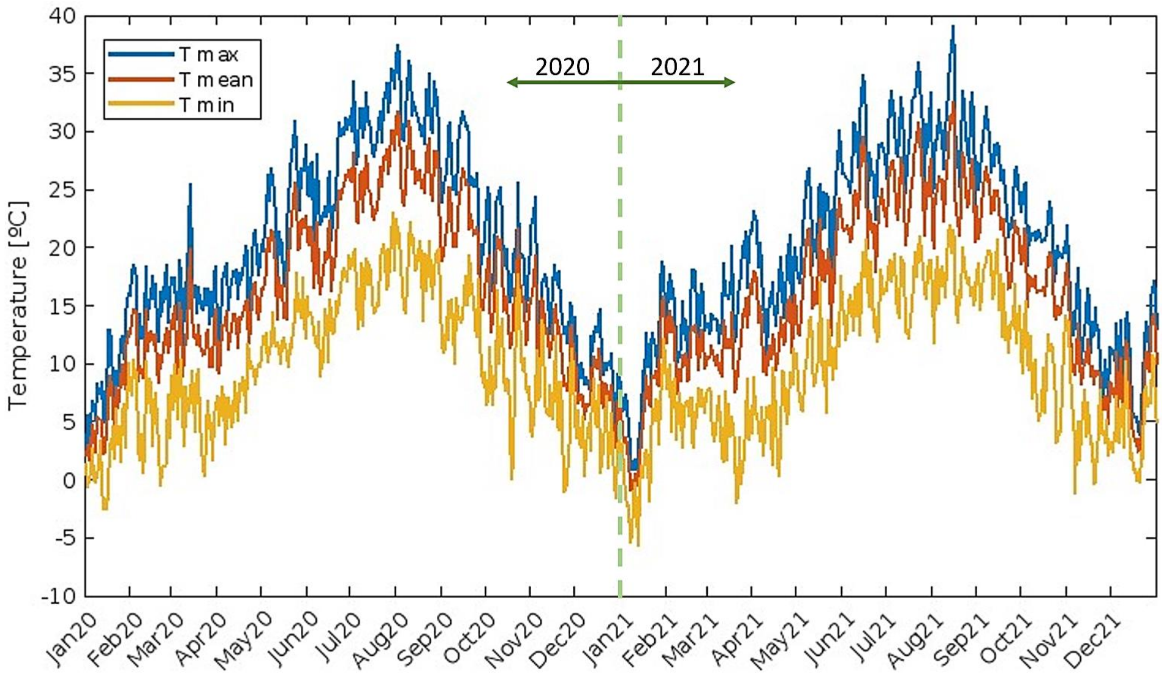

Figure 18. Daily temperature measurements in Cervià during sunlight hours (2020-2021). (Author's own, adapted with MATLAB).

Logically, winters are the coldest time of year, and summers are hot, representing a temporary distribution of similar temperatures between the two years. Examining the daily average, it can be seen that there are a few days in the year that exceed 25ºC. It is calculated that only 52 days a year have an average of more than 25 ºC. Precisely, it is computed that of the 4603 hours of sunshine in Cervià, 3664 hours do not exceed 25ºC at any time. Therefore, despite representing a warm location, the assessment for the installation is favourable due to the suitable conditions of the zone.

3.6.2 Wind resource availability

The operation of the wind turbine is reasonably simple. The incident wind moves the blades of the wind turbine which, with a mechanical multiplier system, transmits the energy to the generator (Zbigniew Lubosny, 2003). Once the electricity has been generated, it follows the same structure as with the PV panels (Figure 16). Currently, there are two types of wind turbines, the vertical and the horizontal axis. As mentioned in section 2.5.3, due to the characteristics and location of the project, a domestic turbine must be installed to avoid creating a visual impact and vibrations. Moreover, it is recommended to install the wind turbine at least 10 metres above any obstacle to be able to operate at the speed needed by the generator to produce the constant power for which it was designed (nominal or rated speed). Vertical axis turbines are well-integrated into landscapes and have the advantage that they are always aligned with the wind without matter the direction. (Juan *et al.*, 2015).

Likewise, it is only necessary to study the wind speed obtained in Cervià. As with solar energy, the availability of the natural resource is analysed comprehensively. Figure 19 represents the distribution of the variable during the years 2020 and 2021, using daily averages and the daily maximum and minimum values. The code MATLAB used in this section is attached in Appendix III.5 and in MS OneDrive folder.

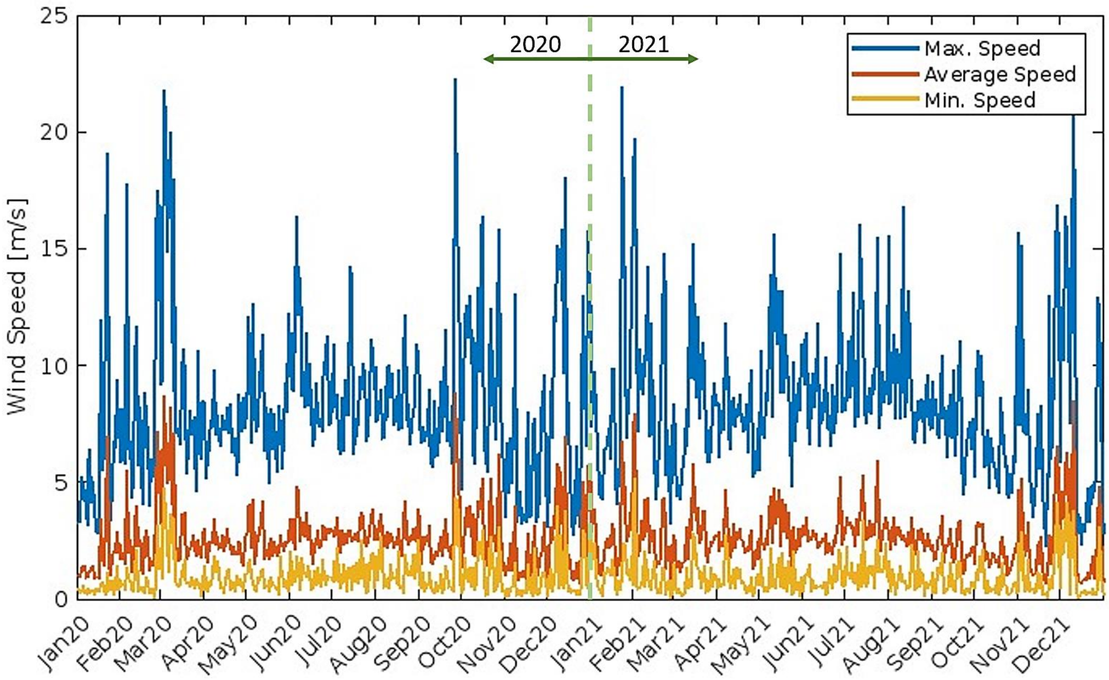

Figure 19. Daily wind measurements in Cervià (2020-2021). (Author's own, adapted with MATLAB).

As can be extracted from Figure 19, as with temperature and solar radiation data, the two years are resemblant. Although they have a relatively higher daily average in summer, the strongest gusts occur during the rest of the year. The average is more proximate to the minimum than the maximum, indicating that strong wind gusts are not lasting. Moreover, the maximum values are almost identical. To analyse the variable in more detail, the statistical procedure is performed in Table 8.

Table 8. Annual wind speed statistics for Cervià

	2020	**2021**
Average [m/s]	2.6052	2.6325
Median [m/s]	2.3271	2.4092
Maximum value [m/s]	22.269	22.3344
Minimum value [m/s]	0.0549	0.0548
Average of Daily Maximum [m/s]	4.9719	5.0546
Standard deviation [m/s]	1.6771	1.5881
Coefficient of variation [%]	64.3726	60.3256

(Author's own, adapted with MATLAB).

The statistical values reaffirm that the variability from one year to another is low between contiguous years and that the choice of the year is indifferent to performing the study. The average is approximately 2.6 m/s. Nevertheless, the map of the average annual wind speed (Figure 11) indicates that an average range of [5.5-6.0] m/s (at 80 m high) should theoretically be obtained for Cervià. If the wind profile formula used in section 3.5.2 is applied (alpha = 0.2), in Cervià a value of 3.9 m/s is calculated. The value is significantly lower than expected. In case, the interpolation process is meticulously reviewed and the data obtained is manually compared with the data of the three locations without encountering any errors. The other stations have similar statistical values. For example, Ulldemolins is the weather station with a higher average wind speed, with a value of 2.9496 m/s. Additionally, a momentary arbitrary simulation with SAM using the created wind data file and a domestic turbine is executed. The output power obtained is about 1.500 kWh/yr and the capacity factor is 2%. It corroborates the infeasibility of installing a wind turbine with the desired characteristics since the normal capacity factor of wind energy is 20% (Boccard, 2009).

Due to the values obtained, a detailed wind turbine study is accomplished by comparing the different types, manufacturers, models, and characteristics. Although they admit a high range of different speeds, it is observed that the nominal speeds of the devices are significantly higher than the average obtained in Cervià. Figure 20 indicates the shape of the typical power curve of a wind turbine with the specific values of three domestic turbines suitable for installation. Note that the ST-1000 is not a vertical axis turbine but is one of the turbines with the lowest nominal speed value on the market.

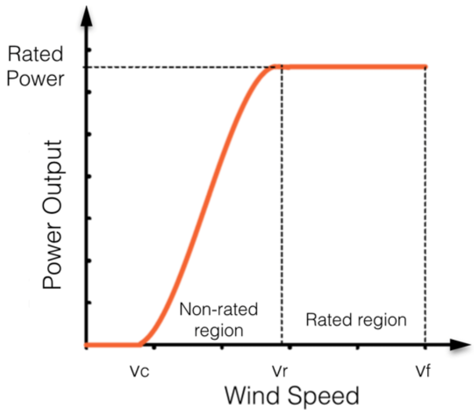

Model	Rated power [W]	Cut-in speed (Vc) [m/s]	Cut-off speed (Vf) [m/s]	Nominal speed (Vr) [m/s]
Aeolos-V 300w	300	1.5	50	10
DS700	700	2.2	15	12
ST-1000	1000	1	20	7.55

Figure 20. Typical power curve and comparison between three domestic wind turbines. (Elsevier (2017); Hi-vawt (2012); Bauer (2018)).

Considering the average wind speed, it is estimated that the wind turbine would generally start but operate in the non-rated region. Observing the maximum daily values in Figure 19, it is appreciated that the wind speed should reach these values constantly for the correct operation of the turbines. Additionally, the value of the standard deviation confirms that the data is close to the measure of the mean. Despite obtaining a high coefficient of variation, assuming the data for 2020 and 2021, the annual number of hours where the wind was higher than 7.55 m/s was only 143 h (one year has 8760 h). Despite this conclusion, if the values were more favourable than one during the night than during the day (Table 9), it may be appropriate to consider the installation for some energy flexibility.

Table 9. Annual wind speed statistics for Cervià during the hours without sunlight

	2020	2021
Average [m/s]	2.2882	2.2977
Median [m/s]	1.9676	2.0981
Maximum value [m/s]	20.2022	16.9284
Minimum value [m/s]	0.0775	0.0639
Average of Daily Maximum [m/s]	5.6857	5.9857
Standard deviation [m/s]	1.4694	1.4167
Coefficient of variation [%]	65.4928	61.6573

(Author’s own, adapted with MATLAB).

During the hours when there is no solar radiation, even less advantageous statistical values are obtained, such as the mean and median values. The data is similar during the day and night, indicating that it is not appropriate either. Although the daily averages of the values are slightly more elevated, generally the maximums and minimums of the day do not occur during the night. For these reasons, it is concluded that it is not reasonable to install a wind turbine at the project's location. The wind speed is almost not enough to start rotating the turbine and would cause it to work in an inefficient area. The decision will significantly reduce the centre's energy flexibility because it will primarily use solar energy and, when demand necessitates, the biomass boiler.

Notwithstanding, as mentioned in section 1, the town hall would desire an integrated energy centre. As a consequence, a viable and innovative alternative is proposed that could be considered in the future but will not be studied in detail. Possibly an avant-garde option would be to install the so-called "wind tree". This is a new silent wind turbine that, as its name suggests, has the silhouette of a tree (Figure 21), which is composed of 72 vertical conical turbines representing the leaves. Its dimensions are comparable to those of a standard tree (11 m high and 8 m of diameter) (New World Wind, 2019). The power with the standard turbines is approximately 3kW, but it permits more productive ones to be installed, increasing it to practically 11kW. It is designed to be installed inside cities, being able to generate current with an irregular light breeze of 2 m/s (Barber, 2017).

Figure 21. Wind tree created by the French company New Wind. (Emeara *et al.*, 2021).

3.6.3 Biomass feedstock availability

There are numerous types of boilers with different characteristics, but they all have the same basic principle as a conventional thermal power plant. Biomass is used to generate steam to move the turbine that is connected to the electric generator. Electricity from this resource is valuable because it can be adjustably generated when it is needed. Regarding the weather conditions, none of them directly affect the operation and specific performance of the boiler. Nevertheless, temperature affects energy consumption indirectly. Relative humidity, temperature, and pressure influence the drying of the feedstock.

As mentioned in section 2.5.4, the amount of agricultural waste calculated was the theoretical optimum that could be obtained based on the hectares of land. However, in order to adapt the values to reality and as required by SAM, a percentage called Resource Obtainability is applied. Leveraging the values in Table 2, Table 10 is created to represent the practical biomass data. A breakdown of the calculations of the biomass quantities is attached in Appendix II.6.

Table 10. Cervià's estimated annual biomass production

Crop type	**Cervià's optimum dry production [t/yr]**	**Resource obtainability [%]**	**Cervià's estimated dry production [t/yr]**	**Cervià's estimated energy production [MJ/yr]**
Forest	155,940.40	0	0.00	0
Grain	8.54	2	0.02	290
Vineyards	13.01	5	0.65	7,808
Olive	711.48	5	35.57	426,888
Orchards	275.00	5	13.75	164,997
Olive Pit	1,275.00	70	892.50	17,562,615
Almond Shell	85.00	70	59.50	1,120,266
Total	158,308.43	-	1,001.99	19,282,864

(Autor's own, adapted from Table 2).

SAM offers a typical value of 10%. Even though there is a considerable amount of forest waste, a 0% is assigned to resource obtainability as the clearing of woodlands is performed sporadically by the Generalitat de Catalunya and it would not be feasible to profit from this resource (Departament d'Acció Climàtica, Alimentació i Agenda Rural, 2019). Furthermore, grain is indicated at 2% because it is generally considered that farmers generally use it to make straw. On the other hand, for the Camp Cooperative's resources, an elevated value of 70% is assigned to reflect the high viability that it entails.

Therefore, it is estimated that most of the resources obtained would come from olive pits. This biomass resource has excellent qualities as 2 kg is equivalent to approximately one litre of diesel. Additionally, with 1 kg, it is estimated that it can produce 4.47 kWh (gross), obtaining a considerable energy potential that will possibly exceed solar production. (Lett & Ruppel, 2004; Pellets del Sur, 2020).

The number of biomass tonnes obtained needs a large amount of storage space that will have to be strategically distributed within the industrial buildings. Considering that the warehouses are 5.5 metres high, it is estimated that the 1,002 tonnes will require at least 816.3 m^2 of space because, as Jamileh Shojaeiarani *et al.* argue (according to Mani *et al.*, 2004), a common density is 0.3 tonnes/m^3. For the calculations, a height of 4.5 m has been considered due to it is not recommended to accumulate elevated amounts of biomass (Gobierno de España Ministerio de Industria, Turismo y Comercio, 2007). Moreover, to understand its temporal distribution, the collection times and drying times in Table 2 are analysed (Figure 22).

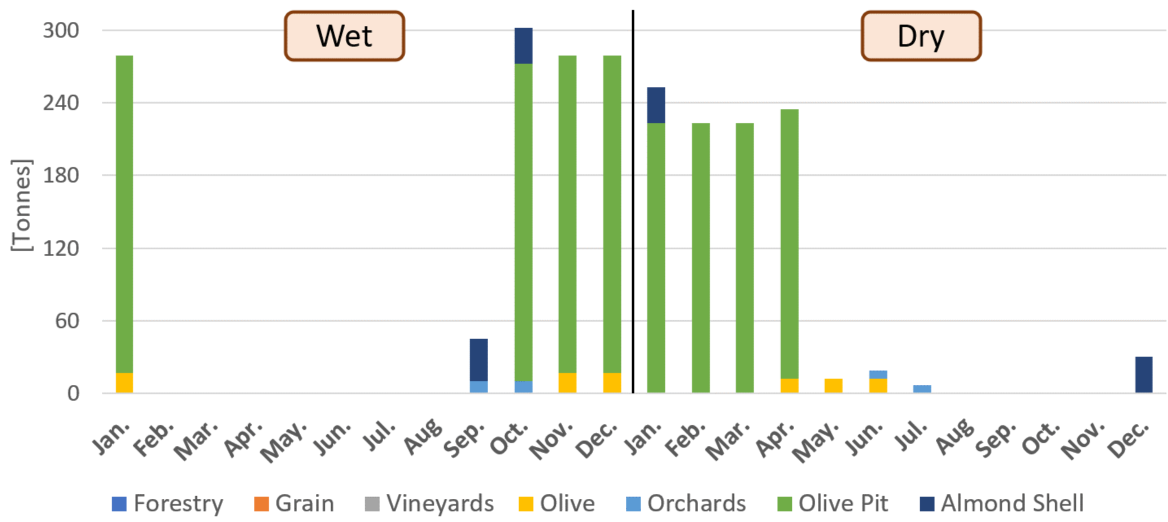

Figure 22. Monthly estimated distribution availability of wet and dry Cervià's biomass. (Author's own).

From Figure 22, it is appreciated that there are noteworthy collection periods as almost all the biomass comes from the same resource, the olive pit. Regarding the dry resource, it is considered only the generated amount without counting the accumulated. Applying the corresponding drying months, most of the resources are obtained from December. However, during the summer and autumn months, no inbound resources are available, but the warehouses for feedstock are considered to be manageable in order to have biomass functional throughout the year.

Finally, the 1002 tonnes would provide 19,282,864 MJ/yr obtainable, which signifies a large amount of annual energy available. Theoretically, by applying the corresponding conversion factor, the harvestable biomass would have 5,356 MWh/yr available. According to the IEA (2015), a typical electrical efficiency is 30%, theoretically obtaining 1,607 MWh/yr. This amount of energy would supply the integral centre of renewable energy and also generate a surplus to compensate for the other municipal facilities.

3.7 Demands and consumption of energy in the village

To model the economic analysis, it is essential to know approximately the energy costs of the village to have a reference point of the consumption to cover. The city council facilitates the annual economic consumption of municipal facilities, the contracted power and their corresponding prices. Unfortunately, a detailed time decomposition of consumption is not available. Consequently, the different electricity price rates cannot be applied according to the time slot (attached in Appendix I.5). The energy timetables group the 24 hours of the day into three-time bands according to supply and demand; peak (expensive), flat (intermediate) and off-peak (cheap). For the performance of the calculations, the intermediate cost has been taken into account to minimise errors. Table 11 indicates the annual results of the energy calculations of the public facilities developed in Appendix II.5.

Table 11. Annual energy calculations of public facilities without the renewable energy centre

Import [€/yr]	**Contracted power [kW]**	**Tax (VAT, 21% BI) [€/yr]**	**Electricity Tax (0,6% BI) [€/yr]**
28,412.48	132	4,906.76	140.19
Rental meters [€/yr]	**Power Import [€/yr]**	**Consumption Import [€/yr]**	**Power Consumption [kWh/yr]**
17.96	1928.33	21419.24	228948.07

(Author's own, adapted from City Council of Cervià de les Garrigues 2022, personal communication, 25 January).

On the other hand, although attempts will be made to maximise power production to market surpluses, the approximate reference for renewable energy centre consumption should also be considered. The consumption that the installation will demand has been estimated considering its infrastructural characteristics and the uses that it will conceive (25,000 kWh/yr). The consumption involved in the installation of the inverters and the energy production systems is not yet considered since it will be simulated by SAM.

With the assistance of tutor Dr. Antonio Palau Ibars, a monthly categorisation has been completed to be able to perform the SAM simulation (Figure 23). The detailed procedure is in Appendix II.7. Basically, the periods of use of each municipal facility and the use that is granted to them have been considered. For example, logically, the municipal swimming pools have their consumption mostly during the summer while the school consumes more during the class months, especially in winter due to the heating.

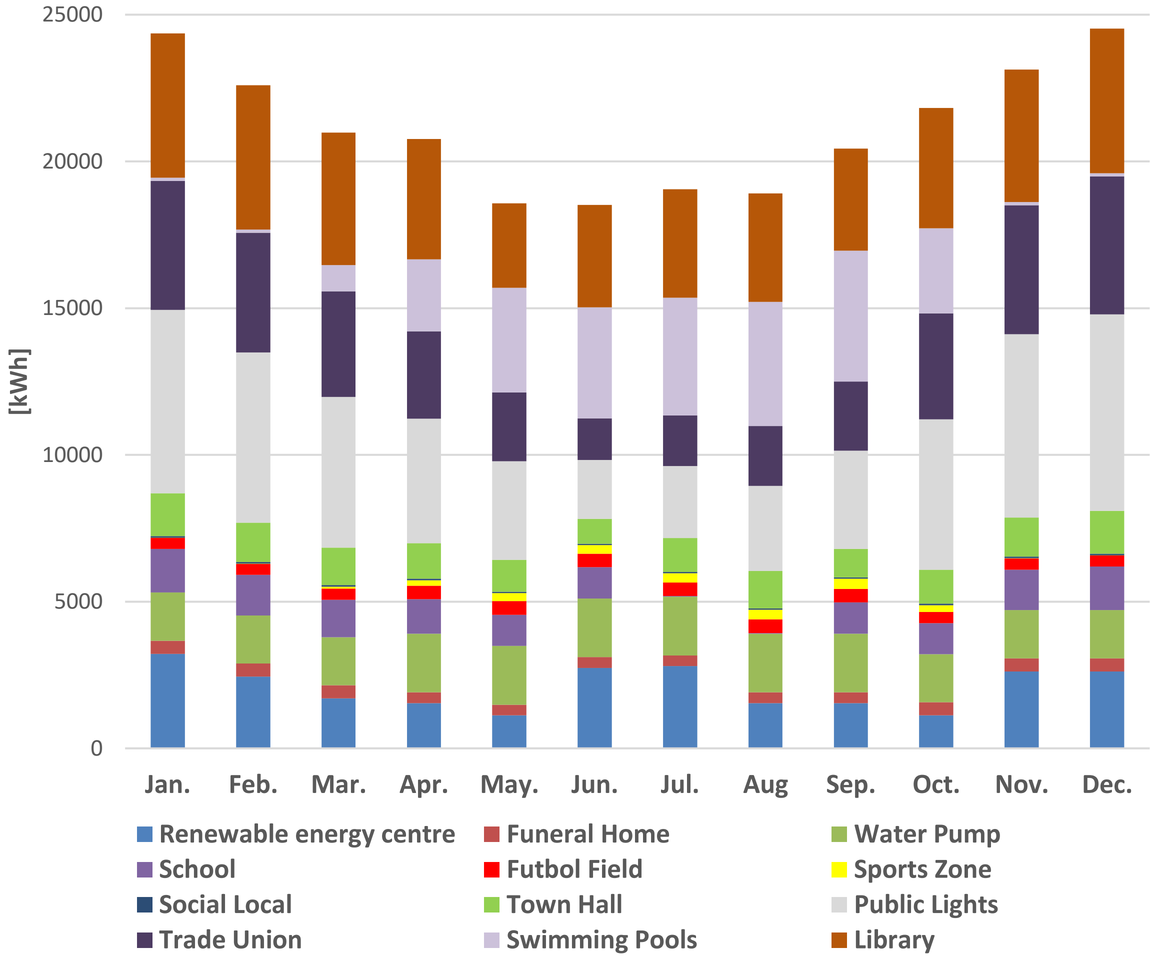

Figure 23. Monthly estimated public electricity demand in Cervià. (Author's own).

As can be remarked from Figure 23, the most elevated annual consumption comes from street lighting and the library. During the summer months, the municipal swimming pools predominate, while the town hall remains almost constant throughout the year. It is estimated that the renewable energy centre will have higher consumption during the summer when people have more leisure time and during the winter due to the consumption of heating.

4 System design simulation with SAM

The installation will not be an autonomous system as it will be connected to the mains to be able to export excess electricity. Additionally, at times when demand requires it, the energy of the distribution company will have to be consumed due to the installation cannot be left without supply. The two types of renewable energy are analysed and designed individually, considering at all times the technical specifications of the simulation software.

Section 4.1 details the PV simulation, while section 4.2 explains the biomass boiler performance. Note that in both cases, the modelling uses the same Weather data file created in section 3.5. Only the different components of the system required are explained without detailing the financial analysis as it is accomplished in the thereafter section 5.

4.1 Photovoltaic system

As mentioned previously in section 2.4, there are three adjacent industrial buildings with an area of about 3000 m^2 facing SE. Despite the construction problem of the asbestos, the study will be calculated considering the roof is already repaired and in satisfactory conditions for the installation of this technology (explained in section 6.3).

For solar energy simulation, the software requires several inputs classified into 7 sections (Table 12). Accordingly, the PV module and the inverter to be used must be determined. Although the program permits manually entering the characteristics of the elements, components that appear in the libraries will be selected to accelerate the simulation. In addition, it is considered that electric companies will not impose any grid limits.

Table 12. Required inputs to the software for the energy simulation of the PV system

Section	Summary
Location and Resource	The weather data file to be used is selected. Then the DNI from GHI and DHI is specified. It allows visualising graphs of the meteorological variables.
Module	The photovoltaic panel specifications are documented. SAM offers libraries that automatically fill in values or the option to enter them manually one by one.
Inverter	The inverter specifications are documented. SAM offers libraries that automatically fill in values or the option to enter them manually one by one.
System Design	The system is dimensioned by specifying the number of panels, inverters, the number in each subarray, their orientation and the land area.
Shading and Layout	Allows creating a 3D model to calculate external shadows, such as buildings, trees, etc. The snow loss option can also be activated.
Losses	All types of losses are defined (irradiance, DC, AC, transformer, etc.) SAM gives default values of most values.
Grid Limits	It is specified in case of a power limit of interconnection with the electric company

(SAM Help's System, 2022).

As can be realised from Table 12, the system must also be specifically designed and dimensioned, calculating the exact number and models of components. In addition, the minimum distance between the panels will be estimated based on the shades of the roof (section 4.1.2) and their shadows (section 4.1.3). Appendix V.1 offers all the variables entered that are used in the program to model the PV system. Moreover, note that SAM offers an instruction manual for the simulation of solar technology (Gilman *et al*., 2018).

4.1.1 Selection of the photovoltaic panel

Nowadays, there are three types of PV panels on the market based on their silicon purity. Monocrystalline is the purest and, consequently, the most powerful and efficient (between 15% and 24%). Despite being the most expensive type, they can operate in low light and tolerate reasonably elevated temperatures. On the other hand, polycrystalline has an efficiency range of 13-16% and is more sensitive to temperatures higher than 25ºC. Finally, amorphous panels are the simplest and most inexpensive. Its useful life is brief and its efficiency is 7%-13%. (Ammar & Dulaimi, 2018).

Due to their appropriate characteristics, the monocrystalline panels are chosen. This type offers a variety of models. Table 13 recapitulates a selection of frequently used models in facilities with features such as this project.

Table 13. Adequate PV panels for an installation with the characteristics of the project

Manufacturer	Model	Efficiency [%] [1]	Temperature Coefficient [% W/ºC] [1]	Peak Power [W]	Long [m]	Width [m]	Cost [€]
AUO SunForte	PM096B00	20.3 %	-0.38	330	1.559	1.046	320
SunPower	MAXEON 3 - 400	22.6	-0.29	400	1.690	1.046	346
SunPower	MAX3-370	20.9	-0.35	370	1.690	1.046	304
REC Solar	Alpha- REC380AA	21’7	-0.26	380	1721	1.016	265
LG Neon R	LG360Q1C-A5	20.8 %	-0.37	360	1.700	1.016	296
SHARP	NQ-R256A	19.8 %	-0.377	256	1.318	0.980	204
Panasonic	VBHN330SJ53	19.7 %	-0.258	330	1.590	1.053	222
Panasonic	VBHN325SJ53	19.4 %	-0.258	325	1.590	1.053	209

1. Measured at optimal conditions (irradiance of 1000 W/m2, 25ºC).

(Adapted from Solarelectricsupply.com, 2014; Europe-solarstore.com, 2015; SunPower Residential, 2021).

The MAXEON 3-400 and Alpha-REC380AA were chosen since they present better efficiency and an impressive power value. The technical specifications of the datasheet are attached in Appendix IV.1 and IV.2. A priori, the SunPower solar panel is more convenient, but it has a worse temperature coefficient and there is a noticeable economic difference between them. For this reason, section 4.1.4 calculates how many modules could be placed and what would be the maximum theoretical power generated in both cases. Contrasting this value with the price will determine which one will be selected.

4.1.2 Calculation of shades generated by roofs

Attending the location of the installation (Figure 7), it can be perceived that no element around it can cast shadows on it. For this reason, the roof itself is first analysed in order to dimension the PV installation. As can be observed in the 3D rendering in Figure 24, each industrial building has its gabled roof. Therefore, the roofs are triangular and an occasional penumbra can occur between them. Moreover, they have been coloured, and a plan view is attached with the assignment of a name to facilitate the subsequent discernment.

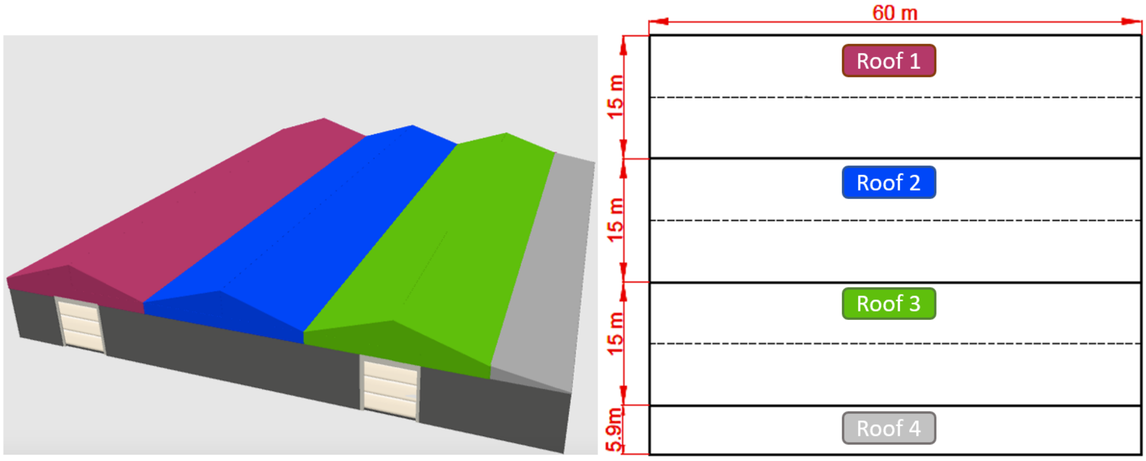

Figure 24. 3D view and floor plant of the installation.
(Author's own, adapted with Sweet Home 3D and AutoCAD).

As can be detected in Figure 24, Roof 3 has an extension (Roof 4). In addition, the first three roofs are identical, with an angle of inclination of 19 degrees and an area of 468 m^2. Roof 4 (facing SE) has a slope of 10º and an area of 360 m^2. To facilitate the understanding of the roofs, the profile view is also attached (Figure 25). In addition, to aid comprehension, the roof names are abbreviated to R1, R2, R3, and R4.

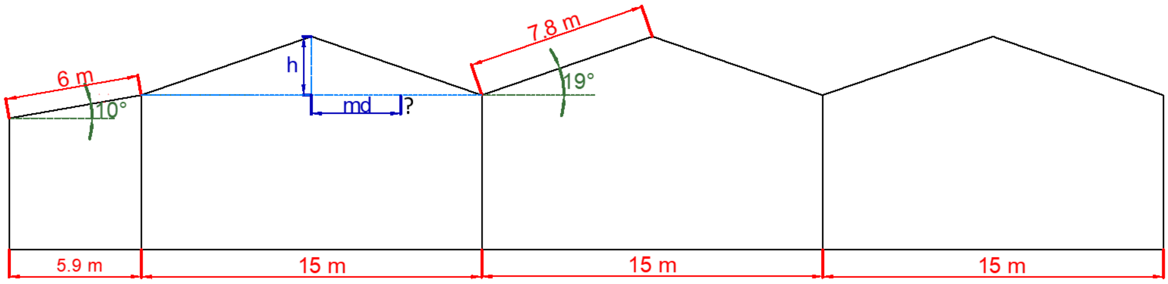

Figure 25. Section plan of the warehouses. (Author's own, adapted with AutoCAD).

Basic trigonometry is applied to estimate the shades that can be produced by the triangular profile of the roof. Furthermore, the formula provided by the Institute for Diversification and Energy Saving (IDAE) is used to calculate the minimum optimal separation distance between them (IDAE, 2011). Logically, due to their form and orientation, the R4 and R1 will not produce any umbra on their adjacent roof. Accordingly, the calculations will be performed for R3 (19º) which will also be used for R2:

$$sen(roof\ angle) = \frac{h}{roof\ length} \tag{5}$$

$$sen(19) = \frac{h}{7.8\ m} \rightarrow h = 2.5394\ m$$

$$Minimum\ distance\ (md) = \frac{h}{tg(60º - latitud)} \tag{6}$$

$$Minimum\ distance\ (md) = \frac{2.5394}{tg(60º - 41.4246)} = 7.55\ m$$

The minimum distance (*md*) obtained is bigger than the distance of the half of the roof (7.5m). Consequently, it is confirmed that, theoretically, panels can be installed on all four roofs, but a horizontal distance of 0.05m should be left at the bottom of the R1 and R2 roofs. Additionally, in the R1, R2 and R3, they will only be able to be installed in the halves facing the SE. However, it is recommended to leave a safety margin (at least 10%) to minimise shadows when the sun is at a low altitude angle, such as in winter, during sunrise or sunset. When distributing the panels, the remaining spaces will be considered and allocated strategically to fulfil this margin of safety.

4.1.3 Calculation of the shadows caused by the panels themselves

Firstly, the optimal tilt angle of the panels to have the maximum production according to the location of Cervià is studied. If the resulting value is excessively distant from the incline of the roof, support structures must be added to rectify the incline. The value depends on the latitude of Cervià and the azimuth of the panel (Figure 26). With Google Earth, the orientation of the three industrial buildings is determined, obtaining an azimuth angle of 42º.

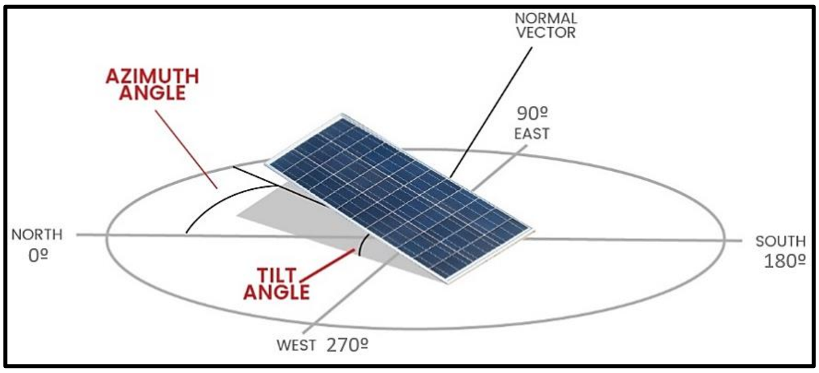

Figure 26. Tilt and azimuth angle clarification of a solar panel. (Adapted from Emeara *et. al*., 2021).

One of the agilest methods to calculate the optimum tilt angle is using the software developed by the European Commission Photovoltaic Geographical Information System (PVGIS; see: https://ec.europa.eu). It is paid software, but it offers a limited gratis version that calculates basic values (Europa.eu, 2016). By entering the coordinates and the azimuth angle of the installation, the software computes the most efficient angle (Figure 27).

Provided inputs:	
Location [Lat/Lon]:	41.425,0.865
Horizon:	Calculated
Database used:	PVGIS-ERA5
PV technology:	Crystalline silicon
PV installed [kWp]:	1
System loss [%]:	14
Simulation outputs:	
Slope angle [°]:	33 (opt)
Azimuth angle [°]:	- 42
Yearly PV energy production [kWh]:	1757.04
Yearly in-plane irradiation [kWh/m^2]:	2245.29
Year-to-year variability [kWh]:	47.74
Changes in output due to:	
Angle of incidence [%]:	-2.38
Spectral effects [%]:	0.98
Temperature and low irradiance [%]:	-7.69
Total loss [%]:	-21.75

Provided inputs:	
Location [Lat/Lon]:	41.425,0.865
Horizon:	Calculated
Database used:	PVGIS-SARAH2
PV technology:	Crystalline silicon
PV installed [kWp]:	1
System loss [%]:	14
Simulation outputs:	
Slope angle [°]:	38 (opt)
Azimuth angle [°]:	- 42
Yearly PV energy production [kWh]:	1566.58
Yearly in-plane irradiation [kWh/m^2]:	1988.74
Year-to-year variability [kWh]:	54.22
Changes in output due to:	
Angle of incidence [%]:	-2.69
Spectral effects [%]:	1.01
Temperature and low irradiance [%]:	-6.82
Total loss [%]:	-21.23

Figure 27. Optimum panel orientation calculated with ERA5 database (left) and SARAH2 database (right). (Europa.eu, 2016).

Remarkably, PVGIS has different databases and, depending on which is used, the resulting optimal angle is different. The result varies significantly between 33º and 38º depending on the library selected. The 38º option is preferred because, according to the EU Science Hub (2022), PVGIS-ERA5 was created for the Nordic countries with a latitude greater than 60º while PBGIS-SARAH2 is the right one for Catalonia. Moreover, to verify the values, an instantaneous arbitrary simulation is performed with SAM maintaining the Cervià meteorological data with all the parameters constant and changing only the inclination of the panel. Observing the results obtained, SAM confirms that 38º is the most productive position.

Consequently, having 10º and 19º roofs, supports must be used. The shadows that will appear between the modules and the inclined roof surface will have to be calculated. It is utilised the same procedure as section 4.1.2. Specifically, the process to calculate the minimum distance (*md1*) is performed for the SunPower MAXEON 3-400 model:

$$cos(tilt\ angle) = \frac{dx}{panel\ length} \rightarrow\ cos(38) = \frac{dx_1}{1.046\ m} \rightarrow dx_1 = 0.8243\ m \qquad (7)$$

$$sen(tilt\ angle) = \frac{h}{panel\ length} \rightarrow\ sen(38) = \frac{h_1}{1.046\ m} \rightarrow h_1 = 0.6439\ m \qquad (8)$$

$$d = \frac{h}{tg(60º - latitude)} \rightarrow\ d_1 = \frac{0.64398}{tg(60º - 41.424637)} = 1.9164 \qquad (9)$$

$$md_1 = dx_1 + d_1 = 2.7407\ \ m \qquad (10)$$

In Appendix II.3, the same procedure is performed for the Alpha-REC380AA. It only changes the dimensions of the PV panel, obtaining a minimum distance (md_2) of 2.6621 m. Those measures are in case they are installed on a completely flat surface. For this reason, the distance on the inclined plane on which the shadow is projected must be calculated. As represented in Figure 28, the distance (*D*) will be less than the minimum distance (d_1) previously calculated for each PV panel length (d_2). It will vary depending on the angles of the roofs (α) and the panels (β) inclination. Using the cosine and Pythagorean theorems, a system of 6 equations with 6 unknowns is raised to calculate all the segments of Figure 28:

$$D^2 = \ (d_1 - x)^2 + y^2 \qquad (11)$$

$$z^2 = \ x^2 + y^2 \qquad (12)$$

$$d_3^2 = d_1^2 + d_2^2 - 2 \cdot d_1 \cdot d_2 \cdot \cos(\alpha + \beta) \qquad (13)$$

$$D^2 = d_1^2 + z^2 - 2 \cdot d_1 \cdot z \cdot \cos(\varphi) \quad (14)$$

$$y^2 = x^2 + z^2 - 2 \cdot x \cdot z \cdot \cos(\varphi) \quad (15)$$

$$y^2 = d_1^2 + D^2 - 2 \cdot d_1 \cdot D \cdot \cos(\alpha) \quad (16)$$

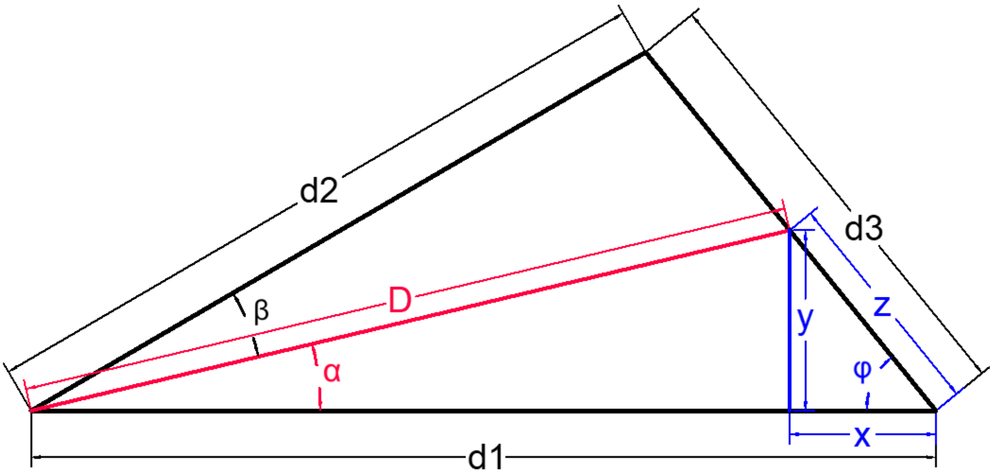

Figure 28. Illustration of the shadow produced by PV panel on a sloping roof.

(Author's own, adapted with AutoCAD).

To solve it efficiently, the equation system is introduced in MATLAB. The results obtained are shown in Table 14. The code MATLAB used in this section is attached in Appendix III.6 and in MS OneDrive folder. The data obtained from the minimum distance on the inclined surface will permit calculating the total number of solar panels that can be installed. Consequently, depending on their characteristics, the installed power and the cost of the investment, it will be decided which one is considered more adequate.

Table 14. Minimum distances between rows of PV panels in the installation

Model	Roof	Panel length [m]	Minimum horizontal distance [m]	Minimum inclined distance [m]
MAXEON 3 - 400	R1, R2, R3	1.046	2.74073	1.4501
	R4	1.046	2.74073	1.5132
Alpha- REC380AA	R1, R2, R3	1.016	2.66212	1.4070
	R4	1.016	2.66212	1.4671

(Author's own, adapted with MATLAB).

4.1.4 Distribution of the panels

To calculate the distribution of the panels, it is necessary to consider the dimensions of the roof and those of the PV modules. The three halves of the R1, R2 and R3 where it is feasible to install them are 60 m x 7.8 m each. R4 is 6 m x 60 m. The physical characteristics of the models to be studied are in Table 13. Additionally, the maximum number of modules that could be fitted in both cases is indicated.

Table 15. Maximum number of PV panels rows in the installation

Solar Panel Model	Weight [kg]	Width [m]	Max. of panels per row R1, R2, R3, R4	Minimum inclined distance R1, R2, R3 [m]	Max. rows R1, R2, R3	Minimum inclined distance R4 [m]	Max. Rows R4
MAXEON 3 - 400	19	1.690	35	1.4501	5	1.5132	3
Alpha-REC380AA	19.5	1.721	34	1.407	5	1.4671	4

(Author's own).

As can be seen from Table 15, the maximum number of panels is practically the same as their dimensions are nearly identical. However, the maximum number cannot be applied because certain spacing must be designed between them to prevent malfunctions. Furthermore, it is recommended to leave at least 0.5 m at the edges of the roof and a margin of error (at least 10%) in the minimum distance required by the shadows. Therefore, applying these conditions, the distribution in Table 16 is obtained.

Table 16. Optimal calculated PV panels distribution in the installation

Solar Panel Model	Nº of panels per row R1, R2, R3, R4	Nº of rows R1, R2, R3	Nº of rows R4	Nº of total panels	P_{max} / panel [W]	Panel price [€]	Installed Power [W]	Total cost [€]
MAXEON3-400	34	4	3	510	400	346	204000	176460
Alpha-REC380AA	34	4	3	510	380	265	193800	135150

(Author's own).

The installed power between the two options could be considered similar, but the price difference is substantially notable. Moreover, the temperature coefficient of the Solar Rec is slightly more optimal. As demonstrated in section 3.6.1, Cervià is in a relatively warm area, with an average of 52 days/yr with a more elevated temperature of 25ºC (considering the hours of sunlight). For these reasons, Alpha-REC380AA panels were selected. Additionally, Rec Solar manufacturer offers a 20-year product guarantee and a 25-year rated power warranty.

Eventually, the panels are spatially distributed. Surplus spaces are strategically and equitably allocated to reduce the likelihood of shadows, obtaining a margin of 20% of the minimum distance value. Horizontally, they are distributed into five groups of six panels each and a single group of four, since the supports for correcting the tilt angle are made for a maximum of six PV modules.

Figure 29 illustrates the profiles of R3 and R4. Note that roofs R1 and R2 are distributed equally as R3. The shadow that a panel could cast from one roof to another is also considered. Finally, Appendix I.4 represents a 3D model of the completed integral centre.

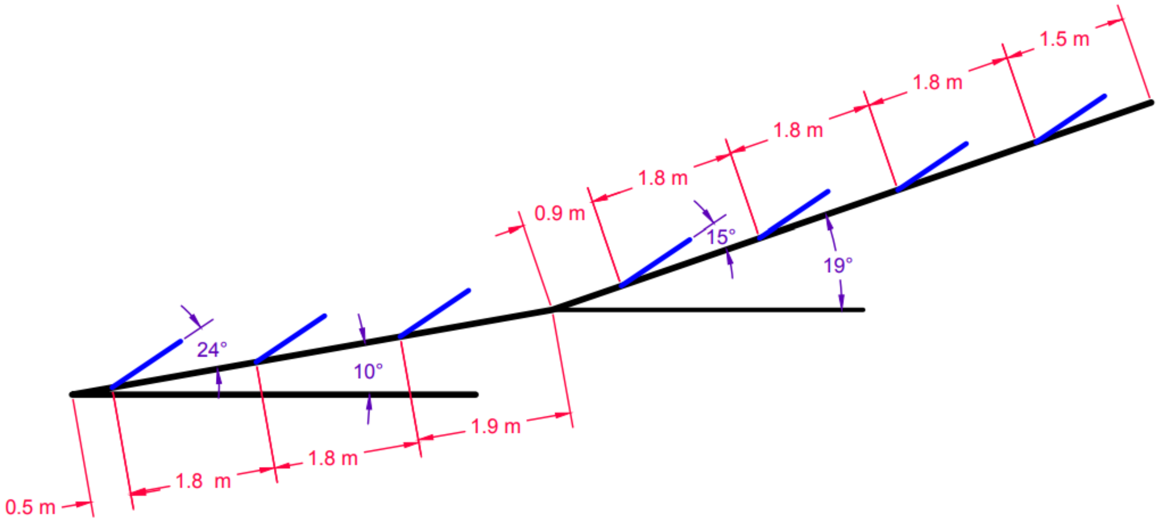

Figure 29. Profile view of roofs R3 and R4 with the installed PV panels.
(Author's own, adapted with AutoCAD).

4.1.5 Inverter selection and system connection

The inverter transforms the DC from the PV cells to AC, adapting the voltage and frequency to that of the mains to be able to use it (230 V and 50 Hz). Likewise, it performs energy optimization tasks, monitoring energy performance, electrical activity, etc. To characterise an inverter, it is necessary to consider its efficiency, the rated voltage, and the rated power. (Saidatul Shema Saad *et al.*, 2011).

There are three main types of inverter configurations such as connections, central inverters, chain inverters, and microinverters. The central inverter is the one that collects the voltage of all the installations at a single point and sends it to the mains. It is used in low-power domestic installations. The chain inverter divides the installation into different strings. If there is any alteration or malfunction somewhere, the overall performance of the system is not harmed. Finally, microinverters are devices that are connected to each board by transforming the current individually and then injecting the current into the grid. It is not typically installed in large infrastructures due to the considerable extra cost (Louwen *et al.*, 2022). Therefore, chain inverters were selected as they are the most suitable for the characteristics of this project.

The power of the inverter is calculated with the capacity of the PV installation, but solar installations rarely generate their maximum power. Generally, it is advisable to install an inverter that has between 80% and 90% of the peak power and, especially, it cannot be less than 75%. If calculated at 100%, most of the time it would be operating in low output power conditions and consequently with more inferior efficiencies. (Qazi, 2017).

To determine the most adequate type of chain inverter for the installation, it is essential to consider its efficiency and it is important to study the MPTT (Maximum Power Point Tracking). This value ensures that the strings of the solar panels are always in operation and at their maximum efficiency. If there are several strings with different orientations, it means that each series of solar cells will receive a different amount of solar radiation, involving different powers (Chitransh *et al.*, 2021). Other components may also be affected, such as price, monitoring components, years of warranty, or technical support included. A selection is made in Table 17 with different types that would be appropriate for the project.

Table 17. Adequate inverters for an installation with the characteristics of the project

Inverter	**SolarEdge three-phase Synergy – SE55 K**	**Fronius Tauro**	**Huawei SUN 2000-40KTL-M340**	**Kostal PIKO CI 50**
AC active power [kW]	50	50	40	50
Max. efficiency (%)	98.3	98.6	98.7	98.3
MPPT	1 per panel	3	4	4
Warranty [yr]	12 - 20	5 - 20	5 - 20	5
Cost [€]	3,499	4,371	3,285	2,700
Technical Service	Yes	Yes	Yes	Yes
Monitoring	Excellent	Good	Normal	Good
Dimensions	558x328x273	644x1038x316	640x530x2770	710x855x285
Temperatures [ºC]	-40 to +60	-40 to +65	-25 to +60	-25 to +60

(Adapted from Solaredge.com, 2018; Fronius.com, 2022; Europe-solar.com, 2021; Krannich Solar, 2022).

Despite the four models being relatively similar, the Huawei SUN 2000-40KTL-M340 is selected because it is the most efficient and the only one that appears in SAM libraries. Its datasheet can be found in Appendix IV.3 The maximum number of modules that can be connected in series per string is given by the temperature and the voltage of the inverter and the arrays (Ruiz, 2021). SAM is able to calculate the ideal value by entering the desired power and the desired DC to AC ratio. According to ABB (2018), the optimal value is 1.2-1.25 and the maximum desired power was previously calculated in Table 17.

As a result, SAM calculates the number of panels and inverters to be connected (Figure 30), obtaining a total of four inverters and 861.9 m^2 of panels, with an approximate estimated annual production of 313 MWh/yr (4.59 kWh/m^2, 21.7% efficiency). The value corresponds with the calculated in section 3.6.1 (335 MWh/yr) and exceeds significantly the public energy demand estimated.

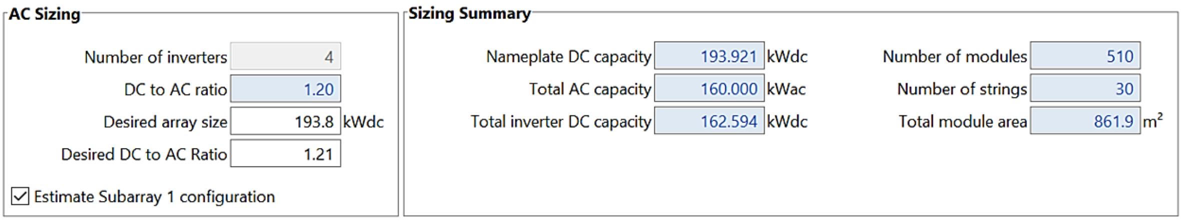

Figure 30. Number of inverters and modules calculated by SAM. (Author's own, adapted with SAM).

4.2 Biomass system

As in the simulation of the PV installation, the inputs required by the biomass modelling software are studied. SAM offers a simulation for boilers with any type of biomass and is capable of adding the additional use of coal without quantitative limits (Nrel.gov, 2022).The software models systems for electricity generation. According to SAM's Help Manual (SAM Help's System, 2022), the software is apt for simulating the first design when system-specific details are still unspecified. The configurable parameters make it possible to determine a possible theoretical model. These are divided into five sections (Table 18). Furthermore, note that SAM offers an instruction manual for the simulation of biomass technology (Jorgenson et al., 2011).

Table 18. Required inputs to the software for the energy simulation of the biomass system

Name	Summary of the requirements
Ambient Conditions	The weather data file to be used is selected. Then the DNI from GHI and DHI is specified. It allows visualising graphs of the meteorological variables.
Feedstock	The amount of biomass available is specified. It has a limited number of types and only allows you to enter two additional types.
Plant Specs	You can choose from three types of combustion systems. Boiler parameters are also specified. SAM provides all parameters, by default.
Emissions	The contamination of the transport of the raw material is specified as well as the type of processing that is applied (chipping, heavy grinding, or pellet).
Grid Limits	It is specified in the case of an interconnection power limit with the electric company.

(SAM Help's System, 2022).

Dissimilar to solar energy, the program does not have commercial libraries of different models of boilers. SAM is only limited to modelling three simple types of biomass combustion systems that pursue the process of conventional thermal power plants (Figure 31). It is not able to simulate other methods of electricity generation, such as gasification and pyrolysis, because their viability has not been sufficiently studied and they are not yet commercially modellable. For these reasons, it is not viable to simulate the pre-selected type of biofuel boiler (CHP). However, the type used in SAM only influences the proportion of carbon that is wasted and, consequently, the efficiency of the system. The main influence of the selection must be considered manually in the financial model as the cost of the installed technology will have to be accounted for.

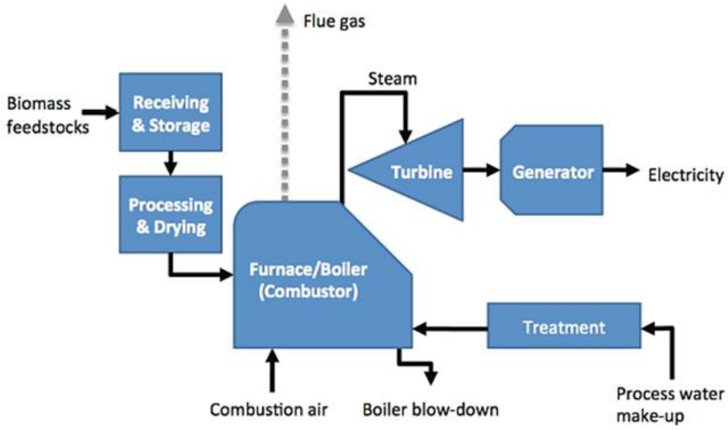

Figure 31. SAM's biomass power process flow diagram. (Jorgenson *et al.*, 2011).

Therefore, SAM only offers standard values for grate stoker furnaces, fluidized-bed combustor (FBC), and cyclone furnaces. In all three types, the raw material obtained is processed and burned in the boiler, which functions as a heat exchanger. It performs a standard Rankine cycle for the production of mechanical energy and, accordingly, electricity. The grate stoker furnace is discarded as, according to the manual, it is the most polluting and is suitable for huge energy installations with elevated burning speeds (34-317 t/h). Cyclone furnaces are also discarded because they are not commonly used for power generation. They are predominantly used in industrial plants for thermal generation and have a 3% fuel loss. Finally, fluidized bed combustion (FBC) is selected due to it being the most efficient, with a fuel loss of 0.25%. Nevertheless, the operating speed is lower and it is the most expensive technology. In addition, this type works with reduced steam temperatures (400 and 450 ºC). It is recommended for applications with limited space and also supports various types of feedstocks. Appendix V.2 lists all the variables entered that are used in the program to model the system, mostly using those provided by SAM by default. (Jorgenson *et al.*, 2011; Nrel.gov, 2022).

5 Financial model simulation with SAM

After modelling the energy analysis, the financial model is dimensioned, taking advantage of the toolkit provided by the Software Advisor Model to study its economic aspect. As specified in section 3.1, the main idea is to simulate both projects separately and then use a generic system to analyse them together. Section 5.1 studies the different types of financial analysis offered by SAM, and section 5.2 summarises the inputs it requests.

5.1 Types and selection of the SAM's financial model

When the interface is started and a project is created, the first parameter to select is the financial model type that is desired. Apart from the Helps' SAM manual, the Manual for the Economic Evaluation of Energy Efficiency and Renewable Energy Technologies produced for the National Renewable Energy Laboratory and Short, W. *et al.* (1995) specifies the definitions, formulas, and methods used by software to calculate financial metrics.

There is a comprehensive range of possibilities, such as Merchant Plant, Sale, Leaseback, Third Owner or simply No Financial Model. The models are similar but have some variables and characteristics that distinguish them. In the project context, the most appropriate option is to use the Residential/Commercial Owner model. This option simulates the purchase and sale of energy based on the demand entered (Nrel.gov, 2021b). The parameters that SAM requests are summarised in Table 19. Moreover, all the values introduced in the software are explained in Appendix VI. Remark that in Land Preparation input, it is considered asbestos management and the reconstruction of the roof. In addition, in the case of biomass, the salary of a worker has been counted (apart from the cost of the installation).

However, at the time of the simulations, it is appreciated that biomass modelling does not support all available financial models, as it is not as developed as solar or wind. Precisely, the Residential/Commercial Owner is not supported. The second most accepted model is the Single Owner. This type has a single owner who manages the profits without having to have different investors (Nrel.gov, 2013). Electricity is sold at an agreed price (PPA price), but the purchase cost is calculated based on the target minimum internal rate of return (IRR).

5.2 Summary of the specifications of the financial models used

Table 19 recapitulates the specified parameters of the most appropriate financial model (Residential/Commercial Owner). SAM divides the inputs into 7 different sections. The simulation of biomass (Single Owner) only changes that the Electricity Rates and Electricity Loan options cannot be configured. There are two new variables called Depreciation and Electricity Purchases, where the estimated depreciation over its estimated useful life and the energy price method must be defined.

Table 19. Required inputs to the software for the financial model used

Name	Summary of the requirements
Life time and degradation	The annual degradation value of the solar panel must be entered.
Installation Costs	The direct and indirect costs of the installation are defined. Sales tax base variables are also described.
Operating Costs	Additional fixed and variable costs are determined. The costs depending on the production and capacity of the system must also be entered.
Financial Parameters	The analysis period and the type of loan (debt fraction, loan rate, loan term, etc.) are defined. Moreover, the different rates (income tax, insurance, property tax, etc.) and the salvage value are established.
Incentives	The credits and state grants received are defined.
Electricity Rates	Specifies the type of billing to be used with consumption and surplus, indicating the purchase and selling prices.
Electricity Load	Detailed Time Load is introduced. SAM also allows entering a generic monthly value.

(SAM Help's System, 2022).

Additionally, as in energy simulation, note that the program is designed for a financial study in the United States with the monetary unit, taxes, fees, and parameters of this country. Despite this, it is not supposed to be a problem as conversion methods are applied and the configurations that do not involve the project are simply discarded by entering zeros in their values. Furthermore, many of the data points are totally unidentified and are determined to be out of scope as the project does not require such a detailed study. For example, the program requests the form of financing the project by specifying the type of loan (interest, federal and state taxes, inflation rate, etc.), the types of insurance that will be provided, or property taxes. In addition, it also requires specific federal and state incentives and grants that the project will receive. As mentioned in section 2.8, there are interesting and feasible options, but they have several bureaucratic processes that do not ensure their grant.

6 Results

This section summarises the results obtained from the thesis. Section 6.1 presents the simulated energy results, thus calculating the annual production, while section 6.2 explains the financial model. Finally, section 6.3 illustrates the design and distribution of the interiors of the three industrial buildings.

6.1 Power results

Solar energy will be the basis since its production is not flexible as it depends on the hours of sunlight (section 6.1.1), while biomass will be used strategically to supply and compensate for it (section 6.1.2). SAM provides an accurate energy production estimate. Despite having only annual consumption data, with the monthly distribution of consumption extrapolated in section 3.7, an estimate of the monthly energy losses and gains can be documented.

6.1.1 Solar energy production

With the characteristics defined in section 4.1 and Appendix V.1, a Nominal Plane of Array (POA) irradiance of 1,924 MWh is received. Observing the various losses (panel performance, inverter, power transformers, wiring, etc.), results in an annual generation of 349 MWh. The biggest losses are for DC modulated deviation from POA front-side soiling loss (5.0%) and DC module deviation from STC (4.2%). The main annual energy results are summarised in Table 20.

Table 20. First-year energy results of the PV system

Year 1	Nominal POA irradiance [kWh]	Net DC electricity [kWh]	Gross AC electricity [kWh]	Annual Production [kWh]	Performance ratio [-]	DC capacity factor [%]	Energy yield [kWh/kW]
Value	1,924,008	375,447	353,513	349,978	0.81	20.6	1,805

(Author’s own, adapted with SAM).

Based on 30 strings with 17 modules for each one, a PV panel array with a capacity of 193 kWdc is modelled. The data obtained is particularly favourable as the annual energy production significantly exceeds the energy consumption of public facilities. In addition, the capacity factor is positively favourable since it is higher than the average value obtained (18%) in a common profitable PV installation (IRENA, 2019).

Moreover, the value agrees with the annual theoretical production calculated in sections 3.6.1 and 4.1.5 (335 MWh/yr and 313 MWh, respectively). The theoretical value is slightly lower than the value obtained because SAM is more accurate in defining the panel efficiency, losses, and decomposition of irradiation (GHI, DNI, and DHI).

Despite the promising production, the results have to be compared with energy needs to determine if it could fulfil the demand during the winter months (Figure 32). With the estimated monthly distribution in section 3.7, a monthly graph is made to determine surpluses and energy shortages.

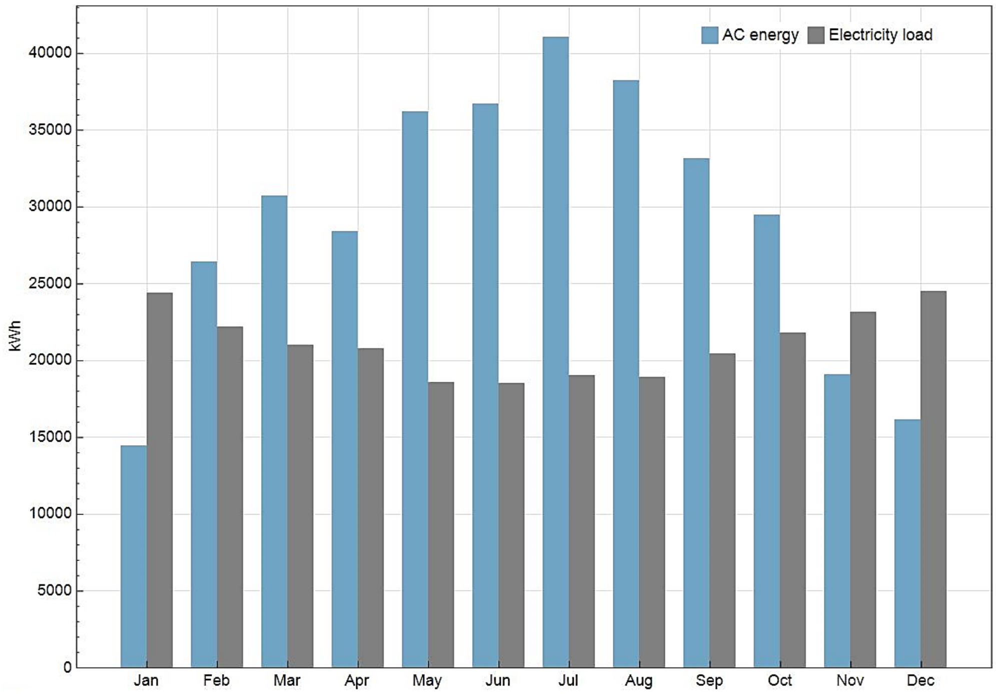

Figure 32. Monthly production and consumption of the PV installation. (Author's own, adapted with SAM).

As can be determined from Figure 32, the summer months are when more energy is produced and less is consumed, producing a consistent surplus. During the winter, there is the opposite circumstance, with a negative month-to-month computation. This deficiency in supply will have to be compensated for using biomass and, if necessary, from the electricity grid. Unfortunately, there is no time distribution of consumption to analyse the periods in detail. Having the appropriate data and contrasting them with the hourly production, it would be possible to determine the approximate periods from which it would be necessary to obtain biomass and external energy. For example, it could be calculated whether during the hours of darkness there would be consumed and therefore it would be necessary to use the biomass boiler. Additionally, analysis over time demonstrates that the selected components are acceptable and that production will decrease gradually as the panels have only 0.25% annual degradation.

On the other hand, an estimated annual energy surplus of 105 MWh is obtained. It is assumed that it will be able to be completely exported to the grid, generating economic benefits. This income will accelerate the payback of the investment. Details of economic results are explained in section 6.2.

6.1.2 Bioelectricity production

Biomass modelling is performed using the parameters defined in Appendix V.2. As described, to conduct the simulation, it is considered that the use of the boiler is constant throughout the year and that its main raw source is estimated to be the olive pit, which can be used to meet the needs of the appropriate boiler. The results are listed in Table 21.

Table 21. First-year energy results of the biomass system

Boiler capacity [kW]	Net electricity to grid [kWh]	Biomass usage [dry tonnes]	Efficiency of the system [%]	Life Cycle g CO2eq released/ dry kg
177.355	1,292,791	1,002	35.78	48.08

(Author’s own, adapted with SAM).

Depending on the amount of feedstock to be burned, SAM automatically models the capacity of the system, in this case, 177 kW. The annual bioelectricity quintuples the production of solar panels, which were originally intended to be the main source of energy. To confirm that the demand can be supplied, the monthly energy balance is shown in Figure 33, also considering the PV production.

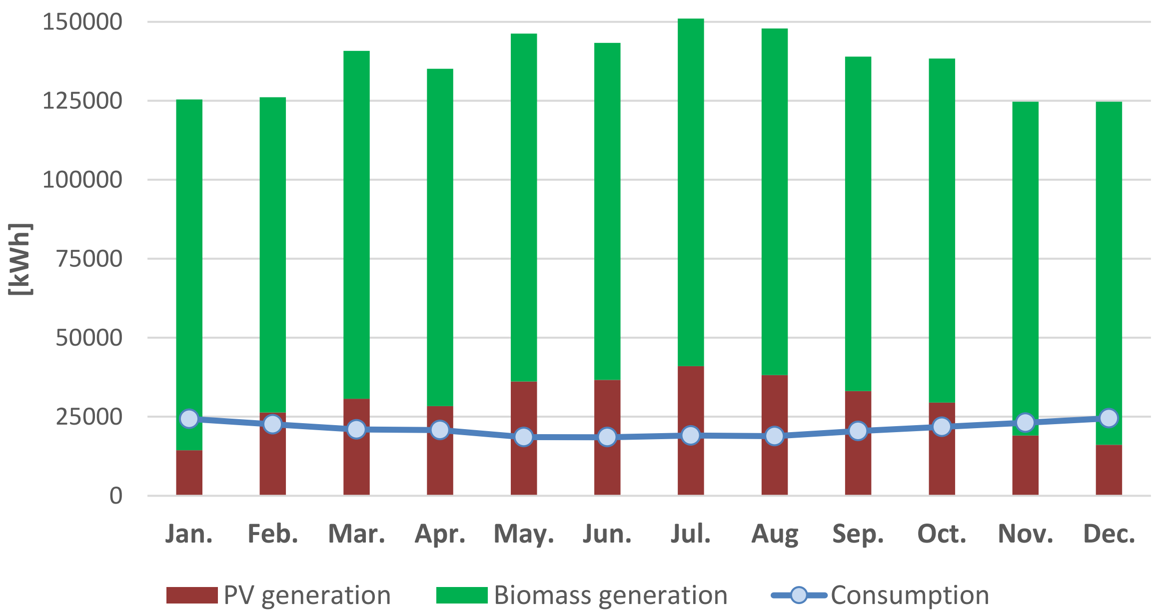

Figure 33. Monthly energy production and consumption of the infrastructure. (Author’s own).

Discerning the results in Figure 33, it can be concluded that the uniform use of agricultural resources fulfils the energy demand that the PV panels could not cover. The shortcomings of the winter are well covered, and the supply is guaranteed. Considering both systems, an annual surplus of 1,389 MWh is obtained, which would provide significant financial income. This plethora of energy could supply a part of the energy demand of the village. It could be sold at a cost price to encourage demographic change and offer unusual services to the municipality.

On the other hand, as mentioned in section 3.6.3, the 1,002 tonnes provide a theoretical energy of 1,607 MWh/yr. According to the SAM's simulation, the system has an efficiency of 35.78%, generating 1,292 MWh/yr. The energy differs due to SAM using its feedstock calorific values from predefined libraries and it is not designed to define more than two custom feedstock types. Moreover, SAM offers some indication of environmental impact in the calculation of the annual production of ash (48.013 tonnes), the biomass CO_2 uptake (-1166 kWh) and the biomass Life cycle CO_2 (164 kWh).

6.2 Financial results

As explained in section 3.1, separate case funding is analysed over a period of 25 years. The purpose is to study the feasibility separately, determining whether the type of technology installed is viable. If practicable, the cost of the investment and the repayment time will be studied. The results of the analysis of the generic system that encompasses the two technologies are demonstrated in sections 6.2.1 and 6.2.2. Remark that the results are obtained in American dollars ($) and the equivalent of $1 = €0.95 (European Commission, 2022) has been applied.

6.2.1 Solar economic viability

The configurations described in Appendix VI.1 are used to analyse the financial model for the installation of PV panels. The most relevant results are summarised in Table 22. The study was conducted using the Residential/Commercial owner, assuming that the initial investment would be made with a single initial payment (without any loan).

Table 22. First-year financial results of the PV system

Energy production [kWh]	Levelized COE [€/kWh]	Electricity bill without system [€]	Electricity bill with system [€]	Net savings with the system [€]	Capital cost [€]	Payback period [yr]
349,789	0.029	21,469	-29.45	21,499	266,707	13.1

(Author's own, adapted with SAM).

With the installation of the PV panels, the annual public demand of the town and the one created by the three industrial buildings would be completely amortized. SAM graphs are not used as they are in values in US dollars. To perform the conversion, the software effortlessly exports the data to a datasheet where the desired graphs are made. The initial investment of €266,000 involves a price of €1.43/kW of installed capacity, which implies a payback period of 13.1 years (Figure 34).

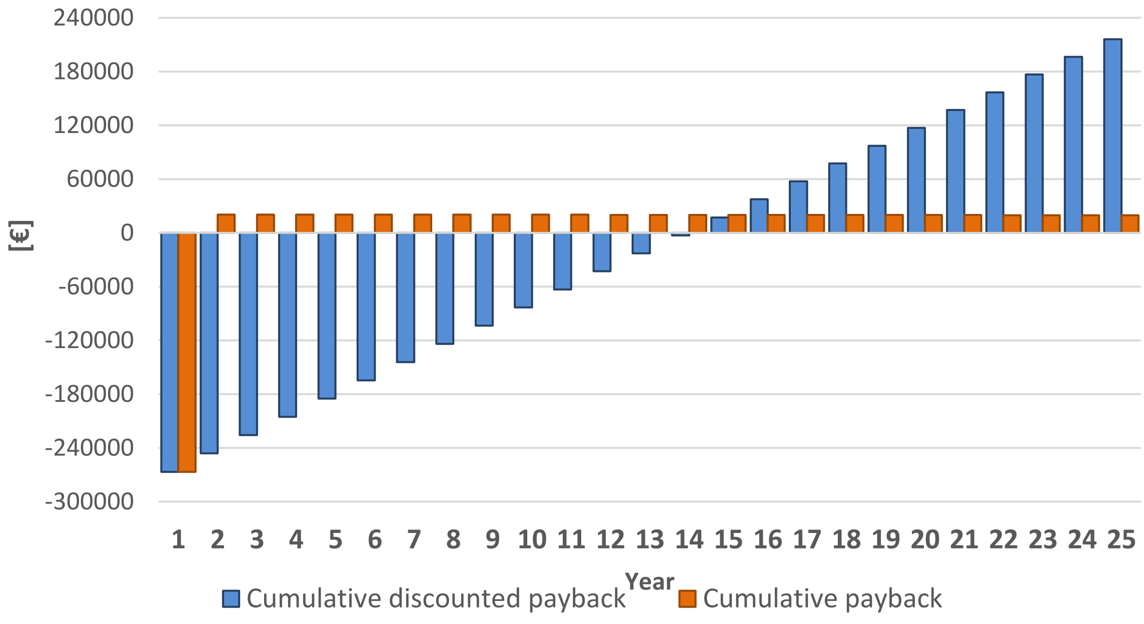

Figure 34. Payback of PV installation. (Author's own).

As assessed, the annual gains indicate that the initial cost of the installation is gradually being amortized until the 13th year, when the accumulated payback is no longer negative because it has been amortized. Note that year 1 denotes the moment when the initial investment is made. Therefore, the graph indicates that the amortisation time reaches the fourteenth year (the identical procedure is applied in succeeding economic analyses). Subsequently, economic gains and energy savings remain nearly constant (approx. €21,000/yr), which causes the accumulated payback to continue increasing practically linearly. The cash flow generated by SAM is attached to Appendix VII.1. For a more detailed study, the monthly electricity bill is studied based on the solar electricity generated (Figure 35).

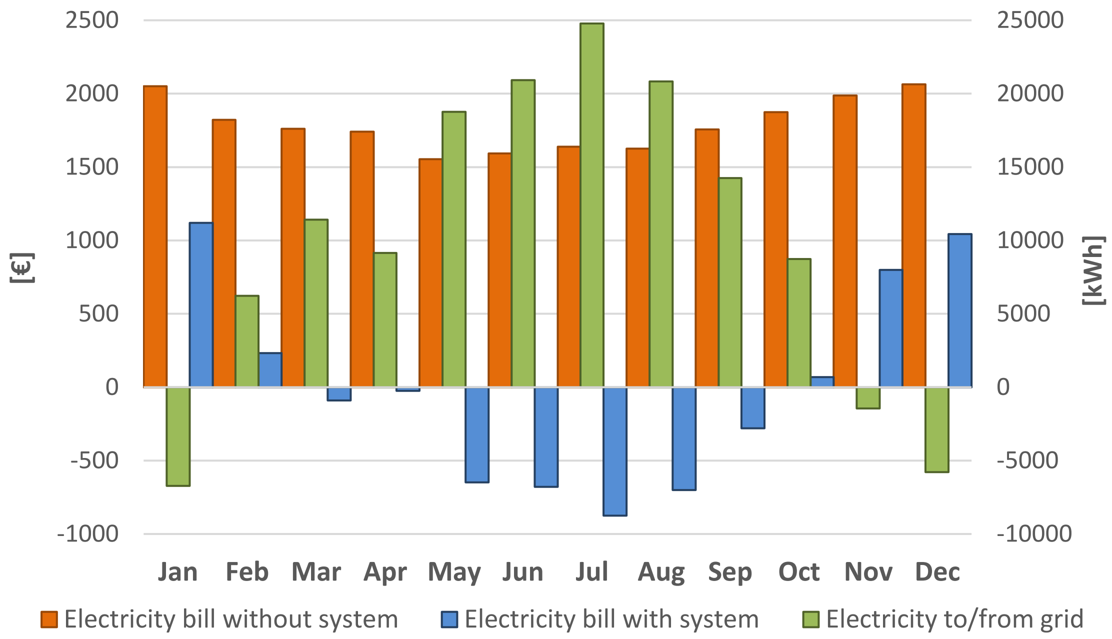

Figure 35. Electricity bill based on PV electricity generated. (Author's own).

As previously discussed in section 6.1.1, January, November, and December generation is not enough to supply the energy demand. As a result, the electricity has to be provided by the power company at a positive cost. Even in February and November, despite supplying energy to the grid, it is not enough to pay the monthly energy costs as the price sold (0.055€/kWh) is cheaper than what is bought (0.09€/kWh). During the remaining months, the total annual consumption is offset by reducing the annual electricity bill to €0 and generating €29 in profits.

6.2.2 Biomass economic viability

The biomass financial study was performed using the parameters defined in Appendix VI.2. The price of the boiler and the installation price have been assessed. Additionally, the hiring of a fixed person throughout the year to manage the use of the machinery and the integrated centre has been considered. No electricity load has been involved due to it having already been applied to the PV system and the financial type selected does not permit it. Feedstock prices have also not been defined, as they are agricultural waste that is currently being disused. Price analysis should be done thoroughly, considering the profitability of the system. Therefore, the value obtained would only cover the amortization of the boiler and the defined menu characteristics. The most significant simulation values are listed in Table 23.

Table 23. First-year financial results of the biomass system (without paying the feedstock)

Energy production [kWh]	Levelized COE [€/kWh]	Net Capital Cost [€]	Profits selling electricity [€]	Internal rate of return (IRR) [%]	Payback period [yr]
1,292,461	0.021	187,188	71103.45	26.70	4

(Author's own, adapted with SAM).

It is relevant to mention that by not using the appropriate financial model, the output obtained is not properly adjusted to the prerequisites of the study. However, it is sufficient to accomplish a general economic viability study. The price per kWh is lower than that obtained from the PV installation, but the value is not realistic since the feedstock is considered to be completely free. Annual economic analyses are performed in Figure 36, and the cash flow generated is attached to Appendix VII.2.

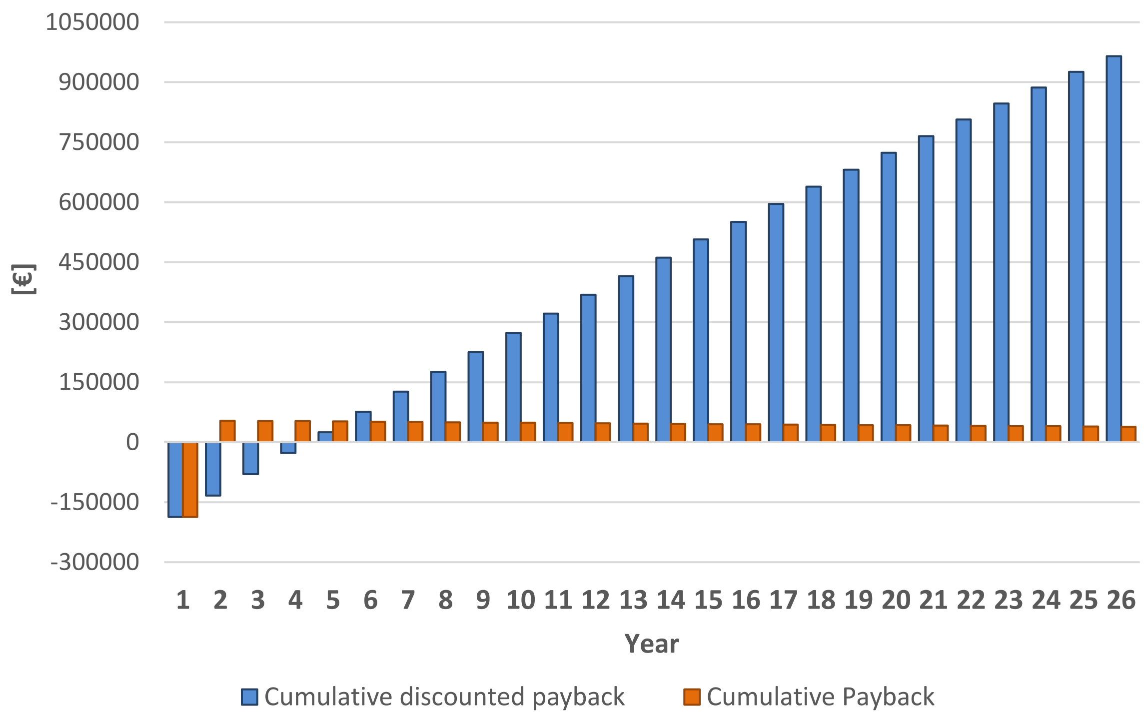

Figure 36. Payback of biomass installation. (Author's own).

From Figure 36, it can be seen that the defined conditions lead to a rapid amortization of the system in four years. Therefore, to calculate more realistic research, a parametric analysis is performed with the SAM. The aim is to calculate the price that the feedstock could be paid to repay the project in about 15 years. An approximate value of 40 €/tonne is calculated and the temporary compensation of Figure 37 is obtained (in 12 years). The cash flow generated by SAM is attached to Appendix VII.3.

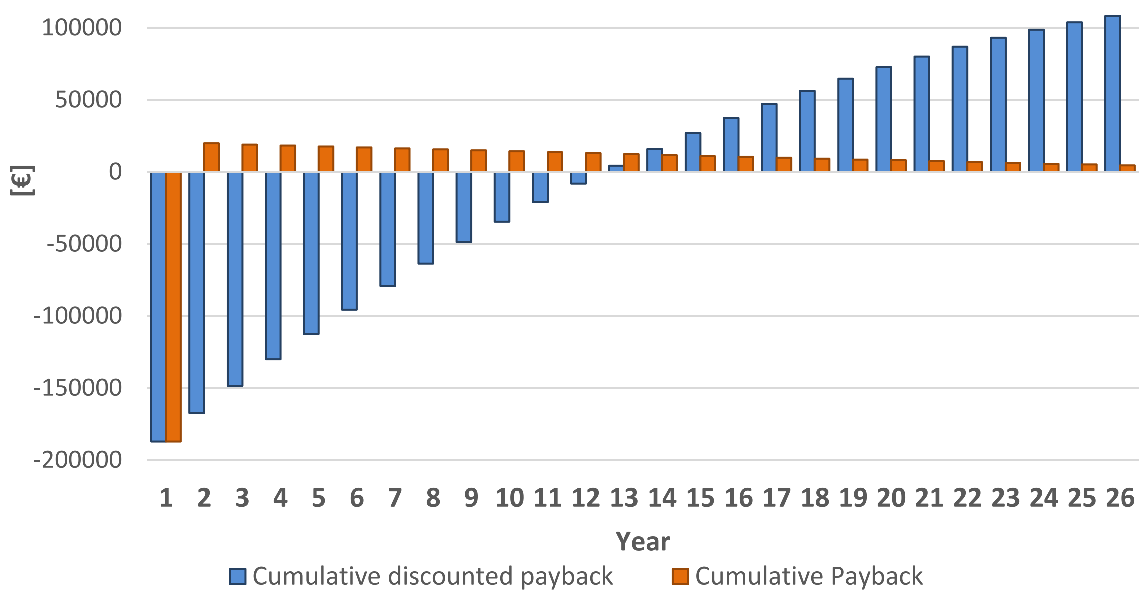

Figure 37. Payback of biomass installation (remunerating agricultural waste). (Author's own).

A cost-effective system is achieved, and farmers would be encouraged to treat agricultural waste properly for the creation of bioenergy. It would aid increase environmental awareness and provide an extra source of economic income. In addition, the residues would generate approximately €40,000 in additional revenue for the Camp Cooperative in exchange for the agro-industrial waste treatment of olive pits and almonds that are currently wasted.

6.2.3 Generic system viability

The Generic System model permits the combination of several cases. However, as the financial models are inevitably selected differently, the program does not properly match the profiles. For this reason, the economic values must be entered manually. The simulation results have been completed, considering that the biomass is paid at 40 €/tonne and one person has been hired. The values entered are indicated in Appendix VI.3 and the results obtained are summarized in Table 24.

Table 24. First-year financial results of the generic system

Energy production [kWh]	Capacity factor [%]	Levelized COE [€/kWh]	Electricity bill without system [€]	Electricity bill with system [€]	Net savings with system [€]	Capital Cost [€]	Payback period [yr]
1,466,290	45.1	0.046	21.469	-66,574	85,047	503,524	14.6

(Author’s own, adapted with SAM).

This model simply adds the values of both simulations in a weighted way to get an overview of the 394 kW of installed capacity. Logically, biomass predominates in the project as approximately 80% of production comes from it. The final rate of return is 14.6 years (Figure 38). The cash flow generated by SAM is attached to Appendix VII.4. The city council could use part of the profits to encourage the population by offering more jobs in the centre or selling the energy at a cost price.

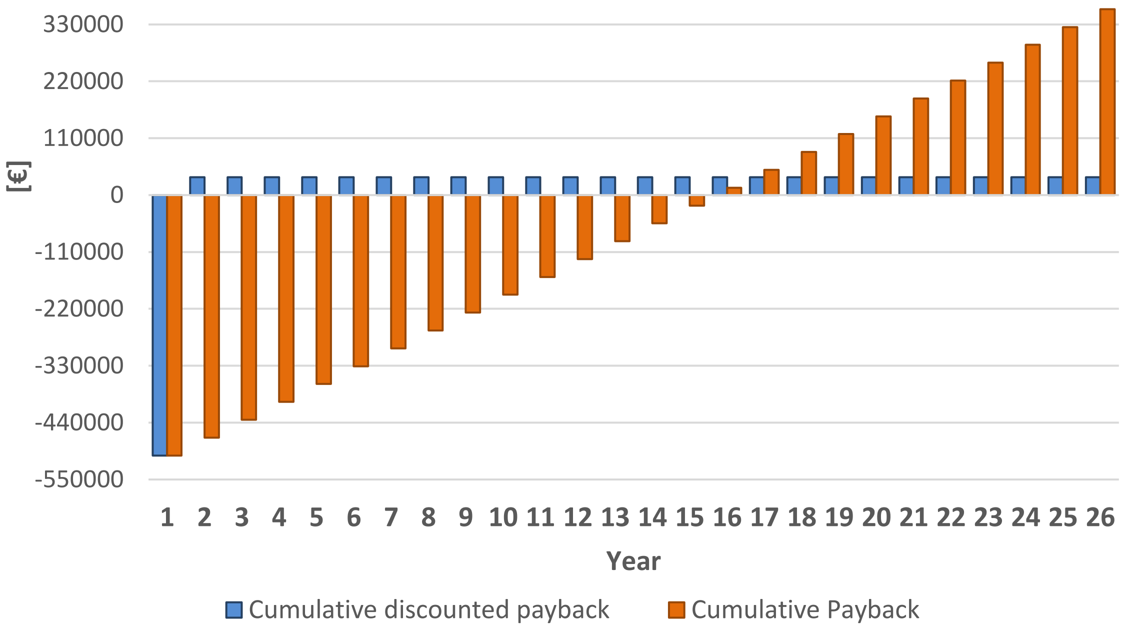

Figure 38. Payback of combined generic system. (Author's own).

6.3 Design of the three industrial buildings

The main purpose of outbuilding planning is to locate the biomass boiler and the corresponding warehouses. To distribute the space in the first place, the boiler has been strategically located in the north (N) corner to avoid the smoke extraction chimney causing shadows on the roof. Furthermore, the dimensions of the different machinery required have been accounted for.

Subsequently, the adjacent biomass warehouses with a space of 1,020 m^2 (minimum space of 816.3 m^2 is calculated in section 3.6.3) have been located. In addition, the current monitoring systems (inverters, bidirectional meters, etc.) for the system have been distributed. With the remaining space, the rest of the sociocultural space is designed to complete the pre-established conditions. Figure 39 represents the floor plan design of the three industrial buildings. Note that in Appendix I.4, the exterior design and 3D views of the final distribution are attached.

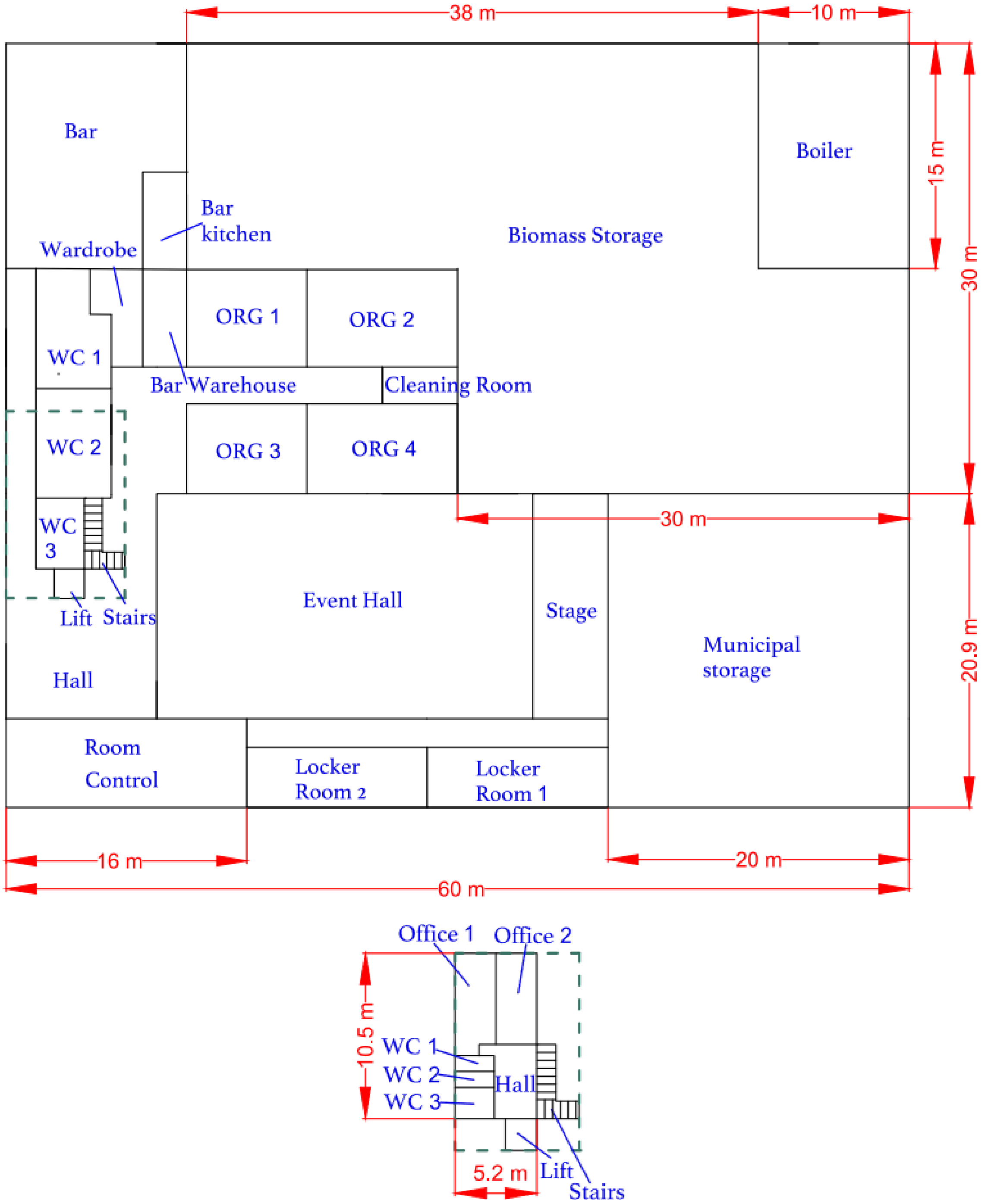

Figure 39. Indoor floor plan design of the three industrial buildings. (Author's own, adapted with AutoCAD).

The asbestos roofs will have to be reconditioned due to the installation of solar panels. Compared to the prices of various local enterprises, it is estimated that the new roof would cost around €100,000. The PV cells adapt effortlessly to different types of roofs. However, the most suitable material would be sheet metal or sandwich panels since they offer stability, resistance, and durability. (Dolomada.com, 2012; HostecServeis, 2015; Desamiantado, 2018; GDA, 2019). In terms of interior design, the cost of the refurbishment is not considered as it is completely relative and would depend on the specific equipment and facilities that would be selected.

7 Discussion

Section 7.1 discusses the thesis results regarding the aims and objectives. Section 7.2 discusses the project limitations, and section 7.3 evaluates the consistencies and inconsistencies within the assessment's results. Finally, section 7.4 suggests improvements for forthcoming studies.

7.1 Aim and objectives result

The purpose of the thesis has been achieved by designing a completely integrated renewable energy centre with an installed capacity of 394 kW. The first specific objective was to install different renewable energies to generate and supply the energy demand of the village. The results obtained with the SAM simulations indicate that the correct management of natural energy resources could generate 1,466 MWh/yr of green electricity.

The subsequent objective was to determine the availability of local agriculture for bioelectricity production. After an exhaustive study, SAM confirms that the 1,002 tonnes of agricultural waste generated mostly by the Camp Cooperative of Cervià are plentiful to produce bioelectricity. If the complete estimated resources were utilised, the exploitation of biomass would quintuple the power converted by PV panels. In addition, with the economic gains, the farmers could be financially encouraged to collect and treat waste properly to maximize bioenergy production with a minimum economically viable price of 40€/tonne.

The third objective was to redesign the three industrial buildings to be able to locate all the machinery needed for renewable energy production as well as to create a multipurpose space for the inhabitants of the municipality. The customer-specified detailed requirements have been accomplished by performing infrastructure planning with AutoCAD.

Finally, to fulfil the last objective, it has been necessary to perform the financial analysis of the project, combining the conclusions obtained in the previous steps. It has been essential to compare the economic benefits of energy production with the various costs of infrastructure (€503,524), obtaining a minimum amortisation of 14.6 years.

7.2 Limitations

Several limitations have materialised during the development of the thesis, most of them related to obtaining data to model the energy and financial systems. There was not enough readily available Cervià documentation to calculate the simulations. For example, temporary energy demand. Moreover, the complete analysis has been calculated with the standard electricity price rate, without considering the hourly discrimination. This could be decisive in determining the system's economic viability since the price of electricity oscillates significantly between 0.0640€/kWh and 0.1646€/kWh (Appendix I.5).

Additionally, there was no prior knowledge of the use of SAM and its specifications. Comprehending its accurate functioning and the requirements it presents has been more complex and time-consuming than predicted. The software is principally designed for the United States with the use of their specific units of measurement, libraries, inputs, and financial parameters, hindering its application. For this reason, it has been considered convenient to manually interpolate and prepare the Cervià meteorological files with the specific characteristics of the SAM.

Likewise, the modulation of SAM biomass is not as well-developed as other more standard renewable energies, such as solar or wind types. Consequently, it does not have the same advantages and does not offer identical perspectives and results. The energy analysis simulates a generic model by selecting one of the three predetermined types of combustion systems to generate electricity without being able to introduce the CHP boiler. In addition, the feedstock data had to be entered manually as it only has specific types of feedstocks common in the US. Furthermore, mention that exclusively two additional types of raw materials can be added, which has caused the use of those already defined with their inaccurate attributes.

7.3 Inconsistencies within the assessment's results

Robust processes and estimates supported by recognised institutions such as NASA and NOAA have been conducted throughout the project. Solar and biomass productions provide great energy potential. However, the results of the interpolation of wind speeds are not favourable, determining that the installation of a domestic wind turbine is not feasible. Decisions and calculations have been justified and verified, contrasting various methods to arrive at a common result.

The energy results obtained from the PV panels coincide rigorously with the estimates made when studying their natural resources. In contrast, for biomass, the values differ relatively because the program assumes unchangeable energy density values different from those used in the theoretical analysis. Conversely, the financial model did not consider some specific factors that would change the amortisation time of the project, such as property devaluation, loan interest, possible subsidies, annual economic decline, inflation rates, etc. For this reason, the analytical consequences of amortisation are considered the minimum periods that would occur in the most satisfactory circumstances.

7.4 Suggestions for assessment improvements

If the project is compared with others accomplished previously, it can be determined that this is not the first integrated renewable energy design (Ramakumar *et al.*, 1995; Bagheri *et al.*, 2019). However, it is a unique study of these characteristics in the area. Therefore, the research may be useful for future investigations of the same nature. But it should be noted that the project only offers an academic and theoretical view of the design of the centre. The values obtained provide a notion of the approximate values that could be obtained.

If the project is to be materialised, an exhaustive study should be accomplished with more accurate data from Cervià. A more detailed examination of temporary demand, biomass collection, and treatment should be conducted, identifying various local data sources. Furthermore, a small weather station should be installed or weather data interpolated with more robust geospatial interpolation methods such as Kringing or CoKringing (En and Porras Velázquez, 2017). Perhaps obtaining more accurate data on the location of the infrastructure could change the decision-making. For instance, the determination to install a domestic wind turbine if favourable wind data is obtained.

Finally, despite the considerable amount of biomass that would provide energy flexibility, the cost-benefit of battery storage could be financially modelled. It would significantly increase energy changeability by using stored power at appropriate times, reducing costs. It would maximise profits by reducing consumption during the hours when electricity is more expensive and charging them when there is a surplus. It would even permit the trading of power on the grid, purchasing it at off-peak hours and vending it at peak times.

8 Conclusions

The decarbonisation of society is an environmental solution that is becoming increasingly important to mitigate human-induced climate change. For this reason, Cervià proposes to engineer an integrated renewable energy centre in three industrial buildings that are currently disused. The main purpose of the facility is to produce power to fulfil the public demand, use agricultural waste in the area and promote various socio-economic activities to revitalise the local demography.

This thesis proposes a repeatable methodology to design infrastructures of these characteristics, studying the different natural resources available and economically viable. Precisely, in Cervià, the exploitation of wind is not favourable as a capacity factor of approximately 2% is obtained. Alternatively, SAM software calculates that solar power provides a capacity factor of 21%, which implies a generation of 349 MWh/yr with a system of 193 kWdc. Likewise, biomass is profitably usable as it is estimated that the available 1002 tonnes can provide net electricity to the grid of 1,292 MWh/yr. The generation using these technologies fulfils plentifully the public consumption of the village, permitting the commercialization of the surplus.

Additionally, the economic viability of the project has been analysed. Despite the initial capital cost of €503,524 for a small-town council such as Cervià, it is estimated that the initial investment will be recovered in a minimum of 14.6 years. The excess energy could be marketed to the villagers at a more affordable expense than the current price and could encourage the local farming economy by purchasing agricultural waste.

To sum up, it can be concluded that the overall purpose of the thesis and the defined objectives have been fulfilled. Moreover, some limitations and improvements in calculations have been proposed, especially concerning the use of more accurate data. Furthermore, the cost-benefit of battery storage could be financially modelled to study maximising the benefits of installation. Therefore, the designed proposal can be studied in detail by the Cervià City Council (or even similar projects) to determine if it is viable to be realised.

9 References

Abas, N., Kalair, A. and Khan, N. (2015). Review of fossil fuels and future energy technologies. *Futures*, [online] 69, pp.31–49. doi:10.1016/j.futures.2015.03.003.

ABB (2018). *Why array oversizing makes financial sense*. [online] Available at: https://new.abb.com/docs/librariesprovider117/default-document-library/solar-inverters/solar_power_world-article.pdf?sfvrsn=80a7614_4.

Adhikary, S.K., Muttil, N. and Yilmaz, A.G. (2017). Cokriging for enhanced spatial interpolation of rainfall in two Australian catchments. *Hydrological Processes*, [online] 31(12), pp.2143–2161. doi:10.1002/hyp.11163.

Ajuntament de Cervià de les Garrigues. (2022). *Ajuntament de Cervià de les Garrigues*. [online] Available at: https://www.cerviadelesgarrigues.cat/.

Ajuts a l'autoconsum. (2021). Autoconsum i emmagatzematge Reial Decret 477/2021. [online] Available at: https://icaen.gencat.cat//26_ajuts_financament/2021_IDAE_EERR/Presentacions-de-les-jornades-de-presentacio/pdf.

Alonso, N., Juan Pedro Ferrio, A. Florit and Jordi Voltas (2004). *Evolució climàtica de la plana occidental catalana durant els darrers 4.000 anys: primers resultats de la...* [online] ResearchGate. Available at: https://www.researchgate.net/Evolucio_climatica_de_la_plana_catalana_durant_els_4000_anys_primers_resultats_de_la_discriminacio_isotopica_del_carboni_D13C.

Altas, I.H. and Sharaf, A.M. (2014). Solar Energy and PV Systems. *International Journal of Photoenergy*, [online] 2014, pp.1–2. doi:10.1155/2014/408285.

Ammar and Dulaimi, A. (2018). *Design of an Off-Grid Solar PV System for a Rural Shelter*. [online] ResearchGate. doi: 10.13140/RG.2.2.24352.07689

Apar Chitransh and Kumar, S. (2021). *The Different Type of MPPT Techniques for Photovoltaic System*. [online] ResearchGate. doi:10.35940/ijee.A1809.111221

Bagheri, M., Delbari, S.H., Pakzadmanesh, M. and Kennedy, C.A. (2019). City-integrated renewable energy design for low-carbon and climate-resilient communities. *Applied Energy*, [online] 239, pp.1212–1225. doi:10.1016/j.apenergy.2019.02.031.

Barber, M. (2017). *Urban 'Wind Trees' generate electricity from breezes*. [online] Curbed. Available at: https://archive.curbed.com/2017/3/14/14914302/wind-tree-turbine-for-sale.

Bárdossy, A. and Li, J. (2008). Geostatistical interpolation using copulas. *Water Resources Research*, [online] 44(7). doi:10.1029/2007wr006115.

Bauer, L. (2018). Aeolos Aeolos-V 300W - 0,30 kW - Wind turbine. [online] Wind-turbine-models.com. Available at: https://en.wind-turbine-models.com/turbines/1849-aeolos-aeolos-v-300w.

Benmedjahed, Rachid Maouedj and Samir Mouhadjer (2017). *Wind turbine selection and wind farm design in Tindouf*. [online] ResearchGate. Available at: https://www.researchgate.net/publication/319645078_Wind_turbine_selection_and_wind_farm_design_in_Tindouf.

Berthet, L. (2009). *Polluted site assessment using Inverse Distance Weighted and Ordinary Kriging -Advantages and limitations*. [online] Available at: https://www.diva-portal.org/smash/get/diva2:1020215/FULLTEXT01.pdf.

Blair, N., Diorio, N., Freeman, J., Gilman, P., Janzou, S., Neises, T. and Wagner, M. (2018). *System Advisor Model (SAM) General Description (Version 2017.9.5)*. [online] Available at: https://www.nrel.gov/docs/fy18osti/70414.pdf.

Boccard, N. (2009). Capacity Factor of Wind Power: Realized Values vs. Estimates. SSRN Electronic Journal. [online] doi:10.2139/ssrn.1285435.

BOE. (2022). *BOE.es - Buscar*. [online] Available at: https://www.boe.es/buscar/ .

Bogdanov, D., Ram, M., Aghahosseini, A., Gulagi, A., Oyewo, A.S., Child, M., Caldera, U., Sadovskaia, K., Farfan, J., De Souza Noel Simas Barbosa, L., Fasihi, M., Khalili, S., Traber, T. and Breyer, C. (2021). Low-cost renewable electricity as the key driver of the global energy transition towards sustainability. *Energy*, [online] 227, p.120467. doi:10.1016/j.energy.2021.120467.

BOP. (2021). Número 36 Butlletí Oficial de la Província de Lleida Dimarts, 22 de febrer de 2022. [online] Available at: https://bop.diputaciolleida.cat/faces/consultaF/servlets/donarEdicte/?id=2022_36_1365.

Bratton, D.C. and Womeldorf, C.A. (2011). The Wind Shear Exponent: Comparing Measured Against Simulated Values and Analyzing the Phenomena That Affect the Wind Shear. *ASME 2011 5th International Conference on Energy Sustainability, Parts A, B, and C*. [online] doi:10.1115/es2011-54823.

Britannica. (2022). In: Encyclopædia Britannica. [online] Available at: https://www.britannica.com/science/Koppen-climate-classification.

Campdecervia.com. (2022). *Camp de Cervià – Cooperativa del Camp de Cervià SCCL*. [online] Available at: https://campdecervia.com/.

Cantero. (2021). *Estratègia per promoure l'aprofitament energètic de la biomassa forestal i agrícola*. [online] Available at: https://icaen.gencat.cat/plansprogrames/estrategia_biomassa/.

Catalunya.com (2013). *Cervià de les Garrigues*. [online] Catalunya.com. Available at: https://www.catalunya.com/cervia-de-les-garrigues-2-1-577322?language=ca.

Ccoo.es. (2015). *Legislación sobre el Amianto*. [online] Available at: https://educarsinamianto.fe.ccoo.es/legislacion/informacion-destacada.html.

CIDO. (2020). *Pressupost i plantilla per a l'any 2021 | Ajuntament de Cervià de les Garrigues | Normativa local | Cercador d'Informació i Documentació Oficials (CIDO) - Diputació de Barcelona*. [online] Available at: https://cido.diba.cat/pressupost-i-plantilla-per-a-lany-2021.

Clean Energy. (2012). *Clean Energy Solutions Center | System Advisor Model (SAM)*. [online] Available at: https://cleanenergysolutions.org/fr/resources/system-advisor-model-sam.

Climate Action. (2018). *2050 long-term strategy*. [online] Available at: https://ec.europa.eu/clima/eu-action/climate-strategies-targets/2050-long-term-strategy_en.

Craighead, J.E. and Gibbs, A.R. (2009). *Asbestos and Its Diseases*. [online] ResearchGate. doi: 10.1093/acprof:oso/9780195178692.001.0001.

CTE (2021). *Documentos CTE*. [online] Available at: https://www.codigotecnico.org/DocumentosCTE/DocumentosCTE.html.

De, M. (2020). *El clima de Catalunya - Servei Meteorològic de Catalunya*. [online] Servei Meteorològic de Catalunya. Available at: https://www.meteo.cat/wpweb/climatologia/el-clima-ahir/el-clima-de-catalunya/.

De, M. (2021). *Petició de dades i d'informes per dies concrets - Servei Meteorològic de Catalunya*. [online] Servei Meteorològic de Catalunya. Available at: https://www.meteo.cat/wpweb/serveis/formularis/peticio-dinformes-i-dades-meteorologiques/peticio-dinformes-meteorologics/.

Departament d'Acció Climàtica, Alimentació i Agenda Rural. (2019). *Gestió forestal*. [online] Available at: http://agricultura.gencat.cat/ca/ambits/medi-natural/gestio-forestal/.

Desamiantado. (2018). *Retirada de amianto Lleida ¡Precio DESAMIANTADO, Lleida! por RERA*. [online] Available at: https://desamiantado.net/retirada-de-amianto-fibrocemento-asbestos-lleida-lerida/.

Díaz, G. and Manuel, J. (n.d.). *Universidad Central de Venezuela Venezuela*. [online] Available at: https://www.redalyc.org/pdf/721/72130181006.pdf.

Diego, V. (2013). Perfiles de generación eólica para la simulación de mediano y largo plazo de sistemas eléctricos. Uchile.cl. [online] doi:https://repositorio.uchile.cl/handle/2250/113644.

Diego, J.C. (2019). *Diego 2020 TESIS Desarrollo de una metodologia de valoracion de impacto visual*. [online] ResearchGate. Available at: https://www.researchgate.net/publication/350236507_Diego_2020_TESIS_Desarrollo_de_una_metodologia_de_valoracion_de_impacto_visual.

DiOrio, N., Dobos, A. and Janzou, S. (2015). Economic Analysis Case Studies of Battery Energy Storage with SAM. [online] doi:10.2172/1226239.

Dolomada.com. (2012). *Grupo DOLOMADA SL | Desamiantado | Gestión de Uralita | Manipulación y Gestión integral de Amianto |(Lleida)*. [online] Available at: http://www.dolomada.com/desamiantado.php.

Eia.gov. (2022). *Renewable energy explained - U.S. Energy Information Administration (EIA)*. [online] Available at: https://www.eia.gov/energyexplained/renewable-sources/.

Elsevier (2017). Global available wind energy with physical and energy return on investment constraints. *Applied Energy*, [online] 209, pp.322–338. doi:10.1016/j.apenergy.2017.09.085.

Emeara, M.S., Ahmed El Abagy and Ahmed Abdel Gawad (2021). *Orientation-Optimization Simulation for Solar Photovoltaic Plant of Cairo International Airport*. [online] ResearchGate. Available at: https://www.researchgate.net/publication/352750112_Orientation-Optimization_Simulation_for_Solar_Photovoltaic_Plant_of_Cairo_International_Airport.

Emeara, M.S., Hamdy, E. and Ahmed Abdel Gawad (2021). *Hybrid Renewable Energy System for a Sustainable House-Power-Supply...* [online] ResearchGate. Available at: https://www.researchgate.net/publication/Hybrid_Renewable_Energy_System_for_a_Sustainable_House-Power-Supply_Journal_of_Advanced_Research_in_Fluid_Mechanics_and_Thermal_S.

En, M. and Porras Velázquez, G. (2017). *Método Kriging de inferencia espacial*. [online] Available at: https://centrogo.repositorioinstitucional.mx/Kriging%20de%20Inferencia%20espacial%20-%20%20Diplomado%20en.

Energia.gob.es. (2019). *Ministerio para la Transición Ecológica y el Reto Demográfico - Normativa*. [online] Available at: https://energia.gob.es/renovables/Paginas/normativa.aspx.

Energia.gob.es. (2021). *Plan estratégico de estimaciones de los impactos socio-económicos de un parque eólico*. [online] Available at: https://energia.gob.es/renovables/regimen-economico/Documents/EOL_PE21%20GREENALIA%20WIND%20POWER.

Energy. (2022). *Renewable energy*. [online] Available at: https://energy.ec.europa.eu/topics/renewable-energy_en.

Es, C. (2020). *Selectra*. [online] tarifaluzhora.es. Available at: https://tarifaluzhora.es/info/pvpc.

Estudi de disponibilitat de biomassa i demanda energètica. (2020). [online] Available at: http://www.forestal.cat/bdds/imatges_db/biblioteca/BIBLIOTECA_DOCUMENT1_4820100013250004.pdf.

EU Science Hub. (2022). *PVGIS 5.2*. [online] Available at: https://joint-research-centre.ec.europa.eu/pvgis-photovoltaic-geographical-information-system/pvgis-releases/.

Europa.eu. (2016). *JRC Photovoltaic Geographical Information System (PVGIS) - European Commission*. [online] Available at: https://re.jrc.ec.europa.eu/pvg_tools/en/tools.html#PVP.

Europa.eu. (2021). *Combating climate change | Fact Sheets on the European Union | European Parliament*. [online] Available at: https://www.europarl.europa.eu/factsheets/en/sheet/72/combating-climate-change.

European Commission. (2022). *Tipo de cambio (InforEuro)*. [online] Available at: https://ec.europa.eu/info/funding-tenders/procedures-guidelines-tenders/information-contractors-and-beneficiaries/exchange-rate-inforeuro_es.

Europe-solarstore.com. (2015). *Panasonic VBHN330SJ53 solar panel*. [online] Available at: https://www.europe-solarstore.com/panasonic-vbhn330sj53.html.

Florinsky, I.V. (2016). Digital Elevation Models. *Digital Terrain Analysis in Soil Science and Geology*, [online] pp.77–108. doi:10.1016/b978-0-12-804632-6.00003-1.

Freeman, J.M., DiOrio, N., Blair, N., Guittet, D., Gilman, P. and Janzou, S. (2019). Improvement and Validation of the System Advisor Model. [online] doi:10.2172/1495693.

Fronius.com. (2022). *Fronius Tauro - commercial solar inverter for large-scale PV systems*. [online] Available at: https://www.fronius.com/en/solar-energy/products-solutions/commercial-energy-solutions/tauro-commercial-solar-inverter-for-large-scale-pv-systems.

Fung, K.F., Chew, K.S., Huang, Y.F., Ahmed, A.N., Teo, F.Y., Ng, J.L. and Elshafie, A. (2022). Evaluation of spatial interpolation methods and spatiotemporal modeling of rainfall distribution in Peninsular Malaysia. *Ain Shams Engineering Journal*, [online] 13(2), p.101571. doi:10.1016/j.asej.2021.09.001.

GDA (2019). *Servicio de Retirada de Amianto en Lleida*. [online] La Plataforma del Amianto de España. Available at: https://gestiondelamianto.com/retirada-amianto-lleida/ .

GENCAT. (2019). [online] Available at: http://www.gencat.cat/mediamb/publicacions/Estudis/EDIS_sector_energetic.pdf.

Gencat.cat. (2013). *Informació general – Article Categories – API REST de Dades Meteorològiques | Meteocat*. [online] Available at: https://apidocs.meteocat.gencat.cat/informacio-general/.

General Forest Policy Plan of Catalonia. (2014). [online] Available at: http://agricultura.gencat.cat/web/.content/06-medi-natural/boscos/planificacio-forestal/pla-general/05_Appendix_05_Appendixos.pdf.

Gilman, P., DiOrio, N.A., Freeman, J.M., Janzou, S., Dobos, A. and Ryberg, D. (2018). SAM Photovoltaic Model Technical Reference 2016 Update. [online] doi:10.2172/1429291.

GitHub. (2022). *Sandia National Laboratories*. [online] Available at: https://github.com/sandialabs.

Gobierno de españa ministerio de industria, turismo y comercio. (2009). [online] Available at: https://www.idae.es/uploads/documentos/doc_Biomasa_Edificios_A2007_6862bde5.pdf.

Gueymard, C. (2010). *PROGRESS IN DIRECT IRRADIANCE MODELING AND VALIDATION*. [online] Available at: https://www.solarconsultingservices.com/Gueymard-DNI_models_validation.

Halit Apaydin, Fajri Kemal and Re, E. (2004). Spatial interpolation techniques for climate data in the GAP region in Turkey. *Climate Research*, [online] 28, pp.31–40. doi:10.3354/cr028031.

Hi-vawt. (2012). Hi-VAWT DS-700 Vertical Axis Wind Turbines. [online] Available at: http://www.hi-vawt.com.tw/en/ds700w.html.

HostecServeis. (2015). *Precio Retirada Uralita en 2022 | ¿Cuanto Cuesta? retiradauralita.org*. [online] Available at: https://www.retiradauralita.org/retirar-uralita.

IDAE. (2011). [online] Available at: https://www.idae.es/sites/default/files/documentos_5654_FV_pliego_condiciones_tecnicas_instalaciones_conectadas_a_red_C20_Julio_2011_3498eaaf.pdf.

Idae.es. (2020). *Nuevo Reglamento de diseño ecológico para calderas de biomasa, 'ECODISEÑO 2020' | Idae*. [online] Available at: https://www.idae.es/noticias/nuevo-reglamento-de-diseno-ecologico-para-calderas-de-biomasa-ecodiseno-2020.

Idae.es. (2021). *Evaluación del potencial de energía geotérmica | Idae*. [online] Available at: https://www.idae.es/publicaciones/evaluacion-del-potencial-de-energia-geotermica.

Idescat.cat. (2022). *Idescat. El municipi en xifres*. [online] Available at: https://www.idescat.cat/emex/?id=250735.

IEA – International Energy Agency (2015). [online] Biomass for Heat and Power. Technology Brief. Available at: https://www.irena.org/-/media/Files/IRENA/Agency/Publication/2015/IRENA-ETSAP_Tech_Brief_E05_Biomass-for-Heat-and-Power.pdf.

IEA – International Energy Agency (2022). [online] IEA. Available at: https://www.iea.org/.

INE. (2016). *Instituto Nacional de Estadística*. [online] Available at: https://www.ine.es/dyngs/INEbase/es/operacion.htm?c=Estadistica_C&cid=1254736176951&menu=ultiDatos&idp=1254735572981.

Informe del sector de l'energia, 2009. [online] Available at: http://www.gencat.cat/mediamb/publicacions/Estudis/EDIS_sector_energetic.pdf.

Institut Català d'Energia. (2019) Pla de biomassa a Catalunya en l'àmbit agrícola. Convenio de colaboración entre la Universidad de Lleida y el Institut Català de l'Energia. Generalitat de Catalunya, Departament d'Indústria, Comerç i Turisme. [online] Available at: https://icaen.gencat.cat/ca/plans_programes/estrategia_biomassa/.

IRENA (2019). *FUTURE OF SOLAR PHOTOVOLTAIC Deployment, investment, technology, grid integration and socio-economic aspects A Global Energy Transformation paper About IRENA*. [online] Available at: https://irena.org/-/media/Files/IRENA/Agency/Publication/2019/Nov/IRENA_Future_of_Solar_PV_2019.pdf.

Jamileh Shojaeiarani, Bajwa, D.S. and Bajwa, S. (2019). *Properties of Densified Solid Biofuels in Relation to Chemical Composition, Moisture Content, and Bulk...* [online] ResearchGate. Available at: https://www.researchgate.net/publication/332530709_Properties_of_Densified_Solid_Biofuels_in_Relation_to_Chemical_Composition_Moisture_Content_and_Bulk_Density_of_the_Biomass.

Jorgenson, J., Gilman, P. and Dobos, A. (2011). *Technical Manual for the SAM Biomass Power Generation Model*. [online] Available at: https://www.nrel.gov/docs/fy11osti/52688.pdf.

Juan, Lamas, M.I., Antonio Couce Casanova and Damota, J. (2015). *Vertical Axis Wind Turbines: Current Technologies and Future Trends*. [online] ResearchGate. Available at: https://www.researchgate.net/publication/274318535_Vertical_Axis_Wind_Turbines_Current_Technologies_and_Future_Trends.

Juan Carlos Santamarta and Jarabo, F. (2013). *Aprovechamientos Energéticos. Biomasa*. [online] ResearchGate. doi:10.13140/RG.2.1.1459.4167

Kalina, M., Fonseca, M., IlbayYupa, M. and Srta Alisson Iza (2018). Comparison of interpolation methods for the estimation of temperature of cease reservoir. [online] ResearchGate. Available at: https://www.researchgate.net/publication/INTERPOLATION_METHODS.

Krannich Solar. (2022). *PIKO CI 50*. [online] Available at: https://shop.krannich-solar.com/de-en/products/inverters/solar-inverters/23331/piko-ci-50.

Kumari, N., Sakai, K. and Gunarathna (2018). *Are geostatistical interpolation techniques better than deterministic interpolation methods?* [online] ResearchGate. Available at: https://www.researchgate.net/publication/329906037_ARE_GEOSTATISTICAL_INTERPOLATION_TECHNIQUES_BETTER_THAN_DETERMINISTIC_INTERPOLATION_METHODS.

Lett, R.G. and Ruppel, T.C. (2004). Coal, Chemical and Physical Properties. *Encyclopedia of Energy*, [online] pp.411–423. doi:10.1016/b0-12-176480-x/00283-7.

Liu, H. (2011). Biomass fuels for small and micro combined heat and power (CHP) systems: resources, conversion and applications. *Small and Micro Combined Heat and Power (CHP) Systems*, [online] pp.88–122. doi:10.1533/9780857092755.1.88.

Louwen, A., Moser, D. and van Sark, W.G.J.H.M. (2022). Design and Components of Photovoltaic Systems. *Comprehensive Renewable Energy*, [online] pp.644–661. doi:10.1016/b978-0-12-819727-1.00100-x.

Malik, B., Bilal, T., Sheikh Tajamul Islam and Reiaz ul Rehman (2015). Biomass Pellet Technology: A Green Approach for Sustainable Development. *Agricultural Biomass Based Potential Materials*, [online] pp.403–433. doi:10.1007/978-3-319-13847-3_19.

Mani, S., Tabil, L.G. and Sokhansanj, S. (2004). Grinding performance and physical properties of wheat and barley straws, corn stover and switchgrass. *Biomass and Bioenergy*, [online] 27(4), pp.339–352. doi:10.1016/j.biombioe.2004.03.007.

María Paz Aguilera, Domingo Ortega Calderón, Beltrán, G. and Marino Uceda Ojeda (2004). *Influencia del régimen hídrico en la formación de aceite de Arbequina*. [online] ResearchGate. Available at: https://www.researchgate.net/publication/28279937_Influencia_del_regimen_hidrico_en_la_formacion_de_aceite_de_Arbequina.

Martin-Vide, J., Prohom, M., Busto, M. and Jordi Camins (2016). *Evolució recent de la temperatura, la precipitació i altres variables climàtiques a Catalunya*. [online] ResearchGate. Available at: https://www.researchgate.net/publication/311681257_Evolucio_recent_de_la_temperatura_la_precipitacio_i_altres_variables_climatiques_a_Catalunya.

Maxwell, E. (1987). *A Quasi-Physical Model for Converting Hourly Global Horizontal to Direct Normal lnsolation*. [online] Available at: https://www.nrel.gov/docs/legosti/old/3087.pdf.

Menacho, T., María, A. and Domingo, A. (2002). *Demografía y crecimiento de la población española durante el siglo XX*. [online] ResearchGate. Available at: https://www.researchgate.net/Demografia_de_la_poblacion_espanola_durante_el_siglo_XX.

Meteo.cat. (2012). *Llistat d'estacions meteorològiques automàtiques de Catalunya*. [online] Available at: https://www.meteo.cat/observacions/llistat-xema.

Meteo.cat. (2019). *Climatologies comarcals - Servei Meteorològic de Catalunya*. [online] Servei Meteorològic de Catalunya. Available at: https://www.meteo.cat/wpweb/climatologia/el-clima-ahir/climatologia-comarcal/.

Meteo.cat. (2022). *Dades de l'estació automàtica la Granadella - Servei Meteorològic de Catalunya*. [online] Available at: https://www.meteo.cat/observacions/xema/dades?codi=UM.

Miteco.gob.es. (2012). *Objetivos de reducción de emisiones de gases de efecto invernadero*. [online] Available at: https://www.miteco.gob.es/mitigacion-politicas-y-medidas/objetivos.

Monin-Obukhov. (1954). Basic laws of turbulent mixing in the ground layer of the atmosphere. Trud. Geofiz. Inst. Akad. Nauk. SSSR, No. 24, 151, pp. 163–187. Traducción del Ruso en 1959, por American Meteorological Society. [online] Available at: http://handle.dtic.mil/100.2/AD672723.

Nasa.gov. (2020). Application of a global-to-beam irradiance model to the NASA GEWEX SRB dataset: An extension of the NASA Surface meteorology and Solar Energy datasets | FIREX-AQ. [online] Available at: https://espo.nasa.gov/firex-aq/content/Application_of_a_global-to-beam_irradiance_model_to_the_NASA_GEWEX_SRB_dataset_An_extension.

National Geographic Society (2019). *Renewable Resources*. [online] National Geographic Society. Available at: https://www.nationalgeographic.org/encyclopedia/renewable-resources/.

New World Wind. (2019). *The Wind Tree - New World Wind*. [online] Available at: https://newworldwind.com/en/wind-tree/.

NOAA (2022). *Calculating zenith and azimuth angles for GridSat-B1* [online]. Noaa.gov. Available at: https://www.ncdc.noaa.gov/gridsat/docs/Angle_Calculations.pdf

Nrel.gov. (2013). *Power Purchase Agreement (PPA) - My site*. [online] Available at: https://sam.nrel.gov/financial-models/utility-scale-ppa.html.

Nrel.gov. (2014). *Weather Data - My site*. [online] Available at: https://sam.nrel.gov/weather-data.html

Nrel.gov. (2021a). *Recent Topics*. [online] Available at: https://sam.nrel.gov/forum/recent.html.

Nrel.gov. (2021b). *Residential and Commercial - My site*. [online] Available at: https://sam.nrel.gov/financial-models/residential-and-commercial.html.

Nrel.gov. (2021c). *Software Development Kit (SDK) - My site*. [online] Available at: https://sam.nrel.gov/weather-data.html.%20Accessed:%2007/19/19.

Nrel.gov. (2022). *Biomass Combustion - My site*. [online] Available at: https://sam.nrel.gov/biomass/55-biomass.html.

OECD (2022). *OECD.org - OECD*. [online] Available at: https://www.oecd.org/.

Olah, G.A., Alain Goeppert and Surya, K. (2018). *Fossil Fuels and Climate Change*. [online] ResearchGate. doi: 10.1002/9783527805662.ch7

Pellets del Sur. (2020). *Venta de Hueso de Aceituna a un Precio Increíble al Por Mayor y al Por Menor.* [online] Available at: https://pelletsdelsur.com/projects/hueso-de-aceituna-calidad-a1/.

Perez, R., Stewart, R., Seals, R. and Guertin, T. (1988). *The development and verification of the Perez diffuse radiation model*. [online] www.osti.gov. Available at: https://www.osti.gov/servlets/purl/7024029 .

Perez, R., P. Ineichen, R. Seals, J. Michalsky and R. Stewart. 1990. "Modeling Daylight Availability and Irradiance Components from Direct and Global Irradiance," Solar Energy, Vol. 44, pp. 271-289.

Perez, R. R., P. Ineichen, E. Maxwell, F. Seals and A. Zelenda. 1991. "Dynamic Models for Hourly Global-to-direct Irradiance Conversion," in 1991 Solar World Congress: Proceedings of the Biennial Congress of the International Solar Energy Society, Vol. 1 (II): pp. 951-956.

Prieto, G. (2017). *El reparto de las horas de sol en el mundo - Geografía Infinita*. [online] Geografía Infinita. Available at: https://www.geografiainfinita.com/2017/07/reparto-las-horas-sol-mundo/.

Qazi, S. (2017). Mobile Photovoltaic Systems for Disaster Relief and Remote Areas. *Standalone Photovoltaic (PV) Systems for Disaster Relief and Remote Areas*, [online] pp.83–112. doi:10.1016/b978-0-12-803022-6.00003-4.

Quelart, R. (2013). *Más de un centenar de pueblos están abandonados en Catalunya*. [online] La Vanguardia. Available at: https://www.lavanguardia.com/pueblos-abandonados-catalunya.html.

Ramakumar, R., Abouzahr, I., Krishnan, K. and Ashenayi, K. (1995). Design scenarios for integrated renewable energy systems. *IEEE Transactions on Energy Conversion*, [online] 10(4), pp.736–746. doi:10.1109/60.475847.

Rossi, R.E., Dungan, J.L. and Beck, L.R. (1994). Kriging in the shadows: Geostatistical interpolation for remote sensing. *Remote Sensing of Environment*, [online] 49(1), pp.32–40. doi:10.1016/0034-4257(94)90057-4.

Ruiz, J. (2021). *Generador De Energia Fotovoltaica Dc/Ac Para Corporacion Expresiones Artisticas Arcoiris De Bogota -USME*. [online] Available at: https://repository.ucatolica.edu.co/bitstream/10983/27025/1/GENERADOR%20DE%20ENERGIA%20FOTOVOLTAICA%20DCAC%20PARA%20CORPORACION%20EXPRESIONES.

Saidatul Shema Saad, Daut, I., Muhammad Irwanto and Nor. (2011). Study of inverter design and topologies for photovoltaic system. *International Conference on Electrical, Control and Computer Engineering 2011 (InECCE)*. [online] doi:10.1109/inecce.2011.5953934.

SAM Help's System (2022). [online] Available at: https://sam.nrel.gov/images/web_page_files/sam-help-2021-12-02r1.pdf.

SAM file format description from Help (2020). [online] Available at: https://sam.nrel.gov/images/web_page_files/sam-help-2020-2-29-r2_weather_file_formats.pdf

Sandialabs (2016). *GitHub - sandialabs/MATLAB_PV_LIB: MATLAB PV function library*. [online] GitHub. Available at: https://github.com/sandialabs/MATLAB_PV_LIB [Accessed 13 May 2022].

Sathe, A., Gryning, S.-E. and Peña, A. (2011). Comparison of the atmospheric stability and wind profiles at two wind farm sites over a long marine fetch in the North Sea. *Wind Energy*, [online] 14(6), pp.767–780. doi:10.1002/we.456.

Sciencing. (2020). *How to Calculate Height & Velocity*. [online] Available at: https://sciencing.com/calculate-height-velocity-8115675.html.

Sedecatastro.gob.es. (2022). *Sede Electrónica del Catastro - Inicio*. [online] Available at: http://www.sedecatastro.gob.es/.

Short, W., Packey, D. and Holt, T. (1995). *A Manual for the Economic Evaluation of Energy Efficiency and Renewable Energy Technologies*. [online] Available at: https://www.nrel.gov/docs/legosti/old/5173.pdf.

Shylaja, B.S. (2015). From navigation to star-hopping: forgotten formulae. *Resonance*, [online] 20(4), pp.352–359. doi:10.1007/s12045-015-0190-7.

Sluiter, R. (2009). *Interpolation methods for climate data*. [online] ResearchGate. Available at: https://www.researchgate.net/publication/242783501_Interpolation_methods_for_climate_data

Solar Power | Renewable Energy | Green Energy. (2021). *A Simple Guide to Grid-Tied Solar Energy Systems*. [online] Available at: https://sunedisoninfra.com/blog/a-simple-guide-to-grid-tied-solar-energy-systems/.

Solaredge.com. (2018). *SolarEdge Technologies Inc.* [online] Available at: https://www.solaredge.com/us/products/pv-inverters/synergy-inverter#/.

Solarelectricsupply.com. (2014). *REC Alpha REC380AA 380 Watt Solar Panel*. [online] Available at: https://www.solarelectricsupply.com/rec380aa-rec-alpha-solar-panel.

Spain. Royal Decree *1367/2007, of 19th October, por el que se desarrolla la Ley 37/2003, de 17 de noviembre, del Ruido, en lo referente a zonificación acústica, objetivos de calidad y emisiones acústicas.* [online] Available at: https://www.boe.es/act.php?id=BOE-A-2007-18397.

Spain. Royal Decree *178/2021, of 23rd March, por el que se modifica el Real Decreto 1027/2007, de 20 de julio, por el que se aprueba el Reglamento de Instalaciones Térmicas en los Edificios.* [online] Available at: https://www.boe.es/buscar/doc.php?id=BOE-A-2021-4572 .

Spain. Royal Decree *244/2019, of 5th April, por el que se regulan las condiciones administrativas, técnicas y económicas del autoconsumo de energía eléctrica.* [online] Available at: https://www.boe.es/buscar/doc.php?id=BOE-A-2019-5089

Spain. Royal Decree *396/2006, of 1st March, por el que se establecen las disposiciones mínimas de seguridad y salud aplicables a los trabajos con riesgo de exposición al amianto.* [online] Available at: https://www.boe.es/buscar/act.php?id=BOE-A-2006-6474.

Spain. Royal Decree *436/2004, of 12th March, por el que se establece la metodología para la actualización y sistematización del régimen jurídico y económico de la actividad de producción de energía eléctrica en régimen especial.* [online] Available at: https://www.boe.es/buscar/doc.php?id=BOE-A-2004-5562.

Spain. Royal Decree *477/2021, of 29th June, por el que se aprueba la concesión directa a las comunidades autónomas y a las ciudades de Ceuta y Melilla de ayudas para la ejecución de diversos programas de incentivos ligados al autoconsumo y al almacenamiento, con fuentes de energía renovable, así como a la implantación de sistemas térmicos renovables en el sector residencial, en el marco del Plan de Recuperación, Transformación y Resiliencia.* [online] Available at: https://www.boe.es/diario_boe/txt.php?id=BOE-A-2021-10824.

Spain. Royal Decree *692/2021, of 3rd August, por el que se regula la concesión directa de ayudas para inversiones a proyectos singulares locales de energía limpia en municipios de reto demográfico (PROGRAMA DUS 5000), en el marco del Programa de Regeneración y Reto Demográfico del Plan de Recuperación, Transformación y Resiliencia.* [online] Available at: https://www.boe.es/diario_boe/txt.php?id=BOE-A-2021-13269.

Spain, Law *24/2013, of 26th December, del Sector Eléctrico.* [online] Available at: https://www.boe.es/buscar/act.php?id=BOE-A-2013-13645.

Statista. (2022). *Topic: Wind energy in Spain*. [online] Available at: https://www.statista.com/topics/9046/wind-energy-in-spain/.

SunPower Residential (2021). *SunPower X-Series Residential AC SPR-X22-370-E-AC | EnergySage*. [online] Energysage.com. Available at: https://www.energysage.com/solar-panels/sunpower/1436/spr-x22-370-e-ac/.

Turisme de les Garrigues. (2021). *Rutes - Turisme de les Garrigues*. [online] Available at: https://www.turismegarrigues.com/ca/comarca/poblacions/cerviadelesgarrigues/rutes/.

Uab.cat. (2022). *Regió Forestal VIII: Cobertes del sól per municipis*. [online] Available at: http://www.creaf.uab.cat/iefc/pub/regions/Comarques/CobertesGarrigues.htm.

US (2022). *ESRL Global Monitoring Laboratory - Global Radiation and Aerosols*. [online] Noaa.gov. Available at: https://gml.noaa.gov/grad/solcalc/calcdetails.html

Vega, I. (2022). *EL PAÍS: el periódico global*. [online] El País. Available at: https://elpais.com/espana/2022-02-09/la-poblacion-de-los-municipios-pequenos-y-rurales-en-espana-crece-casi-un-10-de-media-en-los-ultimos-25-anos.html.

Velasquez Giron, Botero Fernandez and Ignacio Velez (2011). Rainfall Distribution Based on a Delaunay Triangulation Method. *2010 International Symposium on Voronoi Diagrams in Science and Engineering*. [online] doi:10.1109/isvd.2010.11.

Wagner, H.-J. . (2017). Introduction to wind energy systems. *EPJ Web of Conferences*, [online] 148, p.00011. doi:10.1051/epjconf/201714800011.

Wuebbles, D.J. and Jain, A.K. (2001). Concerns about climate change and the role of fossil fuel use. *Fuel Processing Technology*, [online] 71(1-3), pp.99–119. doi:10.1016/s0378-3820(01)00139-4.

Www.boe.es. (2012). *BOE.es - DOUE-L-2001-82354 Directiva 2001/77/CE del Parlamento Europeo y del Consejo, de 27 de septiembre de 2001, relativa a la promoción de la electricidad generada a partir de fuentes de energía renovables en el mercado interior de la electricidad.* [online] Available at: https://www.boe.es/buscar/doc.php?id=DOUE-L-2001-82354.

Yang, T., Clements-Croome, D. and Marson, M. (2017). Building Energy Management Systems. Encyclopedia of Sustainable Technologies, [online] pp.291–309. doi:10.1016/b978-0-12-409548-9.10199-x.

Zbigniew Lubosny (2003). Wind Turbine Operation in Electric Power Systems. *SpringerLink*. [online] doi:10.1007-978-3-662-10944-1.

Appendix I. Description of the area and proprietorship

1. Information about the area

1.1 Cadastral map of the area

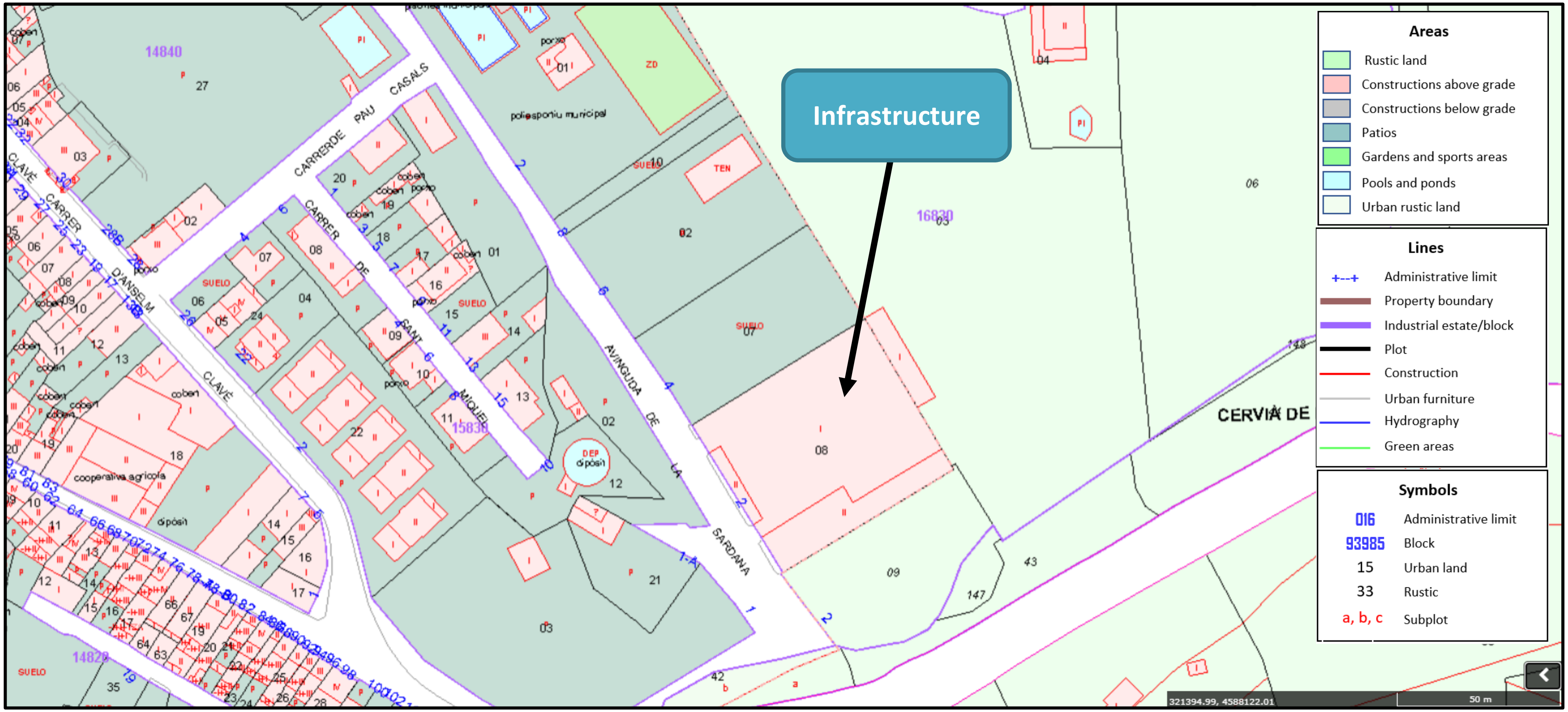

(Adapted from Sedecatastro.gob.es, 2022.)

1.2 Soil classification map of Cervià de les Garrigues

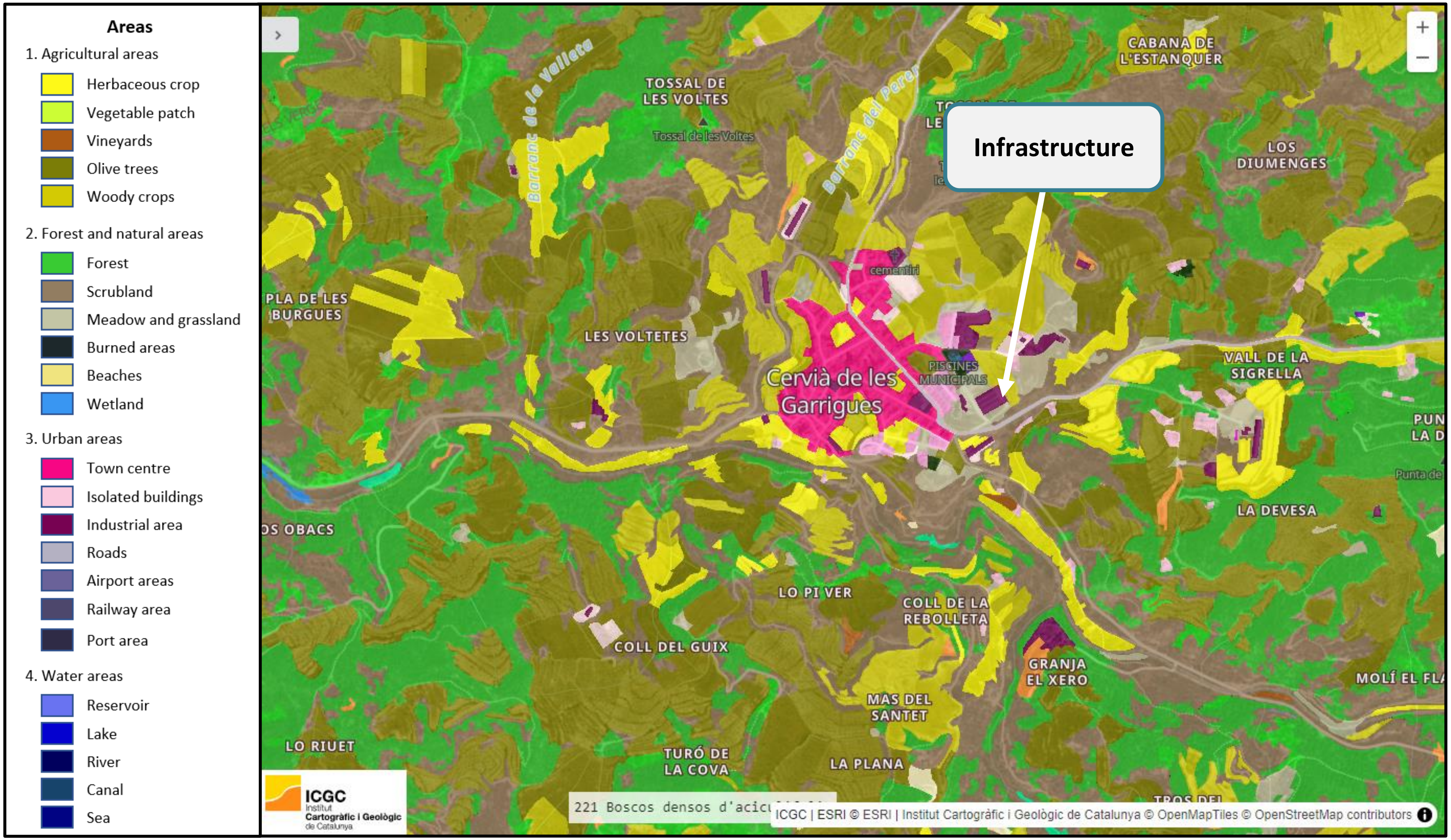

(Adapted from Icgc.cat, 2018.)

2. Infrastructure plans

Attached in this appendix are the plans of the three industrial buildings provided by the town council of Cervià de les Garrigues. Note that the plans are from a 1993 document and only an old scanned version is available. Therefore, it has been reconstructed and edited in the clearest and most understandable form in order to give a notion of infrastructure.

2.1 Section plan of the infrastructure

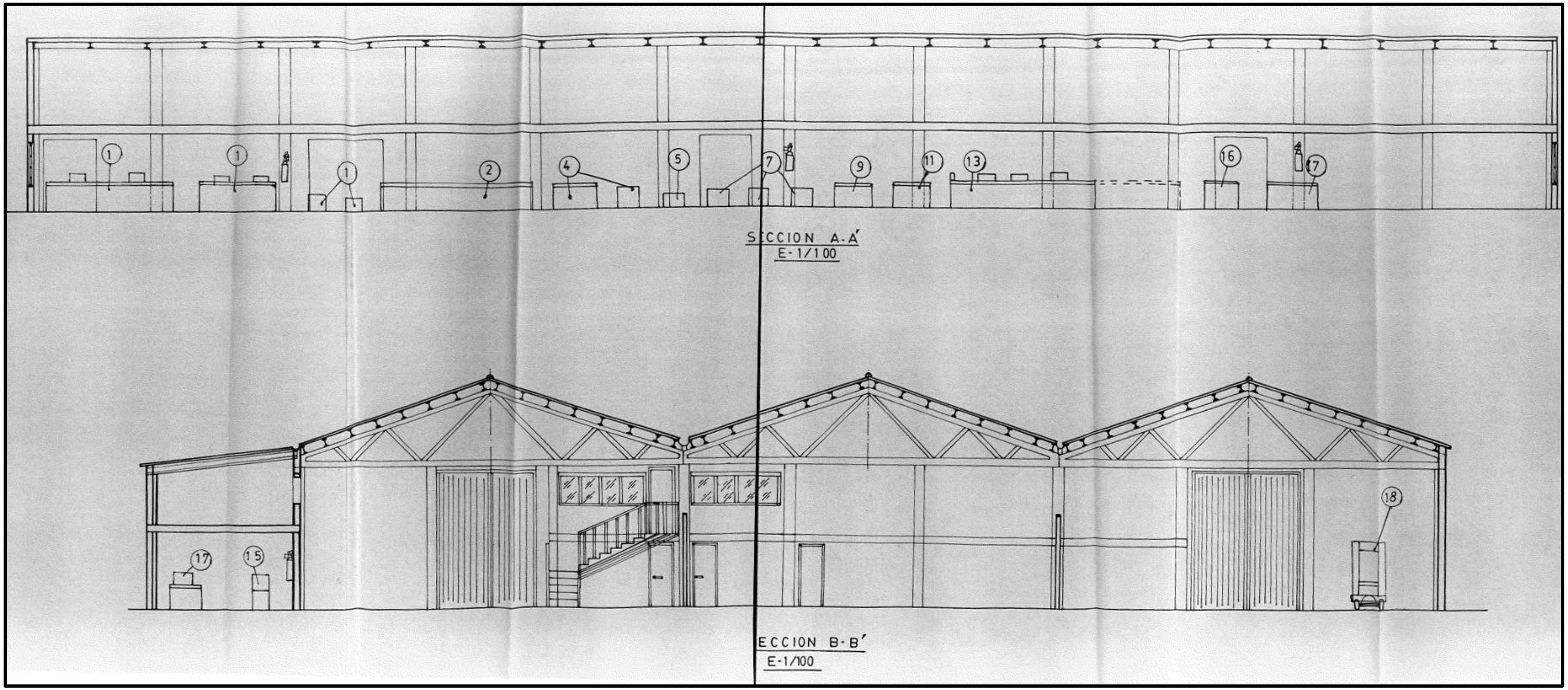

(City Council of Cervià de les Garrigues 2022, personal communication, 22 January).

2.2 Floor plan of the three industrial buildings

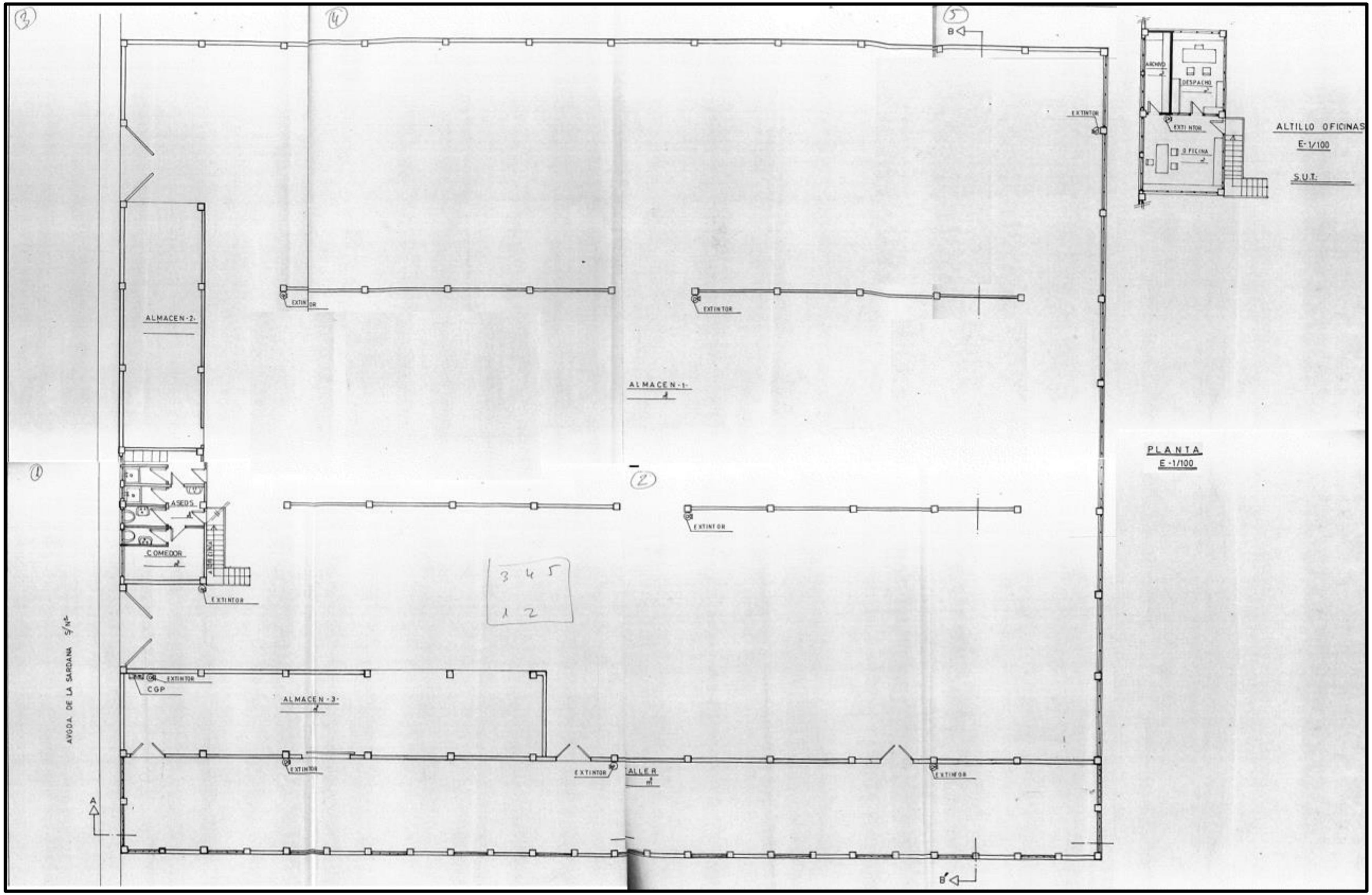

(City Council of Cervià de les Garrigues 2022, personal communication, 22 January).

2.3 Electrical wiring installation diagrams

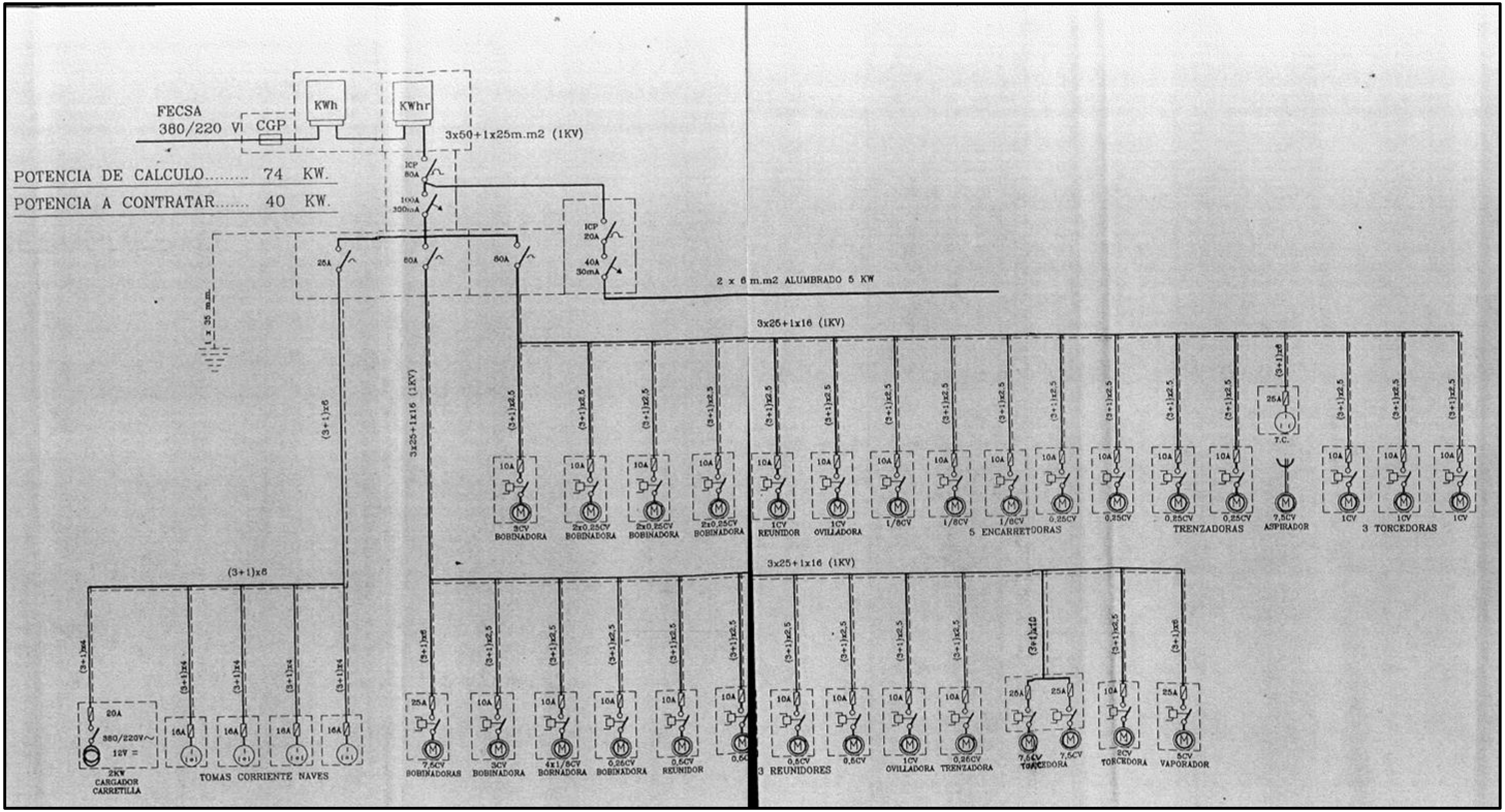

(City Council of Cervià de les Garrigues 2022, personal communication, 22 January).

3. Classification and explication of the relevant legal regulations for the project

A compendium of the national laws is held online for the public. Full details of this legislation can be found in the references indicated in the table.

	European Legislation	Spanish Legislation	Catalan Legislation
Energy efficiency and savings	**European Directive 2006/32/CE of 5th April 2006:** Encourage cost-effective efficiency improvements in energy end-use. **Community Program SAVE:** Promoting energy efficiency and energy saving in different sectors through policy measures, studies, pilot actions, and the creation of Energy Management Agencies.	**Royal Decree 56/2016 of 12th February:** Efficiency in the power supply system. **Energy Saving and Efficiency Action Plan:** efficiency improvements in energy end-use. **Royal Decree 900/2015 of 9th October:** The administrative and economic conditions of the supply of electrical energy through self-consumption are regulated.	**Energy Sector Plan:** It envisages scenarios that reflect imminent growth in energy consumption with initiatives to improve energy efficiency and promote savings.
Renewable Energies use	**Directive 2009/28/CE of 23rd April 2009:** This directive acts as an incentive to use more environmentally friendly methods of obtaining energy such as renewable energy. **Directive (EU) 2018/2001 of 11th December 2018:** the use of energy from renewable sources is promoted.	**Royal Decree 413/2014 of 6th June:** The production of electricity from renewable energy sources, cogeneration and waste is regulated. **Renewable Energy Plan:** aims to ensure that renewable sources represent at least 20% of Spain's final energy consumption by 2025. **Royal Decree (436/2004) of 12th March:** the owner of the installation can vend the electricity generated to the distribution company at an agreed regulated rate or sell it to the market. **Climate Change and Energy Transition Law (May 2019):** Reduction of greenhouse gas emissions, implementation of renewable energy and energy efficiency.	**Energy Sector Plan:** It envisages scenarios that reflect imminent growth in energy consumption with initiatives to improve the use of renewable energy.
Efficiency Certifications	**European Green Deal:** reduce greenhouse gas emissions in the European Union by at least 55% compared to 1990 by 2030.	**Royal Decree 235/2013 of 5th April:** when building, selling or renting a building, it is accompanied by a certificate of energy efficiency (certification of the energy efficiency of buildings). **Royal Decree (244/2019) and Law (24/2013) of 5th April:** define the two different forms of self-consumption.	**Since 1/6/2013:** It is mandatory to have an energy certificate for existing buildings and homes that are rented or sold, and for buildings frequented and occupied by the public. **Law (16/2017) of 1st August:** established the objectives of reducing greenhouse gas emissions by 40% in 2030, 65% in 2040 and 100% in 2050.

Solar energy	**Clean Energy for All Europeans:** allows production, storing and selling of energy generated with photovoltaic panels.	**Royal Decree 14/2010 of 23rd December:** Set limits on the equivalent hours of operation of photovoltaic installations. **Royal Decree 1003/2010 of 5th August:** The settlement of the premium equivalent to special-regime photovoltaic technology power generation facilities is regulated. **Royal Decree 1663/2000 of 29th September:** connection of photovoltaic installations to the low-voltage network.	**Decree 352/2001 of 18th December:** Defines the administrative procedure applicable to photovoltaic solar energy installations connected to the electricity grid.
Wind energy	**EU Biodiversity Strategy to 2030:** focuses on the causes of biodiversity loss, such as unsustainable use of land and sea, overexploitation of natural resources, and pollution caused by wind energy.	**Royal Decree (947/2015) of 16th October:** a specific remuneration regime is established for new wind technology installations.	**Decree 174/2002 of 11th June:** regulates the execution of wind energy in Catalonia
Biomass energy	**Renewable Energy Directive 2018/2001 of 11th December 2018:** establish sustainability criteria to cover large-scale biomass for heat and power.	**Royal Decree (178/2021) of 23rd March:** applies the UNE 303-5 standard, which establishes minimum requirements for energy efficiency and emission values depending on the characteristics of the boiler	**Generalitat de Catalunya, Law 22/2011 of 28th June:** states that the materials to be used for biomass production are excluded from the state law on waste and polluting soils (Law 22/2011, of 28-07-2011)

(Adapted from Energy, 2022; BOE, 2022; GENCAT, 2009).

4. Final design simulation

It should be noted that the biomass boiler's chimney has not been simulated because its characteristics and dimensions are not calculated.

(Author’s own, adapted with Sweet Home 3D).

(Author’s own, adapted with Sweet Home 3D).

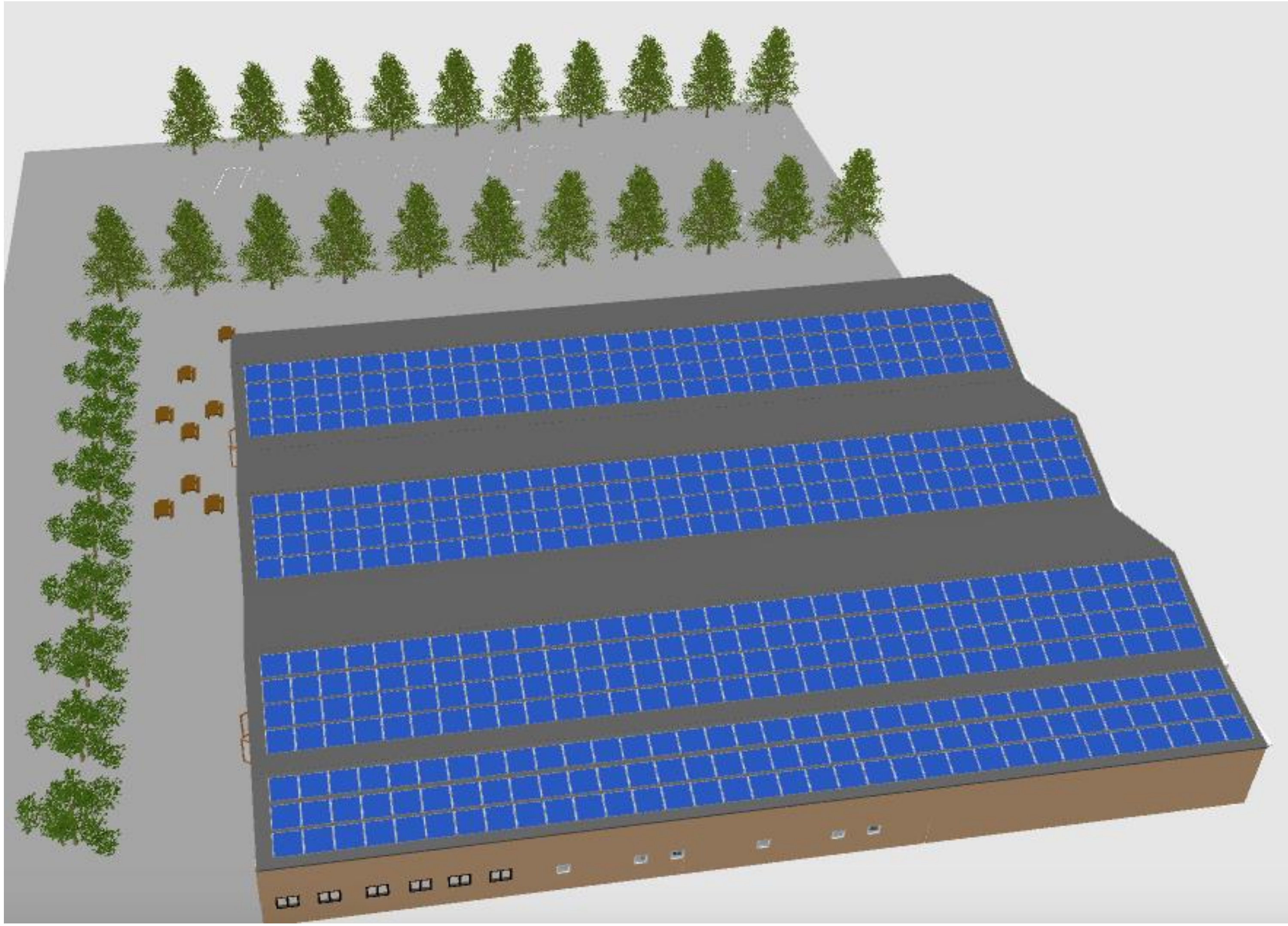

(Author’s own, adapted with Sweet Home 3D).

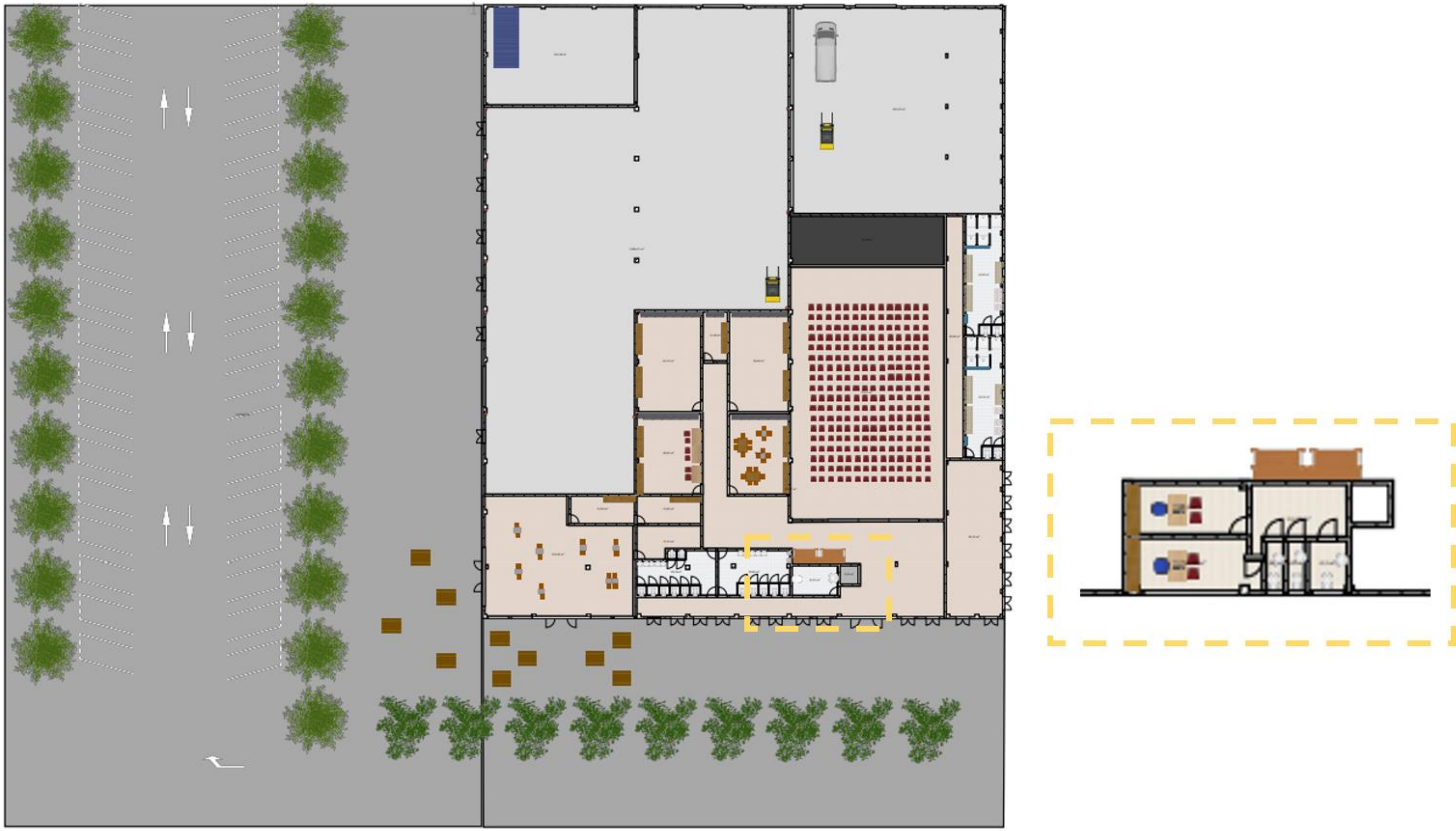

(Author's own, adapted with Sweet Home 3D).

5. Cervià public annual electricity bill

Table of the annual public electricity bill of Cervià de les Garrigues provided by the city council.

Street	Use of the building	Power	Cost [€/yr]
C/Albi, 20	Library	P.1 - 35 kW P.3 - 35 kW P.5 - 35 kW	6225.5
Av. Garrigues, 3	Funeral Home	P.1 - 6 kW P.3 - 6 kW	667.48
Albi 112	Water Pump	P.1 - 7 kW P.3 - 7 kW	2609.74
Av. Paisos Catalans, 5	School	P.1 - 6 kW P.3 - 6 kW	1559.75
11 Septembre	Futbol Field	P.1 - 15 kW P.3 - 15 kW	839.91
11 Septembre	Sports Zone	P.1 - 6 kW P.3 - 6 kW	346.83
Pl. Major 1	Social Local	P.1 - 2 kW P.3 - 2 kW	106.65
Palau 1	Town Hall	P.1 - 14 kW P.3 - 14 K kW	1906.8
Anselm Clave SN699	Public Lights	P.1 - 15 kW P.3 - 15 kW	6362.89
Albi 112	Trade Union	P.1 - 13 kW P.3 - 13 kW	4511.66
Av. Paisos Catalans, 2	Swimming Pools	P.1 - 13 kW P.3 - 13 kW	3275.27

(City Council of Cervià de les Garrigues 2022, personal communication, 25 January).

The purchase price according to the three-time bands was also provided:

	Power Consumption	**Power**	**Power Consumption**	**Power**
	<35 KW		**>35 KW**	
Time Slot	[€/kW]	[€/kW]	[€/kW]	[€/kW]
Peak	0.164681	0.076599	0.099627	0.111586
Standard	0.09521	0.0400235	0.085853	0.066952
Off-Peak	0.064021	0.003448	0.058686	0.0444634

(City Council of Cervià de les Garrigues 2022, personal communication, 25 January).

Appendix II. Calculations procedures

1. Distance between two geographical coordinates applying the Haversine formula

The distance in kilometres between two given locations with their respective coordinates can be calculated by applying spherical trigonometry with the Haversine formula:

$\boldsymbol{Location\ 1} = Latitude_1, Longitude_1[rad]$ $\boldsymbol{Location\ 2} = Latitude_2, Longitude_2[rad]$

It can be calculated by applying the Haversine's formula:

$$\Delta latitude = Latitude_2 - Latitude_1[rad] \quad (I)$$

$$\Delta longitude = Longitude_2 - Longitude_1[rad] \quad (II)$$

$$h = \sin^2\left(\frac{\Delta latitude}{2}\right) + \cos(Latitude_1) * \cos(Latitude_2) * \sin^2\left(\frac{\Delta longitude}{2}\right) \quad [rad] \quad (III)$$

$$distance = R \cdot 2 \cdot \arctan\left(\frac{\sqrt{h}}{\sqrt{1-h}}\right) \quad [km] \quad (IV)$$

Where:

R: Radius of the earth (6378 km)

Adapted from (Shylaja, 2015).

2. Empirical values of wind shear exponent

The table offers different empirical coefficients of wind shear exponents according to the characteristics of the area. However, there is no information about the weather station's environment. For this reason, using Google Earth (see: https://earth.google.com/web/) and introducing its coordinates, it is determined that the surroundings are "Tall row crops, hedges, a few trees" which provides a coefficient of 0.2 (see following table).

Terrain Description	Power law exponent, α
Smooth, hard ground, lake or ocean	0.10
Short grass on untilled ground	0.14
Level country with foot-high grass, occasional tree	0.16
Tall row crops, hedges, a few trees	0.20
Many trees and occasional buildings	0.22 – 0.24
Wooded country – small towns and suburbs	0.28 – 0.30
Urban areas with tall buildings	0.4

(Bratton & Womeldorf, 2011).

3. Calculation of the minimum distance between panels for the Alpha-REC380AA model

The minimum distance (md2) in a horizontal surface between Alpha-REC380AA panels (REC Solar manufacturer) is calculated. Note that the dimensions are 1.016 x 1.721 [m]:

$$cos(tilt\ angle) = \frac{dx}{panel\ length} \rightarrow cos(38) = \frac{dx_2}{1.016\ m} \rightarrow dx_2 = 0.8006\ m \qquad (V)$$

$$sen(tilt\ angle) = \frac{h}{panel\ length} \rightarrow sen(38) = \frac{h_2}{1.016\ m} \rightarrow h_2 = 0.6255\ m \qquad (VI)$$

$$d = \frac{h}{tg(60º - latitude)} \rightarrow d_2 = \frac{0.6255}{tg(60º - 41.424637)} = 1.8613 \qquad (VII)$$

$$md_2 = dx_2 + d_2 = 2.6621\ m \qquad (VIII)$$

4. Correspondence of the selected dates for SAM’s weather files

The table describes the correspondence of the selected dates for the SAM's weather file:

Month	Days	Choosed Year
January	1st - 15th	2019
	15th - 24th	2020
	25th - 31st	2017
February	1st - 28th	2022
March	1st - 15th	2018
	16th - 31st	2021
April	1st - 10th	2017
	11th - 20th	2019
	21st - 30th	2021
May	1st - 8th	2020
	9th - 22nd	2018
	23th - 31st	2019
June	1st - 15th	2021
	16th - 30th	2017

Month	Days	Choosed Year
July	1st - 15th	2019
	16th - 31st	2020
August	1st - 24th	2021
	25th - 31st	2018
September	1st - 4th	2021
	5th - 12th	2017
	13th - 22nd	2019
	23rd - 30th	2021
October	1st - 20th	2020
	21st - 31st	2019
November	1st - 30th	2018
December	1st - 10th	2020
	11th - 20th	2017
	21st - 31st	2021

(Author’s own, adapted from data facilitated by the City Council of Cervià).

5. Estimation of the annual consumption in kWh from the electricity bill and the pricing

Ubication	Municipal equipment	Contracted power [kW]	Import [€/yr]	Import without taxes[1] [€/yr]	Power Import[2] [€/yr]	Consumption Import[3] [€/yr]	Power Consumption[4] [kWh/yr]
Albi, 20	Library	35 kW	6225.50	5119.65	511.30	4606.72	49240.79
Av. Garrigues, 3	Funeral Home	6 kW	667.48	548.91	87.65	459.63	4912.94
Albi 112	Water Pump	7 kW	2609.74	2146.17	102.26	2042.28	21829.67
Av. Paisos Catalans, 5	School	6 kW	1559.75	1282.69	87.65	1193.41	12756.19
11 Septembre	Futbol Field	15 kW	839.91	690.72	219.13	469.95	5023.29
11 Septembre	Sports Zone	6 kW	346.83	285.22	87.65	195.94	2094.36
Pl. Major, 1	Local Space	2 kW	106.65	87.71	29.22	56.86	607.73
Palau, 1	Town Hall	14 kW	1906.80	1568.09	204.52	1361.94	14557.63
Anselm Clave, SN699	Public Lights	15 kW	6362.89	5232.64	219.13	5011.88	53571.47
Albi, 112	Trade Union	13 kW	4511.66	3710.25	189.91	3518.70	37611.06
Av. Paisos Catalans, 2	Swimming Pools	13 kW	3275.27	2693.48	189.91	2501.93	26742.93
TOTAL			28412.48	23365.53	1928.33	21419.24	228948.06

1. 21.6% Taxes
2. 0.0400235 €/kW, 365 days
3. 1.63 € meter rental
4. 0.093555 €/kWh

(Author’s own, adapted from data facilitated by the City Council of Cervià).

6. Biomass source analysis

The following table specifies the different types of biomasses available in Cervià and their respective properties and quantities.

Crop type	Hectares [ha]	Calorific Values [MJ/kg]	Wet optimum production (30% Hum) [t/ha yr]	Dry optimum production [t/ha yr]	Cervià's optimum wet production [t/yr]	Cervià's optimum dry production [t/yr]	Resource Obtainability %	Cervià's estimated wet production [t/yr]	Cervià's estimated dry production [t/yr]	Cervià's estimated energy production [MJ/yr]	Biomass Harvest Time [-]	Drying Time [months]
Forestry	1,342	12.00	166.00	116.20	222,772.00	155,940.40	0	0.00	0.00	0	Apr - May	6
Grain	20	17.00	0.61	0.43	12.20	8.54	2	0.02	0.02	290	Jun - Sep	2
Vineyards	13	12.00	1.43	1.00	18.59	13.01	5	0.93	0.65	7,808	Sep - Oct	4
Olive	1,815	12.00	0.56	0.39	1,016.40	711.48	5	50.82	35.57	426,888	Nov - Jan	5
Orchards	485	12.00	0.81	0.57	392.85	275.00	5	19.64	13.75	164,997	Sep - Oct	8
Olive Pit	-	19.68	-	-	1500	1,275.00	70	1,050.00	892.50	17,562,615	Nov - Jan	3
Almond Shell	-	18.83	-	-	100	85.00	70	70.00	59.50	1,120,266	Sep - Oct	3
Totals	3,675	-	-	-	225,812.04	158,308.43	-	1,191.42	1,001.99	19,282,864	-	-

(Adapted from Estudi de disponibilitat de biomassa i demanda energètica, 2020).

7. Monthly estimated distribution of electricity demand of Cervià de les Garrigues

The subsequent table describes the monthly electricity demand distribution calculated in Cervià.

		Annual consumption	Monthly Average	Jan.	Feb.	Mar.	Apr.	May.	Jun.	Jul.	Aug	Sep.	Oct.	Nov.	Dec.
Library	[kWh]	49240.8	4103.4	4924.1	4924.1	4513.7	4103.4	2872.4	3487.9	3693.1	3693.1	3487.9	4103.4	4513.7	4924.1
	Ratio [-]	12.00	1.00	1.20	1.20	1.10	1.00	0.70	0.85	0.90	0.90	0.85	1.00	1.10	1.20
Funeral Home	[kWh]	4912.9	409.4	450.4	450.4	450.4	368.5	368.5	368.5	368.5	368.5	368.5	450.4	450.4	450.4
	Ratio [-]	12.00	1.00	1.10	1.10	1.10	0.90	0.90	0.90	0.90	0.90	0.90	1.10	1.10	1.10
Water Pump	[kWh]	21829.7	1819.1	1637.2	1637.2	1637.2	2001.1	2001.1	2001.1	2001.1	2001.1	2001.1	1637.2	1637.2	1637.2
	Ratio [-]	12.00	1.00	0.90	0.90	0.90	1.10	1.10	1.10	1.10	1.10	1.10	0.90	0.90	0.90
School	[kWh]	12756.2	1063.0	1488.2	1381.9	1275.6	1169.3	1063.0	1063.0	21.3	21.3	1063.0	1063.0	1381.9	1488.2
	Ratio [-]	12.00	1.00	1.40	1.30	1.20	1.10	1.00	1.00	0.05	0.05	1.00	1.20	1.30	1.40
Futbol Field	[kWh]	5023.3	418.6	376.7	376.7	376.7	460.5	460.5	460.5	460.5	460.5	460.5	376.7	376.7	376.7
	Ratio [-]	12.00	1.00	0.90	0.90	0.90	1.10	1.10	1.10	1.10	1.10	1.10	0.90	0.90	0.90
Sports Zone	[kWh]	2094.4	174.5	8.7	8.7	69.8	192.0	279.2	296.7	314.2	331.6	349.1	226.9	8.7	8.7
	Ratio [-]	12.00	1.00	0.05	0.05	0.40	1.10	1.60	1.70	1.80	1.90	2.00	1.30	0.05	0.05
Social Local	[kWh]	607.7	50.6	55.7	55.7	55.7	45.6	45.6	45.6	45.6	45.6	45.6	55.7	55.7	55.7
	Ratio [-]	12.00	1.00	1.10	1.10	1.10	0.90	0.90	0.90	0.90	0.90	0.90	1.10	1.10	1.10
Town Hall	[kWh]	14557.6	1213.1	1455.8	1334.4	1273.8	1213.1	1091.8	849.2	1152.5	1273.8	970.5	1152.5	1334.4	1455.8
	Ratio [-]	12.00	1.00	1.20	1.10	1.05	1.00	0.90	0.70	0.95	1.05	0.80	0.95	1.10	1.20
Public Lights	[kWh]	53571.5	4464.3	6250.0	5803.6	5133.9	4241.1	3348.2	2008.9	2455.4	2901.8	3348.2	5133.9	6250.0	6696.4
	Ratio [-]	12.00	1.00	1.40	1.30	1.15	0.95	0.75	0.45	0.55	0.65	0.75	1.15	1.40	1.50
Trade Union	[kWh]	37611.1	3134.3	4388.0	4074.5	3604.4	2977.5	2350.7	1410.4	1723.8	2037.3	2350.7	3604.4	4388.0	4701.4
	Ratio [-]	12.00	1.00	1.40	1.30	1.15	0.95	0.75	0.45	0.55	0.65	0.75	1.15	1.40	1.50
Swimming Pools	[kWh]	26742.9	2228.6	111.4	111.4	891.4	2451.4	3565.7	3788.6	4011.4	4234.3	4457.2	2897.2	111.4	111.4
	Ratio [-]	12.00	1.00	0.05	0.05	0.40	1.10	1.60	1.70	1.80	1.90	2.00	1.30	0.05	0.05
Renewable energy centre	[kWh]	25000.0	2083.3	3220.0	2442.0	1700.0	1540.0	1120.0	2738.0	2800.0	1540.0	1540.0	1120.0	2620.0	2620.0
	Ratio [-]	12.00	1.00	1.30	1.25	0.50	0.75	0.55	1.30	1.35	1.20	0.75	0.50	1.25	1.30
Total	[kWh]	253948.1	21162.3	24366.2	22600.7	20982.8	20763.5	18566.7	18518.3	19047.2	18908.6	20442.1	21821.3	23128.3	24526.1
	Ratio [-]	12.00	1.00	1.15	1.07	0.99	0.98	0.88	0.88	0.90	0.89	0.97	1.03	1.09	1.16

(Author’s own, adapted from data facilitated by the City Council of Cervià).

Appendix III. MATLAB codes

The MATLAB codes used are attached in this appendix. Furthermore, the codes are in the subsequent MS OneDrive Folder, in addition to the variables used, the interpolated results, SAM weather files and SAM simulation cases:

- Design and development of an integrated renewable energy centre in Cervià de les Garrigues, Catalonia

1. Distance between geographical coordinates applying the Haversine formula (Haversine.m)

```
%% Code that implements the Harvesine method

% Latitude and longitude of weather stations
Ulldemolins = [41.32000,0.88570]; Granadella = [41.35991,0.66789];
Borges      = [41.51135,0.85617]; Prades     = [41.31481 0.98161];
Espluga     = [41.39241 1.09894]; Blancafort = [41.44237 1.15998];
Margalef    = [41.28521 0.75383];

% Latitude and longitude of Cervia
Cervia      = [41.424637,0.864385];

R = 6378; % Radius of the earth

% Distance (For example) between Granadella and Cervià
% Just change the name and enter the location to measure
LatitudeToMesure = Granadella(1);
LongitueToMesure = Granadella(2);

lat2=Cervia(1)*pi/180;
lat1=LatitudeToMesure(1)*pi/180;
long2=Cervia(2)*pi/180;
long1=LongitueToMesure*pi/180;
lat = lat2-lat1;
long = long2-long1;

h = (sin(lat/2))^2 + cos(lat1) * cos(lat2) * (sin(long/2))^2;
% Desired calculated distance
distance = R * 2 * atan2((h)^(1/2), (1-h)^(1/2));
```

2. Correspondence of the selected dates for SAM's weather files (selectdate.m)

```
%% Code that creates the necessary ordered variables of data
%% Year, Month, Day, Hour, Minute

Year = []; Month = []; Day = []; Hours = []; Minuts = [];
DateSampling = []; InternalCounter = 0;

d = 31;

for yy = 2020:2021
    for hh = 1:12
        if (hh == 2) && (yy == 2020)
            d=29;
        elseif (hh == 2) && (yy == 2021)
            d=28;
        elseif (hh == 1) || (hh == 3)  || (hh == 5)  ...
                || (hh == 7)  || (hh == 8)  || (hh == 10)  || (hh == 12)
```

```
            d=31;
        elseif (hh == 1) || (hh == 4)  || (hh == 6)  ...
                || (hh == 9)  || (hh == 11)
            d=30;
        end

        for kk = 1:d;
            for jj = 0:23
                for ii = 0:30:30
                    Year = [Year; yy];   Month  = [Month; hh]; Day = [Day; kk];
                    Hours = [Hours; jj]; Minuts = [Minuts; ii];
                    DateSampling = [DateSampling, ...
                        datetime('2020-01-01 00:00:00')-...
                        minutes(60)+minutes(30)*InternalCounter];
                    InternalCounter = InternalCounter +1;
                end
            end
        end
    end
end

% February 29 is deleted because the SAM does not need it
Year(2833:2833+47) = []; Month(2833:2833+47)  = []; Day(2833:2833+47) = [];
Hours(2833:2833+47) = [];Minuts(2833:2833+47) = []; DateSampling(2833:2833+47)  = [];
% January
Year(1:720) = [2019]; Year(720+1:1152) = [2020]; Year(1152+1:1488) = [2017];
% February
Year(1488+1:2832) = [2022];
% March
Year(2832+1:3552) = [2018]; Year(3552+1:4320) = [2021];
% April
Year(4320+1:4800) = [2017]; Year(4800+1:5280) = [2019]; Year(4800+1:5760) = [2021];
% May
Year(5760+1:6144) = [2020]; Year(6144+1:6816) = [2018]; Year(6816+1:7248) = [2019];
% June
Year(7248+1:7968) = [2021]; Year(7968+1:8688) = [2017];
% July
Year(8688+1:9408) = [2019]; Year(9408+1:10176) = [2020];
% August
Year(10176+1:11328) = [2021]; Year(11328+1:11664) = [2018];
% September
Year(11664+1:11856) = [2021]; Year(11856+1:12240) = [2017];
Year(12240+1:12720) = [2019]; Year(12720+1:13104) = [2021];
% October
Year(13104+1:14064) = [2020]; Year(14064+1:14592) = [2019];
% November
Year(14592+1:16032) = [2018];
% December
Year(16032+1:16512) = [2020]; Year(16512+1:16992) = [2017];
Year(16992+1:17520) = [2021];

YearMonthDay = [Year, Month, Day, Hours, Minuts];
% Save the values obtained
TimeYMD = YearMonthDay; TimeDat = DateSampling;
save('TimeYMD.mat'); save('TimeDat.mat');
```

3. Interpolation IDW method implementation (IDWinterpolation.m)

```
%% Code that performs the interpolation and creates the necessary files to enter to
%% SAM software. It also executes the method of obtaining the Solar Zenith Angle
% Variables exported from Excel are saved (Ulldemolins)
valorUllDVM = Ulldemolins_DVM; valorUllHRM = Ulldemolins_HRM;
valorUllPM  = Ulldemolins_PM;  valorUllPPT = Ulldemolins_PPT;
valorUllRS  = Ulldemolins_RS;  valorUllTM  = Ulldemolins_TM;
valorUllTN  = Ulldemolins_TN;  valorUllTX  = Ulldemolins_TX;
valorUllVVM = Ulldemolins_VVM; valorUllVVX = Ulldemolins_VVX;
```

```
% Variables exported from Excel are saved (Granadella)
valorGraDVM = Granadella_DVM; valorGraHRM = Granadella_HRM;
valorGraPM  = Granadella_PM;  valorGraPPT = Granadella_PPT;
valorGraRS  = Granadella_RS;  valorGraTM  = Granadella_TM;
valorGraTN  = Granadella_TN;  valorGraTX  = Granadella_TX;
valorGraVVM = Granadella_VVM; valorGraVVX = Granadella_VVX;

% Variables exported from Excel are saved (Borges)
valorBorDVM = Borges_DVM; valorBorHRM = Borges_HRM;
valorBorPM  = Borges_PM;  valorBorPPT = Borges_PPT;
valorBorRS  = Borges_RS;  valorBorTM  = Borges_TM;
valorBorTN  = Borges_TN;  valorBorTX  = Borges_TX;
valorBorVVM = Borges_VVM; valorBorVVX = Borges_VVX;
%Previously created Year, Month, Day, Hour, Minute data
YearMonthDay = TimeYMD;
%Previously created Year, Month, Day, Hour, Minute data for the SolarZenithAngle
DateMostreo  = TimeDat;

% Latitude and longitude of weather stations
Cervia = [41.424637,0.864385];   Ulldemolins = [41.32000,0.88570];
Granadella = [41.35991,0.66789]; Borges = [41.51135,0.85617];

% IDW interpolation method
DistanceUll = ((Cervia(1)-Ulldemolins(1))^2 + (Cervia(2)-Ulldemolins(2))^2)^(1/2);
DistanceGra = ((Cervia(1)-Granadella(1))^2 + (Cervia(2)-Granadella(2))^2)^(1/2);
DistanceBor = ((Cervia(1)-Borges(1))^2 + (Cervia(2)-Borges(2))^2)^(1/2);

wUll = 1/DistanceUll^2; wGra = 1/DistanceGra^2; wBor = 1/DistanceBor^2;

denominator = wUll+wGra+wBor;

valorCerDVM = []; valorCerHRM = []; valorCerPM  = []; valorCerPPT = [];
valorCerRS  = []; valorCerTM  = []; valorCerTN  = []; valorCerTX  = [];
valorCerVVM = []; valorCerVVX = []; valorDewP   = [];

for ii=1:numel(valorUllDVM)
    % Wind correction by applying the vertical profile (alpha=0.2)
    valorGraVVM(ii) = valorGraVVM(ii)*(10/2)^0.2;
    valorGraVVX(ii) = valorGraVVX(ii)*(10/2)^0.2;
    % IDW interpolation method
    NumDVM = (wUll * valorUllDVM(ii) + wGra * valorGraDVM(ii) ...
            + wBor * valorBorDVM(ii)) / denominator;
    NumHRM = (wUll * valorUllHRM(ii) + wGra * valorGraHRM(ii) ...
            + wBor * valorBorHRM(ii)) / denominator;
    NumPM  = (wUll * valorUllPM(ii)  + wGra * valorGraPM(ii)  ...
            + wBor * valorBorPM(ii))  / denominator;
    NumPPT = (wUll * valorUllPPT(ii) + wGra * valorGraPPT(ii) ...
            + wBor * valorBorPPT(ii)) / denominator;
    NumRS  = (wUll * valorUllRS(ii)  + wGra * valorGraRS(ii)  ...
            + wBor * valorBorRS(ii))  / denominator;
    NumTM  = (wUll * valorUllTM(ii)  + wGra * valorGraTM(ii)  ...
            + wBor * valorBorTM(ii))  / denominator;
    NumTN  = (wUll * valorUllTN(ii)  + wGra * valorGraTN(ii)  ...
            + wBor * valorBorTN(ii))  / denominator;
    NumTX  = (wUll * valorUllTX(ii)  + wGra * valorGraTX(ii)  ...
            + wBor * valorBorTX(ii))  / denominator;
    NumVVM = (wUll * valorUllVVM(ii) + wGra * valorGraVVM(ii) ...
            + wBor * valorBorVVM(ii)) / denominator;
    NumVVX = (wUll * valorUllVVX(ii) + wGra * valorGraVVX(ii) ...
            + wBor * valorBorVVX(ii)) / denominator;

    % Save the calculated variables
    valorCerDVM = [valorCerDVM;NumDVM];     valorCerHRM = [valorCerHRM;NumHRM];
    valorCerPM  = [valorCerPM;NumPM];       valorCerPPT = [valorCerPPT;NumPPT];
    valorCerRS  = [valorCerRS;NumRS];       valorCerTM  = [valorCerTM;NumTM];
    valorCerTN  = [valorCerTN;NumTN];       valorCerTX  = [valorCerTX;NumTX];
    valorCerVVM = [valorCerVVM;NumVVM];     valorCerVVX = [valorCerVVX;NumVVX];
end
```

```
% NOAA method for estimating geographic coordinates and time of day
JulianDay = juliandate(DateMostreo);            TimeZoneCervia     = 1;
JulianCentury     = []; GeomMeanLong      = []; GeomMeanAnom      = [];
EccentEarthOrbit  = []; SunEqofCtr        = []; SunTrueLong       = [];
SunAppLong        = []; MeanObliqEcliptic = []; ObliqCorr         = [];
SunDeclin         = []; VarY              = []; EqofTime          = [];
TrueSolarTime     = []; HourAngle         = []; SolarZenithAngle  = [];
for ii=1:numel(JulianDay)
    JulianCentury(ii)=(JulianDay(ii)-2451545)/36525;
    GeomMeanLong(ii)    = mod(280.46646 + JulianCentury(ii) ...
        * (36000.76983 + JulianCentury(ii) * 0.0003032),360);
    GeomMeanAnom(ii)    = 357.52911 + JulianCentury(ii) *...
        (35999.05029 - 0.0001537 * JulianCentury(ii));

    EccentEarthOrbit(ii)  = 0.016708634 - JulianCentury(ii) * ...
        (0.000042037 + 0.0000001267 * JulianCentury(ii));

    SunEqofCtr(ii)        = sin(deg2rad(GeomMeanAnom(ii)))*...
        (1.914602-JulianCentury(ii)* (0.004817+0.000014*JulianCentury(ii)))...
        +sin(deg2rad(2*GeomMeanAnom(ii)))*(0.019993-...
        0.000101*JulianCentury(ii))+sin(deg2rad(3*GeomMeanAnom(ii)))*0.000289;

    SunTrueLong(ii)       = GeomMeanLong(ii) + SunEqofCtr(ii);

    SunAppLong(ii)        = SunTrueLong(ii) -0.00569-0.00478*...
        sin(deg2rad(125.04-1934.136*JulianCentury(ii)));

    MeanObliqEcliptic(ii) = 23+(26+((21.448-JulianCentury(ii)*...
        (46.815+JulianCentury(ii)*(0.00059-JulianCentury(ii)*0.001813))))/60)/60;

   ObliqCorr(ii)         = MeanObliqEcliptic(ii)+0.00256*...
        cos(deg2rad(125.04-1934.136*JulianCentury(ii)));

    SunDeclin(ii)         = rad2deg(asin(sin(deg2rad(ObliqCorr(ii)))*...
        sin(deg2rad(SunAppLong(ii)))));

    VarY(ii)              = tan(deg2rad(ObliqCorr(ii)/2))*...
        tan(deg2rad(ObliqCorr(ii)/2));

    EqofTime(ii)          = 4 * rad2deg(VarY(ii)*...
        sin(2*deg2rad(GeomMeanLong(ii)))- 2*EccentEarthOrbit(ii)...
        *sin(deg2rad(GeomMeanAnom(ii)))+ 4*EccentEarthOrbit(ii)*VarY(ii)*...
        sin(deg2rad(GeomMeanAnom(ii)))*cos(2*deg2rad(GeomMeanLong(ii)))...
        -0.5*VarY(ii)*VarY(ii)*sin(4*deg2rad(GeomMeanLong(ii)))...
        -1.25*EccentEarthOrbit(ii)*EccentEarthOrbit(ii)*...
        sin(2*deg2rad(GeomMeanAnom(ii))));

    TrueSolarTime(ii)     = hour(DateMostreo(ii))*60 +...
        TimeZoneCervia*60 + minute(DateMostreo(ii)) + second(DateMostreo(ii))/60 ...
        + EqofTime(ii) + 4*Cervia(2) - 60*1;

    if (TrueSolarTime/4<0)
        HourAngle(ii)=TrueSolarTime(ii)/4+180;
    else
        HourAngle(ii)=TrueSolarTime(ii)/4-180;
    end

    SolarZenithAngle(ii)  = rad2deg(acos(sin(deg2rad(Cervia(1)))*...
        sin(deg2rad(SunDeclin(ii)))+cos(deg2rad(Cervia(1)))*...
        cos(deg2rad(SunDeclin(ii)))*cos(deg2rad(HourAngle(ii)))));
end% A vector is created that obtains the number of the day of the year
% from 1 to 365, % repeating 48 times each value to be able to apply the DIRINT method
dayofyear  = [];
for hh = 1:365
    for ii = 1:48
        dayofyear = [dayofyear;hh];
    end
end
```

```
% Double the vector to get the two consecutive years
dayofyear = [dayofyear;dayofyear];
% The function that executes the DIRINT method is called
dirintDNI = pvl_dirint(valorCerRS, SolarZenithAngle', dayofyear, 100*valorCerPM);
% The values obtained are stored
CerviaValuesComplete = [YearMonthDay,valorCerTM,valorCerTX,valorCerTN,...
            valorCerHRM,valorCerPPT,valorCerVVM,valorCerVVX,...
            valorCerDVM,valorCerPM,valorCerRS,dirintDNI,SolarZenithAngle'];
TitlesofCerviaComplete = ["Year","Month","Day","Hour",...
                          "Min","TM","TMax","Tmin","H%",...
                          "PPT","VVM","VVMax","DVM","PM","RS",...
                          "DNI Dirint","Solar Zenith"];

% The SAM's files are also created
WindFile    = [valorCerTM(17520+1:end),valorCerPM(17520+1:end)/1000,...
    valorCerDVM(17520+1:end),valorCerVVM(17520+1:end)/3.6];

WeatherFile = [YearMonthDay(1:17520,:),valorCerTM(1:17520),...
    valorCerVVM(1:17520)/3.6,valorCerDVM(1:17520),...
    valorCerRS(1:17520),dirintDNI(1:17520),valorCerPM(1:17520),valorCerHRM(1:17520)];

% The matrix created are exported to .txt files
writematrix([TitlesofCerviaComplete;CerviaValuesComplete],...
    'valorCerviacomes.txt')
writematrix(WindFile,'WindFile.txt')
writematrix(WeatherFile,'WeatherFile.txt')
```

4. Realization of solar irradiation and temperature graphs and calculations (SolarResource.m)

```
% Load the variables saved, consider that the samples are every 30 min
load('ResultatsDefinitius1.mat')
% Calculate the daily average and the daily maximum of the year 2020
RSmeanday2020 = []; RSmaxday2020 = [];
for ii=1:365
    RSmeanday2020 = [RSmeanday2020, mean(valorCerRS((48*(ii-1)+1):48*ii))] ;
    RSmaxday2020  = [RSmaxday2020,  max(valorCerRS((48*(ii-1)+1):48*ii))] ;
end
% Calculate the dayly average and the dayly maximum of the year 2021
RSmeanday2021 = []; RSmaxday2021 = [];
for ii=366:365*2
    RSmeanday2021 = [RSmeanday2021, mean(valorCerRS((48*(ii-1)+1):48*ii))] ;
    RSmaxday2021  = [RSmaxday2021,  max(valorCerRS((48*(ii-1)+1):48*ii))];
end
% Print the graphs
Jan = 0;        Feb = Jan + 31; Mar = Feb + 28; Apr = Mar + 31;
May = Apr + 30; Jun = May + 31; Jul = Jun + 30; Aug = Jul + 31;
Sep = Aug + 31; Oct = Sep + 30; Nov = Oct + 31; Dec = Nov + 30;

day = 1:365*2;

plot(day,[RSmaxday2020,RSmaxday2021],day,[RSmeanday2020,RSmeanday2021],...
     'LineWidth',1.6,'LineWidth',1.6)
legend('RS Max','Rs Mean'); xlim([0,365*2]); ylabel('GHI [W/m^{2}]');
ylim([0,max([RSmaxday2020,RSmaxday2021])+50]);
xticks([Jan Feb Mar Apr May Jun Jul Aug Sep Oct Nov Dec...
       (Dec+Jan+31) (Dec+Feb+31) (Dec+Mar+31) (Dec+Apr+31)...
       (Dec+May+31) (Dec+Jun+31) (Dec+Jul+31) (Dec+Aug+31)...
       (Dec+Sep+31) (Dec+Oct+31) (Dec+Nov+31) (Dec+Dec+31)]);
xticklabels({'Jan20','Feb20','Mar20','Apr20','May20','Jun20',...
              'Jul20','Aug20','Sep20','Oct20','Nov20','Dec20',...
              'Jan21','Feb21','Mar21','Apr21','May21','Jun21',...
              'Jul21','Aug21','Sep21','Oct21','Nov21','Dec21'});
% Obtain the values with RS > 0
RSsun = []; RSsunmean = [];
counterhofsun = 0; % Counter that will count the hours of sunshine
```

```
counter400W   = 0; % Counter that will count the hours > 400 W/m^2
for ii=1:365*2
    for jj=1:48
        if (valorCerRS(ii*jj)>0)
            RSsun = [RSsun valorCerRS(ii*jj)];
            % Store the dayly non-zero RS values
            counterhofsun = counterhofsun+1;
            % Count the number of RS values
        end
        if (valorCerRS(ii*jj)>400)
            counter400W = counter400W+1;
            % Count the number of RS > 400
        end
    end
    RSsunmean = [RSsunmean mean(RSsun)];
    % Calculate the daily mean of
    % stored non-zero RS values
    % and store it
    RSsun = [];
end
% Calculate statistical values
hyearofsun = (counterhofsun/2)/2 % Annual average hours of sunshine
hyear400W  = (counter400W/2)/2   % Annual average hours > 400 W/m^2

Mean20 = mean(valorCerRS(1:365*48))           % Average 2020
Med20  = median(valorCerRS(1:365*48))         % Median 2020
Mean21 = mean(valorCerRS(365*48+1:365*48*2))  % Average 2021
Med21  = median(valorCerRS(365*48+1:365*48*2))% Median 2021

MaxMaxm20 = max(valorCerRS(1:365*48))         % Maximum value 2020
MaxMean20 = mean(RSmaxday2020(1:365))         % Average of maximums 20
MaxMaxm21 = max(valorCerRS(365*48+1:365*48*2))% Maximum value 2021
MaxMean21 = mean(RSmaxday2021(1:365))         % Average of maximums 21

Dev20  = std(valorCerRS(1:365*48))       % Standard deviation 2020
Cvar20 = Dev20 *100/Mean20               % Coefficient of Variation 20
Desv21 = std(valorCerRS(365*48+1:365*48*2))% Standard deviation 21
Cvar21 = Desv21 *100/Mean21           % Coefficient of Variation 21

% Obtain the values with RS > 0
Tmeandaily = []; ArrayTmean = []; Tmadaily   = []; ArrayTmax  = [];
Tmindaily  = []; ArrayTmin  = [];

counter25Dhours = 0; % Counter that will count the hours > 25ºC
counter25Ddays  = 0; % Counter that will count the days  > 25ºC
counterloop     = 1; % Counter for the iterator

for ii=1:365*2
    for jj=1:48

        if (valorCerRS(counterloop)~=0) %  non-zero RS values
            Tmadaily=[Tmadaily valorCerTM(counterloop)];     % T max
            Tmeandaily=[Tmeandaily valorCerTX(counterloop)]; % T mean
            Tmindaily=[Tmindaily valorCerTN(counterloop)];   % T min
            if (valorCerTX(counterloop)<=25)
                counter25Dhours=counter25Dhours+1;
                % Count the number of Tmean > 400
            end
        end
        counterloop = counterloop + 1;
    end
    % Calculate the daily mean, max, min of stored non-zero RS values and store it
    ArrayTmax = [ArrayTmax max(Tmeandaily)]; ArrayTmean = [ArrayTmean mean(Tmadaily)];
    ArrayTmin = [ArrayTmin min(Tmadaily)];
    Tmeandaily = [];Tmadaily = [];Tmindaily = [];

    if (ArrayTmean(ii)>25)
        counter25Ddays=counter25Ddays+1; % Count the days with an average above 25ºC
```

```
    end
end
% Calculate statistical values
hyearof25D = (counter25Dhours/2)/2 % Annual average hours  <=25ºC
dyearof25D = (counter25Ddays)/2    % Annual days with Tmax > 25ºC
% Print the graphs
Jan = 0;        Feb = Jan + 31; Mar = Feb + 28; Apr = Mar + 31;
May = Apr + 30; Jun = May + 31; Jul = Jun + 30; Aug = Jul + 31;
Sep = Aug + 31; Oct = Sep + 30; Nov = Oct + 31; Dec = Nov + 30;
day = 1:365*2;
plot(day,ArrayTmax,day,ArrayTmean,day,ArrayTmin,...
     'LineWidth',1.6,'LineWidth',1.6,'LineWidth',1.6);
legend('T max','T mean','T min'); xlim([0,365*2]); ylabel('Temperature [ºC]');
xticks([Jan Feb Mar Apr May Jun Jul Aug Sep Oct Nov Dec...
       (Dec+Jan+31) (Dec+Feb+31) (Dec+Mar+31) (Dec+Apr+31)...
       (Dec+May+31) (Dec+Jun+31) (Dec+Jul+31) (Dec+Aug+31) ...
       (Dec+Sep+31) (Dec+Oct+31) (Dec+Nov+31) (Dec+Dec+31)]);
xticklabels({'Jan20','Feb20','Mar20','Apr20','May20','Jun20',...
              'Jul20','Aug20','Sep20','Oct20','Nov20','Dec20',...
              'Jan21','Feb21','Mar21','Apr21','May21','Jun21',...
              'Jul21','Aug21','Sep21','Oct21','Nov21','Dec21'});
```

5. Realization of wind speed graphs and calculations (WindResource.m)

```
% Load the variables saved, consider that the samples are every 30 min
load('ResultatsDefinitius1.mat')

% Calculate the daily maximum, minimum and average of the year 2020
% and Convert km/h to m/s
SpeedMean2020 = []; SpeedMax2020 = []; SpeedMin2020  = [];
for ii=1:365
    SpeedMean2020  = [SpeedMean2020, mean(valorCerVVM((48*(ii-1)+1):48*ii))*10/36] ;
    SpeedMax2020  = [SpeedMax2020, max(valorCerVVX((48*(ii-1)+1):48*ii))*10/36] ;
    SpeedMin2020  = [SpeedMin2020, min(valorCerVVM((48*(ii-1)+1):48*ii))*10/36] ;
end

% Calculate the daily maximum, minimum and average of the year 2021 (Convert km/h-m/s)
SpeedMean2021 = []; SpeedMax2021 = []; SpeedMin2021  = [];
for ii=366:365*2
    SpeedMean2021  = [SpeedMean2021, mean(valorCerVVM((48*(ii-1)+1):48*ii))*10/36] ;
    SpeedMax2021  = [SpeedMax2021, max(valorCerVVX((48*(ii-1)+1):48*ii))*10/36];
    SpeedMin2021  = [SpeedMin2021, min(valorCerVVM((48*(ii-1)+1):48*ii))*10/36];
end
% Print the graphs
Jan = 0;        Feb = Jan + 31; Mar = Feb + 28; Apr = Mar + 31;
May = Apr + 30; Jun = May + 31; Jul = Jun + 30; Aug = Jul + 31;
Sep = Aug + 31; Oct = Sep + 30; Nov = Oct + 31; Dec = Nov + 30;

plot(day,[SpeedMax2020,SpeedMax2021],day,[SpeedMean2020,SpeedMean2021],...
    day,[SpeedMin2020,SpeedMin2021],'LineWidth',1.6,'LineWidth',1.6,'LineWidth',1.6);
legend('Max. Speed','Average Speed','Min. Speed');xlim([0,365*2]);
xticks([Jan Feb Mar Apr May Jun Jul Aug Sep Oct Nov Dec...
       (Dec+Jan+31) (Dec+Feb+31) (Dec+Mar+31) (Dec+Apr+31)...
       (Dec+May+31) (Dec+Jun+31) (Dec+Jul+31) (Dec+Aug+31)...
       (Dec+Sep+31) (Dec+Oct+31) (Dec+Nov+31) (Dec+Dec+31)]);
xticklabels({'Jan20','Feb20','Mar20','Apr20','May20','Jun20',...
              'Jul20','Aug20','Sep20','Oct20','Nov20','Dec20',...
              'Jan21','Feb21','Mar21','Apr21','May21','Jun21',...
              'Jul21','Aug21','Sep21','Oct21','Nov21','Dec21'});
ylabel('Wind Speed [m/s]');

% Calculate statistical values of Cervià
Mean20 = mean(valorCerVVM(1:365*48))           % Average 2020
Med20  = median(valorCerVVM(1:365*48))         % Median 2020
Mean21 = mean(valorCerVVM(365*48+1:365*48*2))  % Average 2021
Med21  = median(valorCerVVM(365*48+1:365*48*2))% Median 2021
```

```
MaxMaxm20 = max(valorCerVVX(1:365*48))          % Maximum value 20
MaxMean20 = mean(valorCerVVX(1:365*48))         % Average of maximums 20
MaxMaxm21 = max(valorCerVVX(365*48+1:365*48*2)) % Maximum value 21
MaxMean21 = mean(valorCerVVX(365*48+1:365*48*2))% Average of maximums 21

MinMini20=min(valorCerVVM(1:365*48))            % Minimum value 2020
MinMini21=min(valorCerVVM(365*48+1:365*48*2))   % Minimum value 2021

Dev20  = std(valorCerVVM(1:365*48))         % Standard deviation 2020
Cvar20 = Dev20 *100/Mean20                  % Coefficient of Variation 2020
Dev21  = std(valorCerVVM(365*48+1:365*48*2))% Standard deviation 2022
Cvar21 = Dev21 *100/Mean21                  % Coefficient of Variation 21
```

6. No-linear system of 6 equations with 6 unknowns (6eq6unk.m)

```
fun = @SolarTriangleAngle;      % Call de function
x0 = [1,1,1,1,1,1];             % Solution start values
[x,feval,flag] = fsolve(fun,x0) % Solve system

function E = SolarTriangleAngle(x)

d1 = 2.66212; d2 = 1.016; a  = 10;      b  = 38-a; % Known variables

% Equations . . . . . . . x(1)=d3; % x(2)=D; % x(3)=x; % x(4)=y; % x(5)=z; % x(6)=p;
E(1) = - x(1)^2 + d1^2 + d2^2 - 2*d1*d2*cosd(a+b);
E(2) = - x(2)^2 + d1^2 + x(5)^2 - 2*x(5)*d1*cosd(x(6));
E(3) = - x(2)^2 + (d1-x(3))^2+x(4)^2;
E(4) = - x(5)^2 + x(3)^2 + x(4)^2;
E(5) = - x(4)^2 + x(3)^2 + x(5)^2 -2*x(3)*x(5)*cosd(x(6));
E(6) = - x(5)^2 + d1^2 + x(2)^2 -2*d1*x(2)*cosd(a);

end
```

Appendix IV. Solar panels and inverter datasheets

1. MAXEON 3 – 400 (Source: Sun Power)

SUNPOWER®
MAXEON®

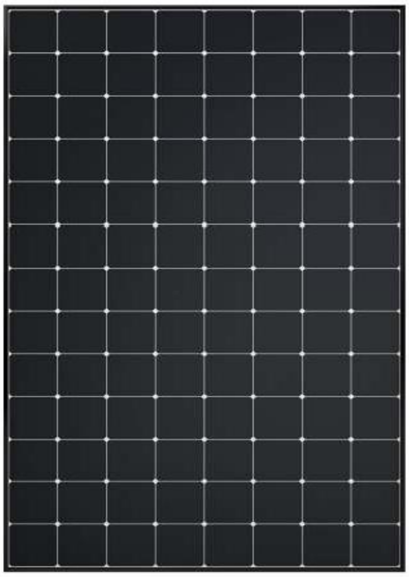

MAXEON® 3 | 400 W

Residential Solar Panel

SunPower Maxeon panels combine the top efficiency, durability and warranty available in the market today, resulting in more long-term energy and savings. [1,2]

Maximum Power. Minimalist Design.

Industry-leading efficiency means more power and savings per available space. With fewer panels required, less is truly more.

Highest Lifetime Energy and Savings

Designed to deliver 60% more energy in the same space over 25 years in real-world conditions like partial shade and high temperatures. [2]

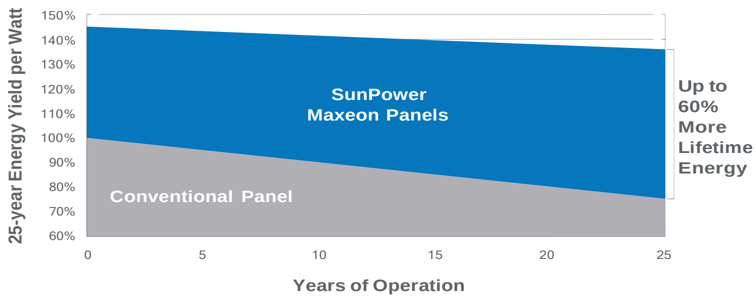

Better Reliability, Better Warranty

With more than 25 million panels deployed around the world, SunPower technology is proven to last. That's why we stand behind our panel with an exceptional 25-year Combined Power and Product Warranty, including the highest Power Warranty in solar.

25-yr SunPower Complete Confidence

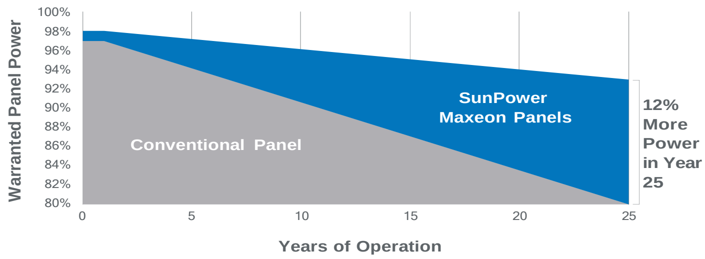

Fundamentally Different. And Better.

The SunPower Maxeon® Solar Cell

- Enables highest efficiency panels available [2]
- Unmatched reliability [3]
- Patented solid metal foundation prevents breakage and corrosion

As Sustainable As Its Energy

- Ranked #1 in Silicon Valley Toxics Coalition Solar Scorecard [4]
- First solar panels to achieve Cradle to Cradle Certified™ Silver recognition [5], *pending*
- Contributes to more LEED categories than conventional panels [6]

MAXEON® 3 | 400 W Residential Solar Panel

Electrical Data			
	SPR-MAX3-400	SPR-MAX3-390	SPR-MAX3-370
Nominal Power (Pnom) [7]	400 W	390 W	370 W
Power Tolerance	+5/0%	+5/0%	+5/0%
Panel Efficiency	22.6%	22.1%	20.9%
Rated Voltage (Vmpp)	65.8 V	64.5 V	61.8 V
Rated Current (Impp)	6.08 A	6.05 A	5.99 A
Open-Circuit Voltage (Voc)	75.6 V	75.3 V	74.7 V
Short-Circuit Current (Isc)	6.58 A	6.55 A	6.52 A
Max. System Voltage	1000 V IEC		
Maximum Series Fuse	15 A		
Power Temp Coef.	−0.29% / °C		
Voltage Temp Coef.	−176.8 mV / °C		
Current Temp Coef.	2.9 mA / °C		

Tests And Certifications	
Standard Tests [8]	IEC 61215, IEC 61730 Class 1 fire rated per UNI 9177
Quality Management Certs	ISO 9001:2015, ISO 14001:2015
EHS Compliance	RoHS (Pending), OHSAS 18001:2007, lead free, REACH SVHC-163 (Pending)
Sustainability	Cradle to Cradle Certified™ (Pending)
Ammonia Test	IEC 62716
Desert Test	10.1109/PVSC.2013.6744437
Salt Spray Test	IEC 61701 (maximum severity)
PID Test	1000 V: IEC 62804, PVEL 600 hr duration
Available Listings	TUV [9]

Operating Condition And Mechanical Data	
Temperature	−40° C to +85° C
Impact Resistance	25 mm diameter hail at 23 m/s
Solar Cells	104 Monocrystalline Maxeon Gen III
Tempered Glass	High-transmission tempered anti-reflective
Junction Box	IP-65, Stäubli (MC4), 3 bypass diodes
Weight	19 kg
Design Load	Wind: 2660 Pa, 274 kg/m² front & back Snow: 4000 Pa, 408 kg/m² front
Max. Load [10]	Wind: 4000 Pa, 408 kg/m² front & back Snow: 6000 Pa, 611 kg/m² front
Frame	Class 1 black anodized (highest AAMA rating)

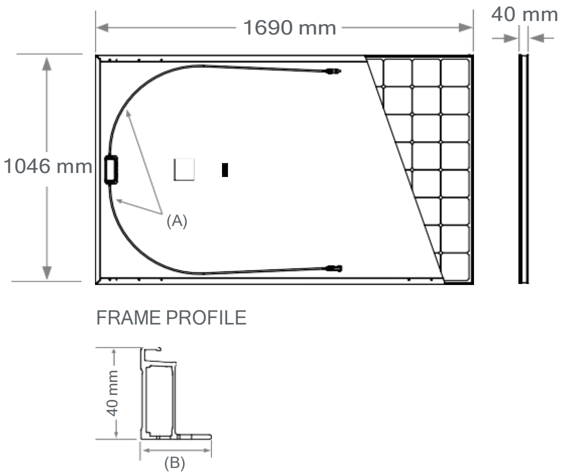

A. Cable Length: 1200 mm +/-10 mm
B. LONG SIDE: 32 mm
SHORT SIDE: 24 mm

Please read the safety and installation guide.

1 SunPower 400 W, 22.6% efficient, compared to a Conventional Panel on same-sized arrays (260 W, 16% efficient, approx. 1.6 m²), 7% more energy per watt (based on PVSyst pan files for avg EU climate), 0.5%/yr slower degradation rate (Jordan, et. al. "Robust PV Degradation Methodology and Application." PVSC 2018).
2 DNV "SunPower Shading Study," 2013. Compared to a conventional front contact panel.
3 #1 rank in "Fraunhofer PV Durability Initiative for Solar Modules: Part 3". PVTech Power Magazine, 2015.
4 SunPower is rated #1 on Silicon Valley Toxics Coalition's Solar Scorecard.
5 Cradle to Cradle Certified is a multi-attribute certification program that assesses products and materials for safety to human and environmental health, design for future use cycles, and sustainable manufacturing.
6 Maxeon2 and Maxeon3 panels additionally contribute to LEED Materials and Resources credit categories.
7 Standard Test Conditions (1000 W/m² irradiance, AM 1.5, 25° C). NREL calibration Standard: SOMS current, LACCS FF and Voltage.
8 Class C fire rating per IEC 61730.
9 Also certified under names SPR-XYY-XXX.
10 Calculated with a 1.5 Safety Factor.

Designed in USA
Made in Philippines (Cells)
Modules Assembled in Mexico

Visit www.sunpowercorp.co.uk for more information.
Specifications included in this datasheet are subject to change without notice.

SUNPOWER®
MAXEON®

2. **Alpha-REC380AA (Source: REC)**

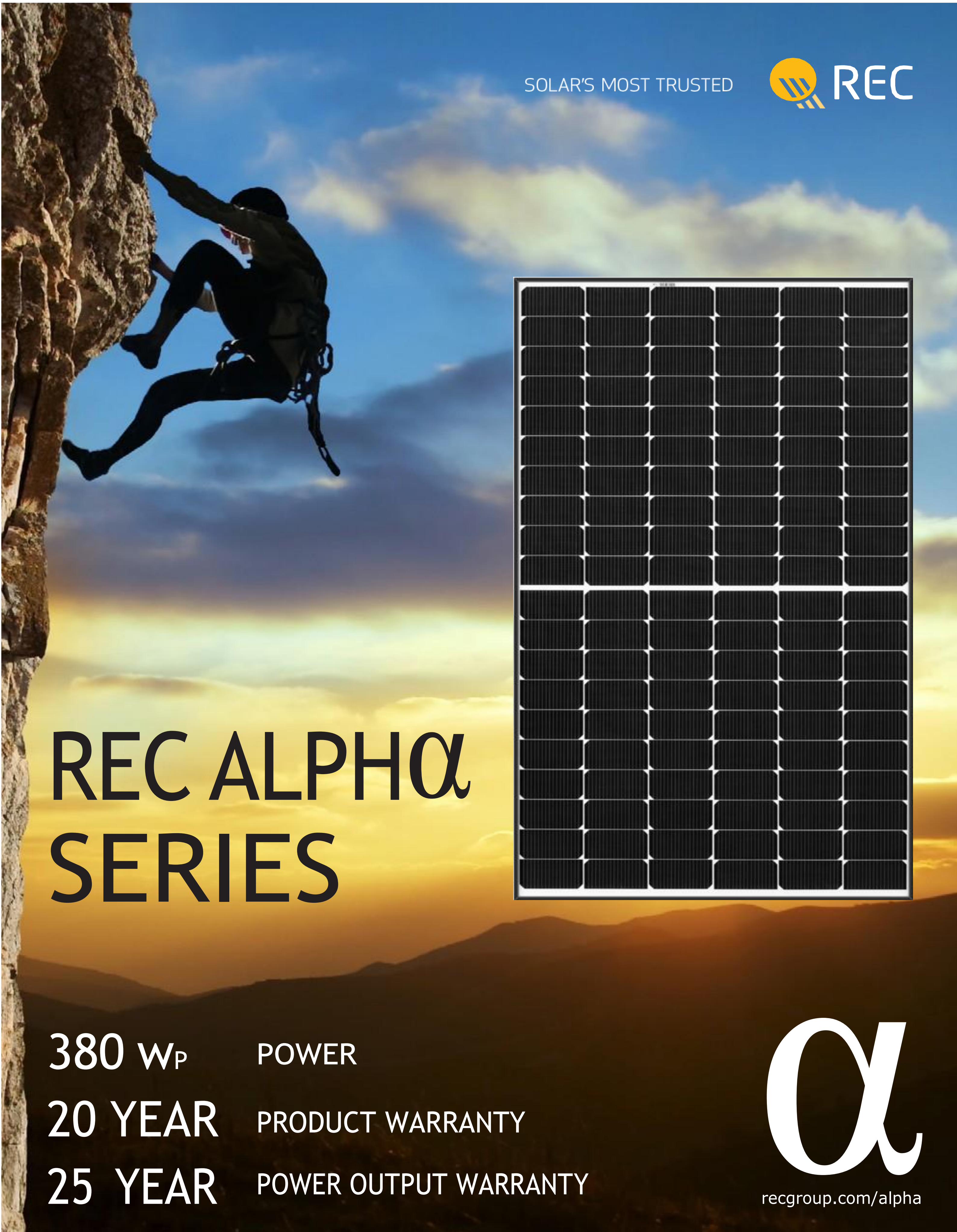

REC ALPHα SERIES

PRODUCT DATASHEET

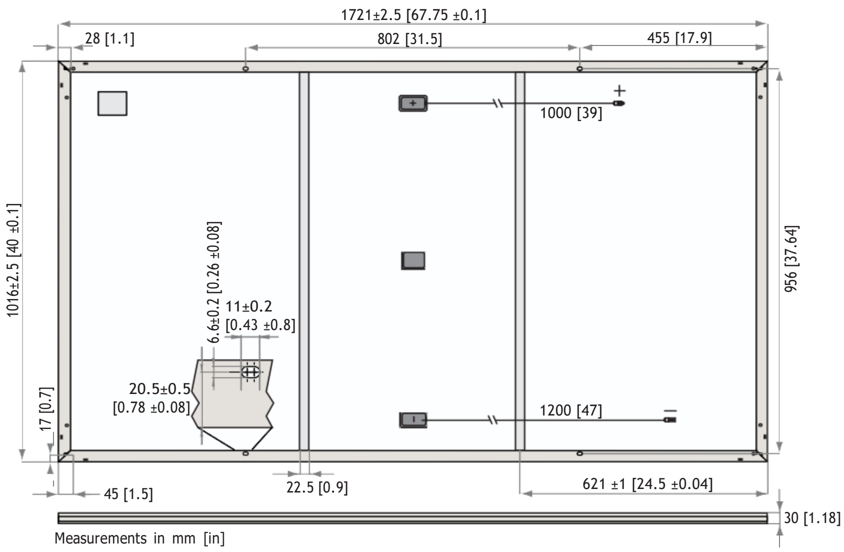

CERTIFICATIONS

IEC 61215:2016, IEC 61730:2016, UL 1703, UL 61730	
IEC 62804	PID
IEC 61701	Salt Mist
IEC 62716	Ammonia Resistance
ISO 11925-2	Ignitability (Class E)
UNI 8457/9174	Ignitability (Class 1)
IEC 62782	Dynamic Mechanical Load
IEC 61215-2:2016	Hailstone (35mm)
AS4040.2 NCC 2016	Cyclic Wind Load
ISO 14001:2004, ISO 9001:2015, OHSAS 18001:2007	

take-e-way WEEE-compliant recycling scheme

WARRANTY

20 year product warranty
25 year linear power output warranty
Maximum annual power degression of 0.25% p.a.
Guarantees 92% of power after 25 years
See warranty conditions for further details.

MECHANICAL DATA

Dimensions:	1721 x 1016 x 30 mm
Area:	1.75 m²
Weight:	19.5 kg

GENERAL DATA

Cell type:	120 half-cut cells with REC heterojunction cell technology 6 strings of 20 cells in series	Junction box:	3-part, 3 bypass diodes, IP67 rated in accordance with IEC 62790
Glass:	3.2 mm solar glass with anti-reflection surface treatment	Cable:	4 mm² solar cable, 1.0 m + 1.2 m in accordance with EN 50618
Backsheet:	Highly resistant polymeric construction	Connectors:	Stäubli MC4 PV-KBT4/KST4 (4 mm²) in accordance with IEC 62852 IP68 only when connected
Frame:	Anodized aluminum (black)	Origin:	Made in Singapore

MAXIMUM RATINGS

Operational temperature:	-40 ... +85°C
Maximum system voltage:	1000 V
Design load (+): snow Maximum test load (+):	4666 Pa (475 kg/m²)⁺ 7000 Pa (713 kg/m²)*
Design load (-): wind Maximum test load (-):	2666 Pa (272 kg/m²)⁺ 4000 Pa (407 kg/m²)*
Max series fuse rating:	25 A
Max reverse current:	25 A

⁺ Calculated using a safety factor of 1.5
* See installation manual for mounting instructions

ELECTRICAL DATA @ STC

Product Code*: RECxxxAA

Nominal Power - P_{MPP} (Wp)	360	365	370	375	380
Watt Class Sorting - (W)	-0/+5	-0/+5	-0/+5	-0/+5	-0/+5
Nominal Power Voltage - V_{MPP} (V)	37.7	38.0	38.3	38.7	39.0
Nominal Power Current - I_{MPP} (A)	9.55	9.60	9.66	9.72	9.76
Open Circuit Voltage - V_{OC} (V)	44.1	44.3	44.5	44.6	44.7
Short Circuit Current - I_{SC} (A)	10.23	10.26	10.30	10.40	10.46
Panel Efficiency (%)	20.6	20.9	21.2	21.4	21.7

Values at standard test conditions (STC: air mass AM 1.5, irradiance 1000 W/m², temperature 25°C), based on a production spread with a tolerance of P_{MPP}, V_{OC} & I_{SC} ±3% within one watt class. * Where xxx indicates the nominal power class (P_{MPP}) at STC above.

TEMPERATURE RATINGS*

Nominal Module Operating Temperature:	44°C (±2°C)
Temperature coefficient of P_{MPP}:	-0.26 %/°C
Temperature coefficient of V_{OC}:	-0.24 %/°C
Temperature coefficient of I_{SC}:	0.04 %/°C

*The temperature coefficients stated are linear values

ELECTRICAL DATA @ NMOT

Product Code*: RECxxxAA

Nominal Power - P_{MPP} (Wp)	274	278	282	286	290
Nominal Power Voltage - V_{MPP} (V)	35.5	35.8	36.1	36.4	36.7
Nominal Power Current - I_{MPP} (A)	7.71	7.76	7.80	7.85	7.88
Open Circuit Voltage - V_{OC} (V)	41.6	41.7	41.9	42.0	42.1
Short Circuit Current - I_{SC} (A)	8.26	8.29	8.32	8.40	8.45

Nominal module operating temperature (NMOT: air mass AM 1.5, irradiance 800 W/m², temperature 20°C, windspeed 1 m/s).
* Where xxx indicates the nominal power class (P_{MPP}) at STC above.

LOW LIGHT BEHAVIOUR

Typical low irradiance performance of module at STC:

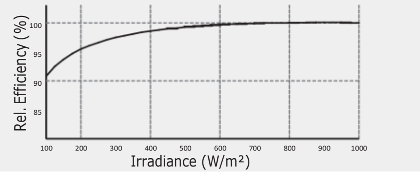

Specifications subject to change without notice.

Ref: PM-DS-12-01-Rev- B 08.19

Founded in Norway in 1996, REC is a leading vertically integrated solar energy company. Through integrated manufacturing from silicon to wafers, cells, high-quality panels and extending to solar solutions, REC provides the world with a reliable source of clean energy. REC's renowned product quality is supported by the lowest warranty claims rate in the industry. REC is a Bluestar Elkem company with headquarters in Norway and operational headquarters in Singapore. REC employs around 2,000 people worldwide, producing 1.5 GW of solar panels annually.

REC
www.recgroup.com

3. Huawei SUN 2000-40KTL-M340 (Source: Huawei)

SUN2000-30/36/40KTL-M3

Smart PV Controller

HUAWEI

Smart

8 strings intelligent monitoring

Efficient

Max. efficiency 98.7%

Safe

Fuse free design

Reliable

Type II surge arresters for DC & AC

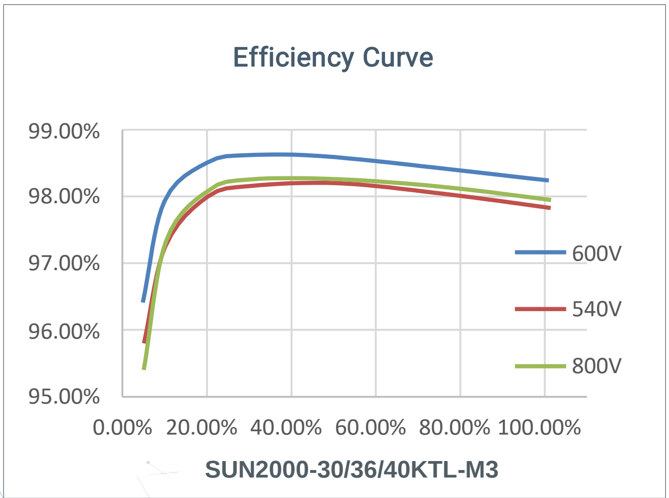

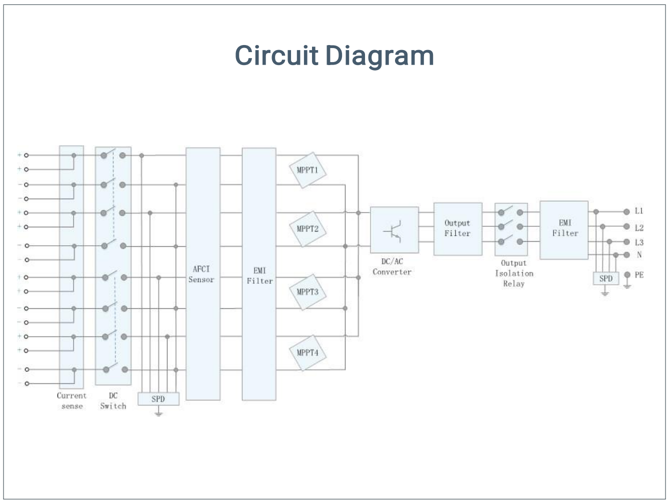

SUN2000-30/36/40KTL-M3
Technical Specification

Technical Specification	SUN2000-30KTL-M3	SUN2000-36KTL-M3	SUN2000-40KTL-M3
Efficiency			
Max. Efficiency	98.7%		
European Efficiency	98.4%		
Input			
Max. Input Voltage [1]	1,100 V		
Max. Current per MPPT	26 A		
Max. Short Circuit Current per MPPT	40 A		
Start Voltage	200 V		
MPPT Operating Voltage Range [2]	200 V ~ 1000 V		
Rated Input Voltage	600 V		
Number of Inputs	8		
Number of MPP Trackers	4		
Output			
Rated AC Active Power	30,000 W	36,000 W	40,000 W
Max. AC Apparent Power	33,000 VA	40,000 VA	44,000 VA
Rated Output Voltage	230 Vac / 400 Vac, 3W/N+PE		
Rated AC Grid Frequency	50 Hz / 60 Hz		
Rated Output Current	43.3 A	52.0 A	57.8 A
Max. Output Current	47.9 A	58.0 A	63.8 A
Adjustable Power Factor Range	0.8 LG .... 0.8 LD		
Max. Total Harmonic Distortion	< 3%		
Protection			
Input-side Disconnection Device	Yes		
Anti-islanding Protection	Yes		
AC Overcurrent Protection	Yes		
DC Reverse-polarity Protection	Yes		
PV-array String Fault Monitoring	Yes		
DC Surge Arrester	Yes		
AC Surge Arrester	Yes		
DC Insulation Resistance Detection	Yes		
Residual Current Monitoring Unit	Yes		
Arc Fault Protection	Yes		
Ripple Receiver Control	Yes		
Integrated PID Recovery [3]	Yes		
Communication			
Display	LED Indicators, Integrated WLAN + FusionSolar APP		
RS485	Yes		
Smart Dongle	WLAN/Ethernet via Smart Dongle-WLAN-FE (Optional)4G / 3G / 2G via Smart Dongle-4G (Optional)		
Monitoring BUS (MBUS)	Yes (Isolation Transformer required)		
General Data			
Dimensions (W x H x D)	640 x 530 x 270 mm (25.2 x 20.9 x 10.6 inch)		
Weight (with mounting plate)	43 kg (94.8 lb)		
Nosie Level	< 46 dB		
Operating Temperature Range	-25 ~ + 60 °C (-13 °F ~ 140 °F)		
Cooling Method	Natural Convection		
Max. Operating Altitude	0 - 4,000 m (13,123 ft.)		
Relative Humidity	0% RH ~ 100% RH		
DC Connector	Staubli MC4		
AC Connector	Waterproof Connector + OT/DT Terminal		
Protection Degree	IP 66		
Topology	Transformerless		
Nighttime Power Consumption	≤ 5.5W		
Optimizer Compatibility			
DC MBUS Compatible Optimizer	SUN2000-450W-P		
Standard Compliance (more available upon request)			
Safety	EN 62109-1/-2, IEC 62109-1/-2, EN 50530, IEC 62116, IEC 60068, IEC 61683		
Grid Connection Standards	IEC 61727, VDE-AR-N4105, VDE 0126-1-1, BDEW, G59/3, UTE C 15-712-1, CEI 0-16, CEI 0-21, RD 661, RD 1699, P.O. 12.3,RD 413, EN-50438-Turkey, EN-50438-Ireland, C10/11, MEA, Resolution No.7,NRS 097-2-1, AS/NZS 4777.2, DEWA		

1. The maximum input voltage is the upper limit of the DC voltage. Any higher input DC voltage would probably damage inverter.
2. Any DC input voltage beyond the operating voltage range may result in inverter improper operating.
3. SUN2000-30~40KTL-M3 raises potential between PV- and ground to above zero through integrated PID recovery function to recover module degradation from PID. Supported module types include: P-type (mono, poly), N-type (nPERT, HIT)

Appendix V. SAM inputs for the energy simulations

The inputs for the two energy simulations run with the System Advisor Model (SAM) software are compiled in this appendix. Only images of the settings used are attached. Section 1 explains the inputs used for the energy simulation of the photovoltaic installation, while section 2 explains those of biomass. It should be remembered that MATLAB codes, weather variables, and SAM simulations are stored in the MS OneDrive folder:

- Design and Development of an Integrated Renewable Energy entre in Cervià de les Garrigues, Catalonia

1. Solar energy

This section explains the various types of inputs that the SAM requires to simulate solar power generation. As mentioned in section 4.1, the main topics are Location and Resource (Appendix V.1.1), Module (Appendix V.1.2), Inverter (Appendix V.1.3), System Design (Appendix V.1.4), Shading & Layout (Appendix V.1.5), Losses (Appendix V.1.6) and Grid Limits (Appendix V.1.7). The procedure used on each of them is described in detail below.

1.1 Location and Resource

Firstly, the Weather Data file of Cervià previously created is chosen. With this data, SAM is able to provide the annual averages of the selected files. Subsequently, the option of estimating the DNI from GHI and DHI is selected. Finally, if the "View Data..." box is pressed, it allows visualising graphs of the meteorological variables.

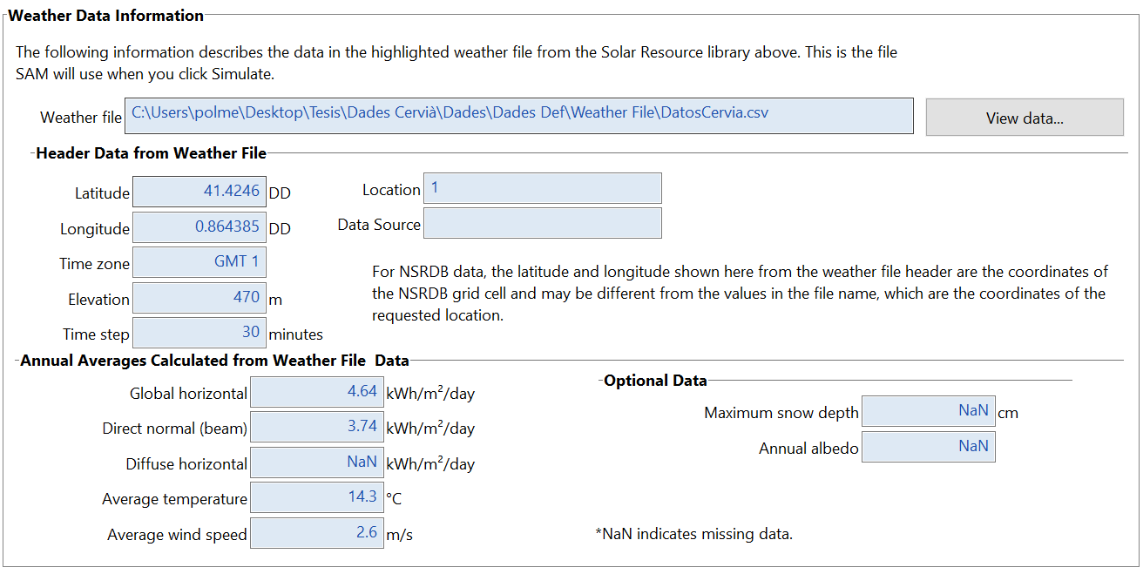

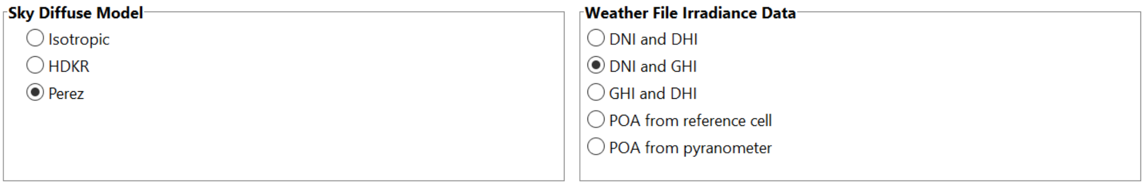

1.2 Module

SAM offers libraries with all kinds of photovoltaic panel models. Evidently, the module chosen in this situation is the same as the one selected during the theoretical research (REC380AA). Selecting a solar panel from those in the software libraries will automatically fill in the simulation data.

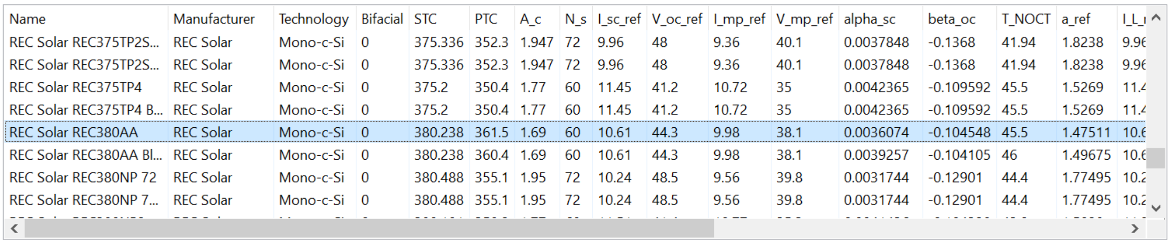

Name	Manufacturer	Technology	Bifacial	STC	PTC	A_c	N_s	I_sc_ref	V_oc_ref	I_mp_ref	V_mp_ref	alpha_sc	beta_oc	T_NOCT	a_ref	I_L_r
REC Solar REC375TP2S...	REC Solar	Mono-c-Si	0	375.336	352.3	1.947	72	9.96	48	9.36	40.1	0.0037848	-0.1368	41.94	1.8238	9.96
REC Solar REC375TP2S...	REC Solar	Mono-c-Si	0	375.336	352.3	1.947	72	9.96	48	9.36	40.1	0.0037848	-0.1368	41.94	1.8238	9.96
REC Solar REC375TP4	REC Solar	Mono-c-Si	0	375.2	350.4	1.77	60	11.45	41.2	10.72	35	0.0042365	-0.109592	45.5	1.5269	11.4
REC Solar REC375TP4 B...	REC Solar	Mono-c-Si	0	375.2	350.4	1.77	60	11.45	41.2	10.72	35	0.0042365	-0.109592	45.5	1.5269	11.4
REC Solar REC380AA	REC Solar	Mono-c-Si	0	380.238	361.5	1.69	60	10.61	44.3	9.98	38.1	0.0036074	-0.104548	45.5	1.47511	10.6
REC Solar REC380AA Bl...	REC Solar	Mono-c-Si	0	380.238	360.4	1.69	60	10.61	44.3	9.98	38.1	0.0039257	-0.104105	46	1.49675	10.6
REC Solar REC380NP 72	REC Solar	Mono-c-Si	0	380.488	355.1	1.95	72	10.24	48.5	9.56	39.8	0.0031744	-0.12901	44.4	1.77495	10.2
REC Solar REC380NP 7...	REC Solar	Mono-c-Si	0	380.488	355.1	1.95	72	10.24	48.5	9.56	39.8	0.0031744	-0.12901	44.4	1.77495	10.2

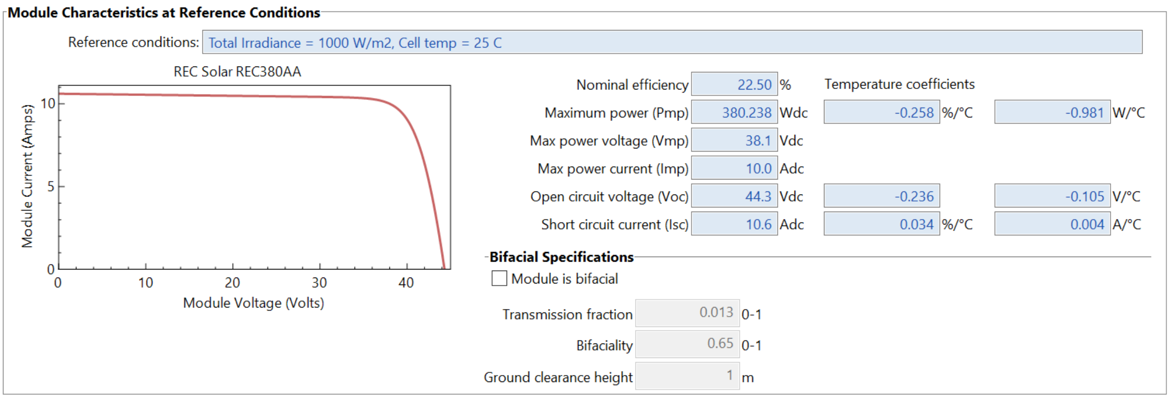

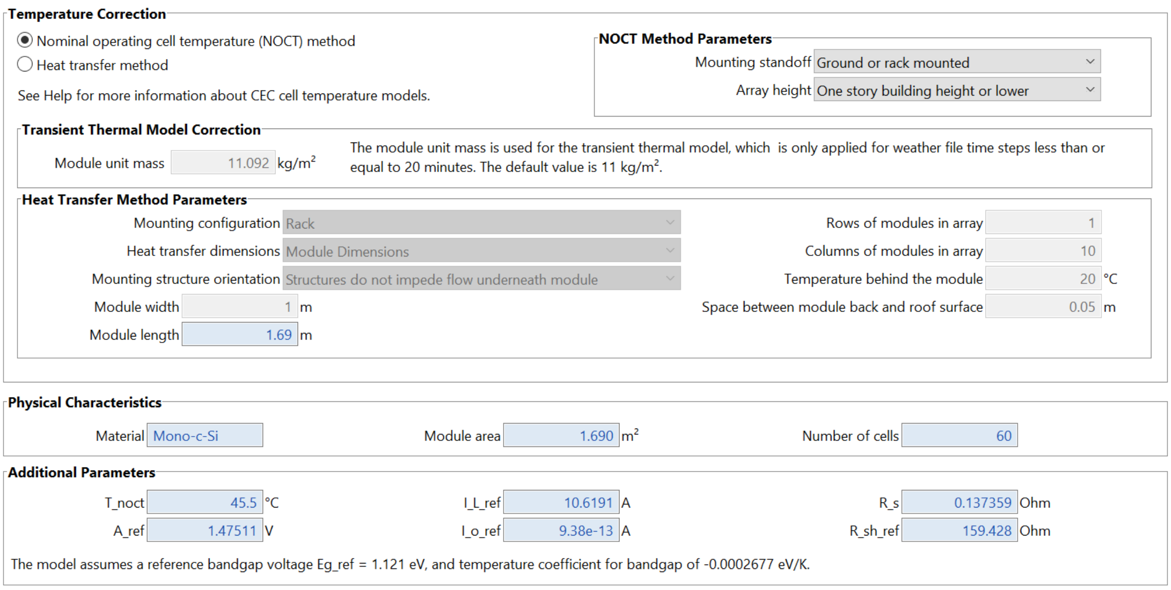

1.3 Inverter

As in the PV panels section, the inverter chosen in the theoretical analysis (Huawei SUN 2000-40KTL-M340) is selected in the libraries of the software. Consequently, all the values for the simulation are filled automatically.

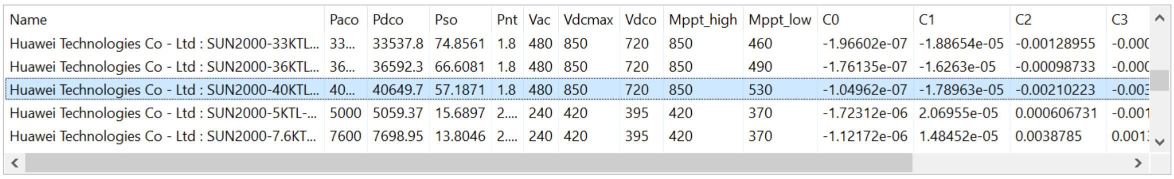

Name	Paco	Pdco	Pso	Pnt	Vac	Vdcmax	Vdco	Mppt_high	Mppt_low	C0	C1	C2	C3
Huawei Technologies Co - Ltd : SUN2000-33KTL...	33...	33537.8	74.8561	1.8	480	850	720	850	460	-1.96602e-07	-1.88654e-05	-0.00128955	-0.00(
Huawei Technologies Co - Ltd : SUN2000-36KTL...	36...	36592.3	66.6081	1.8	480	850	720	850	490	-1.76135e-07	-1.6263e-05	-0.00098733	-0.00(
Huawei Technologies Co - Ltd : SUN2000-40KTL...	40...	40649.7	57.1871	1.8	480	850	720	850	530	-1.04962e-07	-1.78963e-05	-0.00210223	-0.00:
Huawei Technologies Co - Ltd : SUN2000-5KTL-...	5000	5059.37	15.6897	2....	240	420	395	420	370	-1.72312e-06	2.06955e-05	0.000606731	-0.001
Huawei Technologies Co - Ltd : SUN2000-7.6KT...	7600	7698.95	13.8046	2....	240	420	395	420	370	-1.12172e-06	1.48452e-05	0.0038785	0.001:

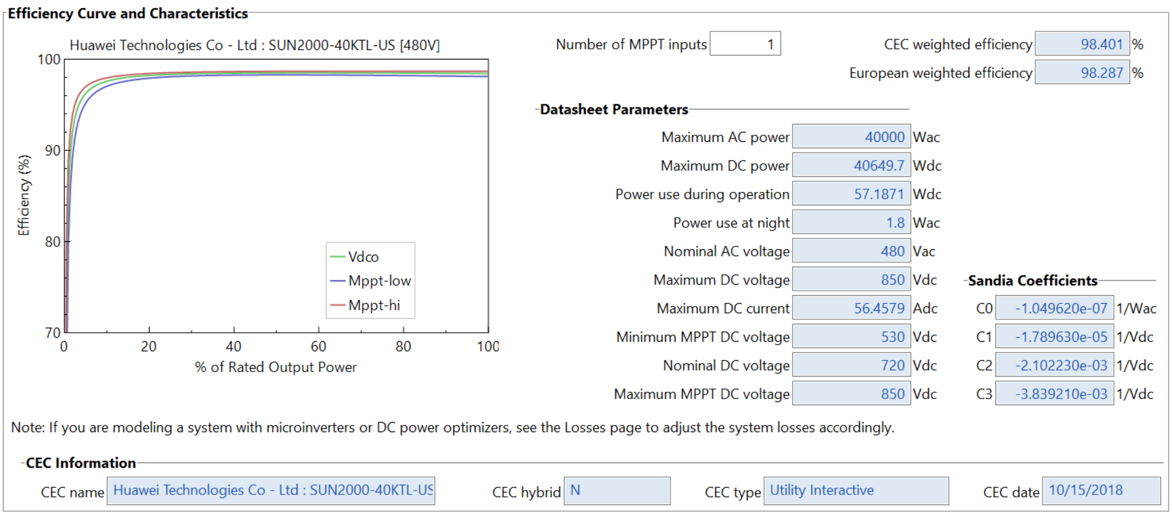

1.4 System Design

In terms of system design, SAM enables the automatic filling of subarray parameters. The option is chosen. Then, the values to calculate (number of investors, string modules, and subarray strings) are entered.

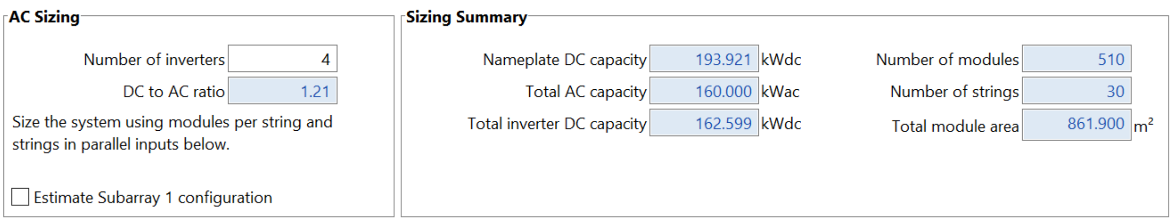

Additionally, the orientation of the previously calculated panels (section 4.1.3) is also introduced. It should be noted that the Ground Coverage Radio is the relationship between the surface of the panels and the surface of the available terrain.

DC Sizing and Configuration

To model a system with one array, specify properties for Subarray 1 and disable Subarrays 2, 3, and 4. To model a sytem with up to four subarrays connected in parallel to a single bank of inverters, for each subarray, check Enable and specify a number of strings and other properties.

Electrical Configuration

	Subarray 1	Subarray 2	Subarray 3	Subarray 4
	(always enabled)	☐ Enable	☐ Enable	☐ Enable
Modules per string in subarray	17			
Strings in parallel in subarray	30			
Number of modules in subarray	510			
String Voc at reference conditions (V)	753.1			
String Vmp at reference conditions (V)	647.7			

Tracking & Orientation

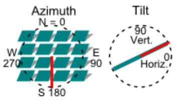

- ◉ Fixed
- ○ 1 Axis
- ○ 2 Axis
- ○ Azimuth Axis
- ○ Seasonal Tilt

☐ Tilt=latitude

Tilt (deg)	38
Azimuth (deg)	138
Ground coverage ratio (GCR)	0.27
Tracker rotation limit (deg)	45
Backtracking	☐ Enable
Terrain slope (deg)	0
Terrain azimuth (deg)	0

Electrical Sizing Information

Ground coverage ratio is used (1) to determine when a one-axis tracking system will backtrack, (2) in self-shading calculations for fixed tilt or one-axis tracking systems on the Shading page, and (3) in the total land area calculation. See Help for details.

Maximum DC voltage	850.0	Vdc
Minimum MPPT voltage	530.0	Vdc
Maximum MPPT voltage	850.0	Vdc

Voltage and capacity ratings are at module reference conditions shown on the Module page.

No system sizing messages.

Finally, the following and last step in the system design section consists of estimating the land area. It is necessary to select the area of the land where the installation will be placed.

Land Area Estimate

The land area estimate is for land purchase and lease calculations for financial models that include land costs. See Help for details.

			acres	ha
Total module area estimate	861.900	m^2	0.478	0.086
Array land area multiplier	1.000			
Additional land area	0.116	ha		
Total estimated land area			0.765	0.310

1.5 Shading and Layout

In the shading and layout section, SAM offers a 3D simulation to calculate the shadows that would occur due to external factors such as buildings, trees, etc. It has been determined not to use this simulation since there is no external object that can cause shadows. Similarly, it happens with the snow losses, which are not considered either because it rarely snows.

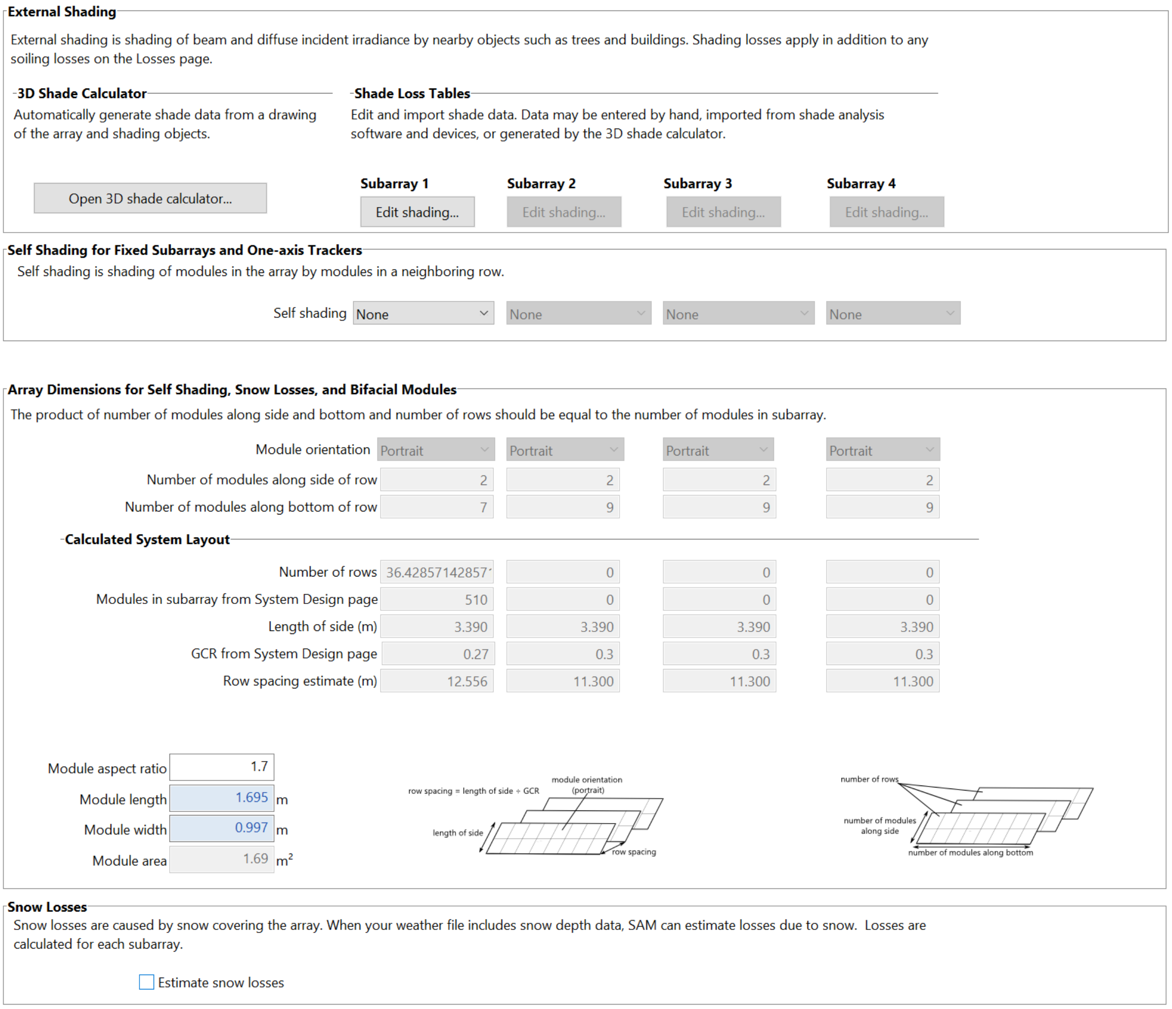

1.6 Losses

SAM offers default loss values. All these default values are selected.

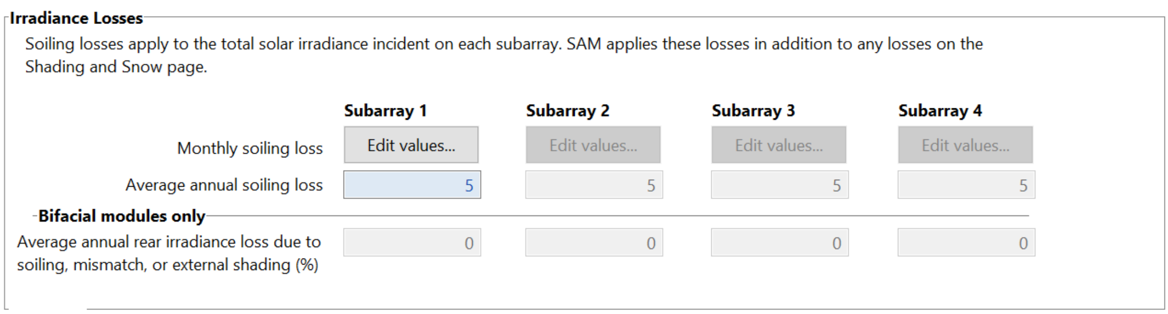

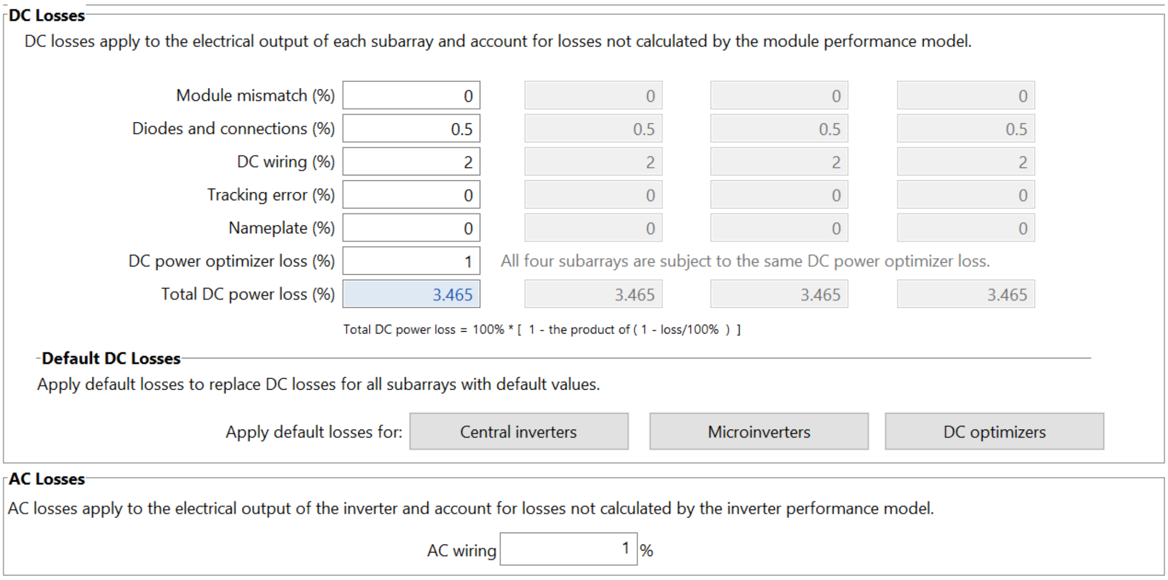

1.7 Grid Limits

Since it is assumed that there are no grid limits, the option is disabled.

2. Biomass energy

The different sections of inputs that the SAM requires to simulate the production of bioelectricity are explained in this section. As mentioned in section 4.2, those are Ambient Conditions (Appendix V.2.1), Feedstock (Appendix V.2.2), Plant Specs (Appendix V.2.3), Emissions (Appendix V.2.4), and Grid Limits (Appendix V.2.5).

2.1 Ambient Conditions

The procedure to follow is the same as used in the Location and Resource section of the solar panels.

2.2 Feedstock

The amount of biomass that is available is defined in Appendix II.6. Moreover, carbon, hydrogen, and nitrogen values have been obtained from Pellets del Sur (2020).

On the other hand, as can be seen in the image, the prevalence of predefined resources does not adapt to the types of Cervià. In fact, although the software allows the introduction of two additional feedstock types, these are not enough. It does not allow to change of the calorific powers of the defined biomass. Furthermore, the need to make conversions in the units is worth noting, as they are different from the system used in the calculations.

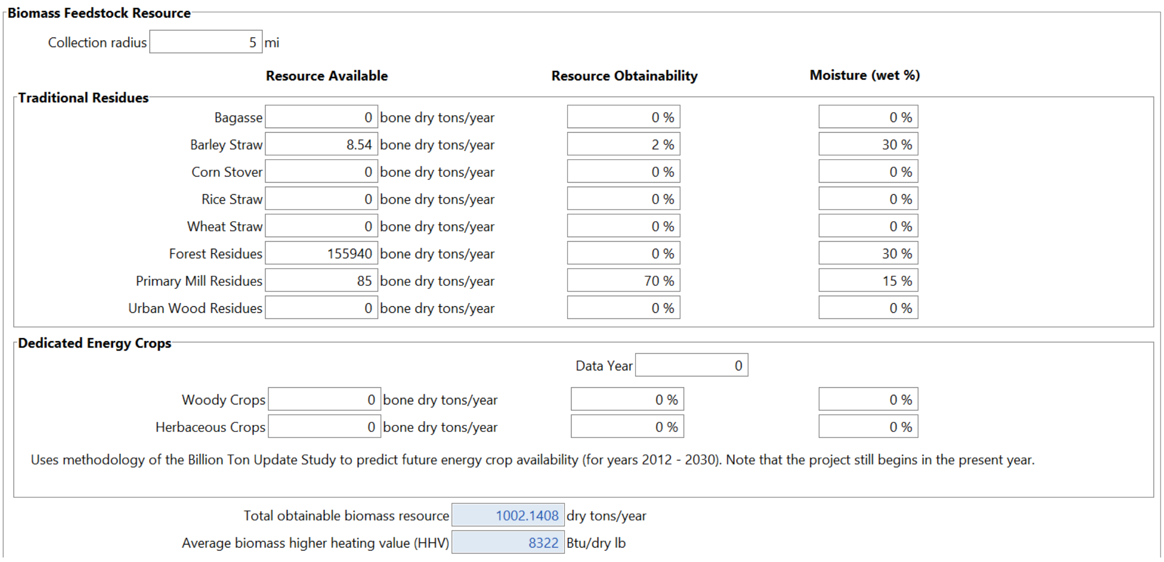

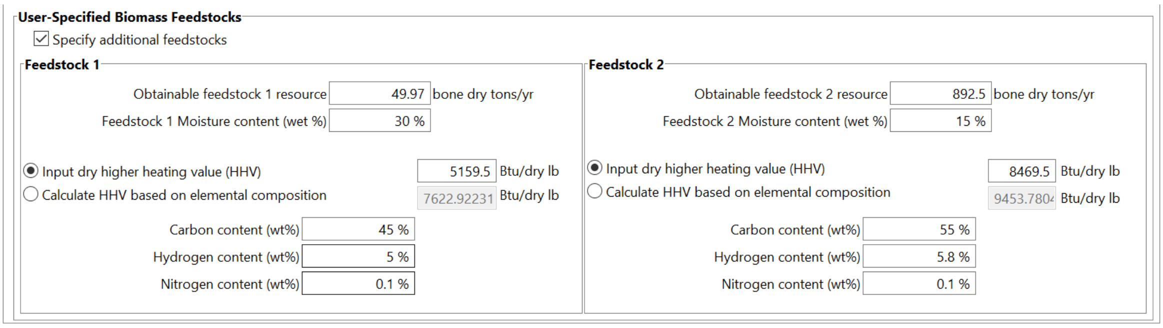

Finally, in the feedstock section, the program calculates the required system capacity based on the amount of feedstock available. It also performs the total biomass calculation.

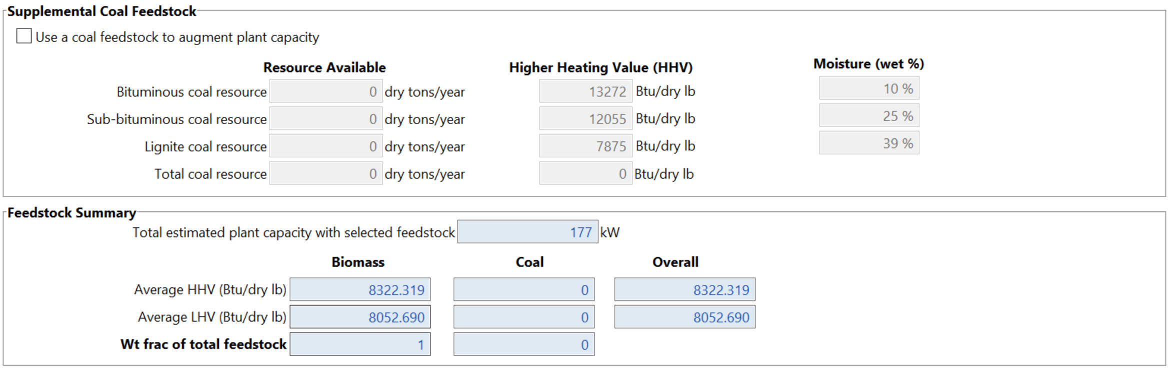

2.3 Plant Specs

This section selects the type of feedstock drying and the type of combustion system. As discussed in section 4.2, a fluidized bed combustor is used. To perform the simulation, SAM uses the default values for this type of system.

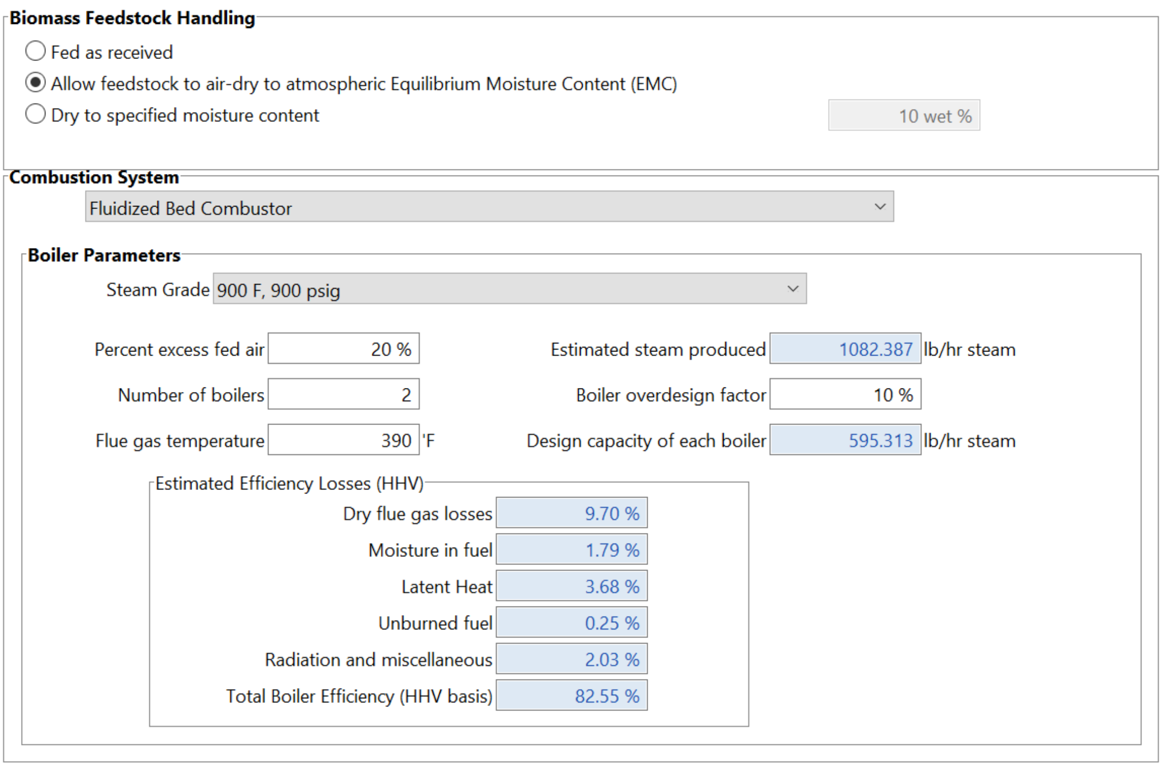

2.4 Emissions

In this section, the emissions that the system will entail are established to calculate the life-cycle impact. It is important to note that the software does not allow you to enter a custom electricity grid value; it only permits to select the stored average data that belong to the United States.

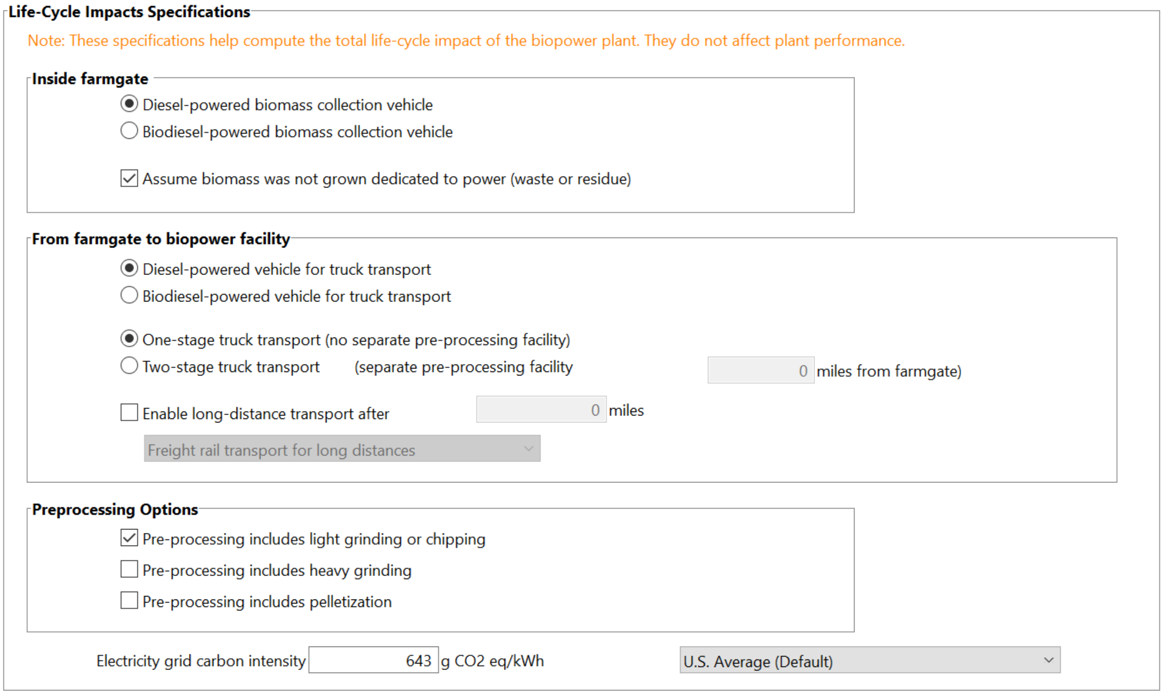

2.5 Grid Limits

In the same way that has been indicated in the simulation of solar energy, there are no grid constraints in this simulation.

Appendix VI. SAM inputs for the financial simulations

The inputs for the three financial simulations run with the System Advisor Model (SAM) software are compiled in this appendix. Only images of the settings used are attached. Section 1 explains the inputs used for the financial simulation of the photovoltaic installation, while section 2 explains those of biomass. Section 3 describes the parameters selected in the Generic System. It should be remembered that MATLAB codes, weather variables, and SAM simulations are stored in the MS OneDrive folder:

- Design and Development of an Integrated Renewable Energy Centre in Cervià de les Garrigues, Catalonia

1. Solar financial

This section explains the different input sections required by the SAM to simulate the financial analysis of the photovoltaic installation. As discussed in section 5.2, they are Lifetime and Degradation (Appendix VI.1.1), Installation Costs (Appendix VI.1.2), Operating Costs (Appendix VI.1.3), Financial Parameters (Appendix VI.1.4), Incentives (Appendix VI.1.5), Electricity Rates (Appendix VI.1.6), Electricity Load (Appendix VI.1.7). Furthermore, as has already been defined, the most representative model for the financial analysis of solar energy is the Residential Owner.

1.1 Life Time and degradation

In this section, lifetime and degradation are discussed. For this reason, the annual degradation value of the solar panel must be entered. This value is easy to obtain since it is found in the technical specifications of the product and therefore in the datasheet attached in Appendix IV.2.

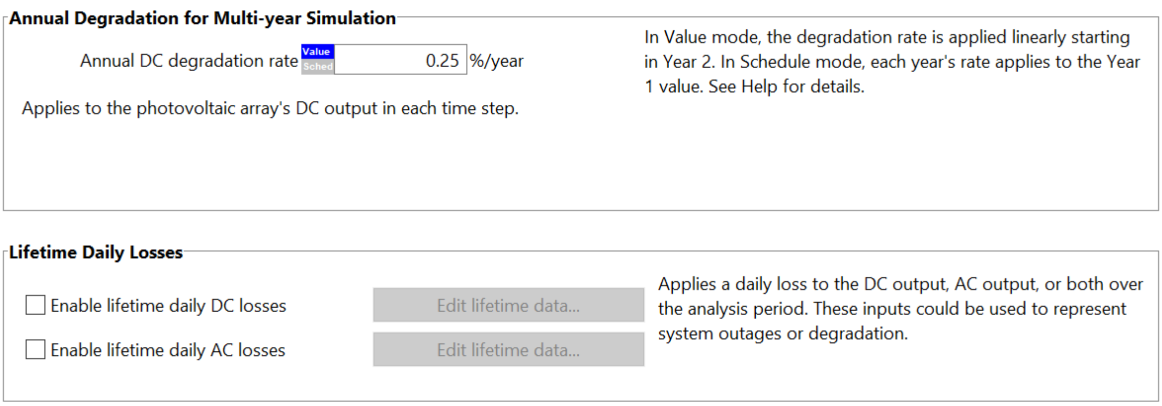

1.2 Installation Costs

In this menu, all installation costs are determined. First of all, direct costs are defined using the unit prices of solar panels and inverters. For the prices, it should be taken into account the units of the system and their respective conversion to our monetary system; \$1 = €0.95 (European Commission, 2022). It is estimated that 10% is due to the system's installation. Furthermore, contingency is defined as the default value of SAM, which is 3%.

Direct Capital Costs

Module	510 units	0.4 kWdc/unit	193.9 kWdc	279.00 \$/Unit	\$ 142,290.00
Inverter	4 units	40.0 kWac/unit	160.0 kWac	3,458.00 \$/Unit	\$ 13,832.00

	\$	\$/Wdc	\$/m^2	
Balance of system equipment	0.00	0.00	0.00	\$ 0.00
Installation labor	14,229.00	+ 0.00	+ 0.00	= \$ 14,229.00
Installer margin and overhead	0.00	0.00	0.00	\$ 0.00
			Subtotal	\$ 170,351.00

Contingency

Contingency	3	% of subtotal	\$ 5,110.53
		Total direct cost	\$ 175,461.53

On the other hand, all indirect costs involved in the project are also established. First of all, the land purchase costs are set at €0 since they are currently owned by the municipality. However, the cost of roof remodelling and the treatment of asbestos is considered (€100000).

Indirect Capital Costs

	% of direct cost	\$/Wdc	\$	
Permitting and environmental studies	0	0.00	0.00	\$ 0.00
Engineering and developer overhead	0	+ 0.00	+ 0.00	= \$ 0.00
Grid interconnection	0	0.00	0.00	\$ 0.00

Land Costs

Land area	0.765 acres				
Land purchase	\$ 0/acre	0	0.00	0.00	\$ 0.00
Land prep. & transmission	\$ 0/acre	+ 0	+ 0.00	+ 105,282.00	= \$ 105,282.00
				Total indirect cost	\$ 105,282.00

Finally, SAM executes the general calculation of installation costs. With the value obtained, establish what will be the capacity cost (\$/Wdc).

Total Installed Cost

The total installed cost is the sum of the indirect, sales tax, and direct costs. Note that it does not include any financing costs from the Financial Parameters page.

Total installed cost	\$ 280,743.53
Total installed cost per capacity	\$ 1.45/Wdc

1.3 Operating Costs

This section configures the operating and maintenance costs. An approximation has been made of what could be an adequate price for its maintenance, and it has been considered to be only €1000 per year. This fee will not only focus on cleaning solar panels but also on periodic inspections and maintenance.

For the estimated calculation, it has been taken into account that the cleaning of the PV modules will be essential as the biomass chimney will produce ash that will eventually spread throughout the environment.

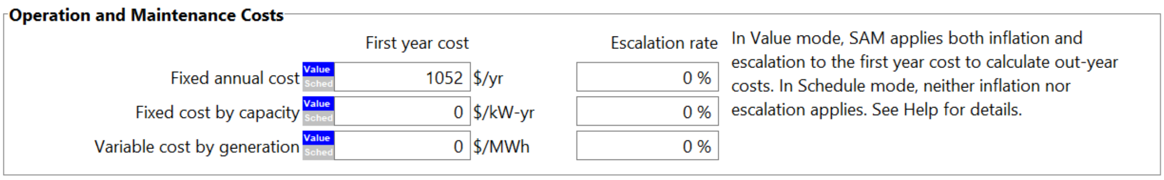

1.4 Financial Parameters

This section provides a variety of inputs that deal with the type of loan. Because a single down payment is considered to be made, all values are configured to 0. Moreover, the year when the financial study will be completed is indicated.

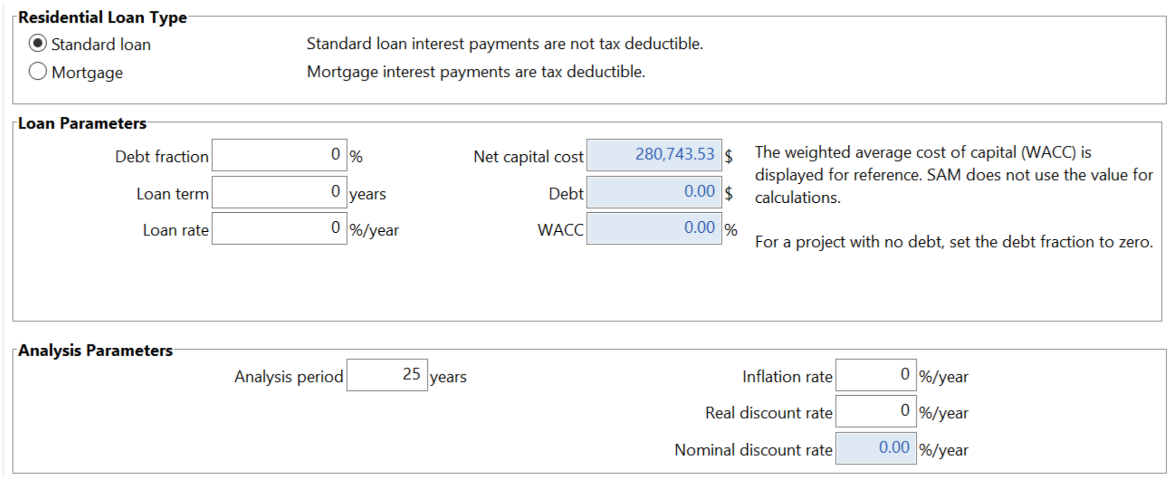

1.5 Incentives

This section deals with the incentives of the project; that is, it describes the credits and state grants received. Since none are supposed to be available, they are all defined as zero.

1.6 Electricity Rates

The type of electricity billing that will be available and the fixed and minimum charges are defined. In this case, the sale of the surplus at a fixed price is selected. Additionally, it is indicated that energy would be purchased if there is not enough generation to cover the demand.

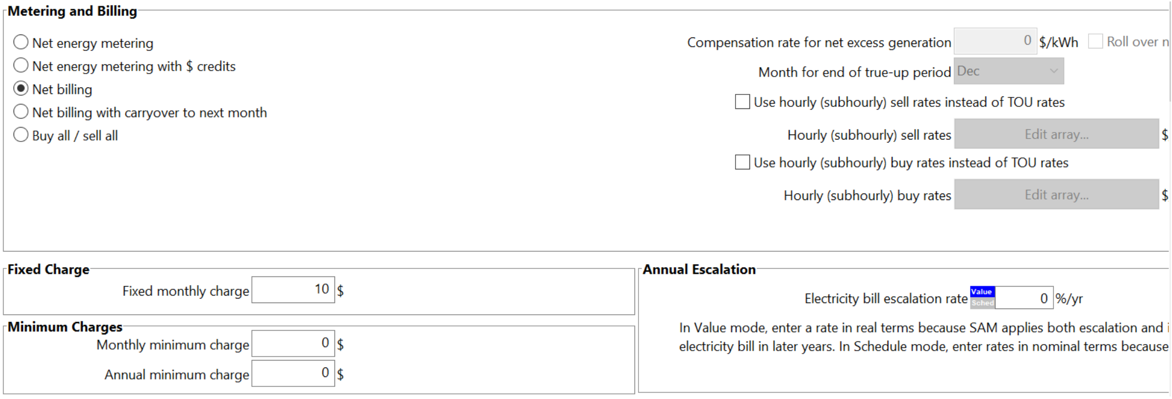

Furthermore, it enables the characterization of energy purchase (0.09€/kWh) and sale values (0.055€/kWh).

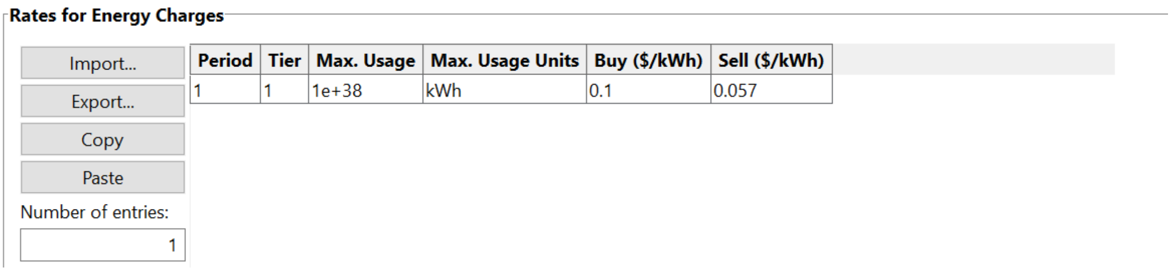

In addition, as shown in the following figure, SAM permits defining a box with different rates, according to the time slot of the day. Note that there is the same box for the weekends. Unfortunately, due to the lack of detailed information on energy demand, this useful tool is not used.

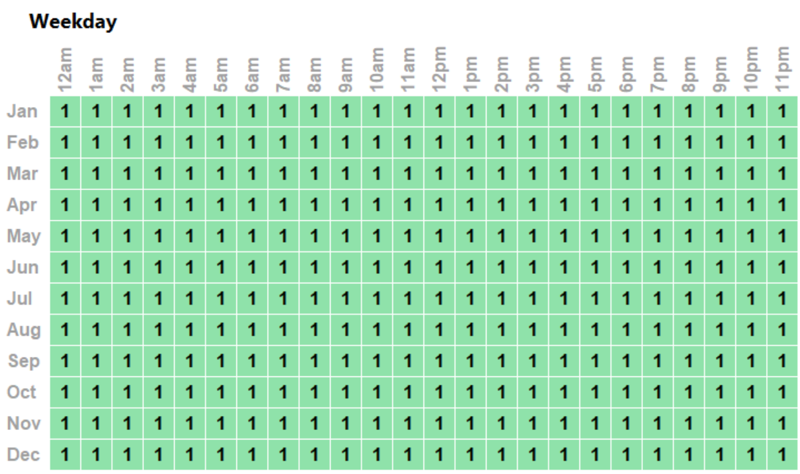

1.7 Electricity Load

This last section deals with the electricity load. In it, hourly or sub-hourly electricity demand is defined. Notwithstanding the lack of this required information, the average monthly values calculated in Appendix II.7 are established.

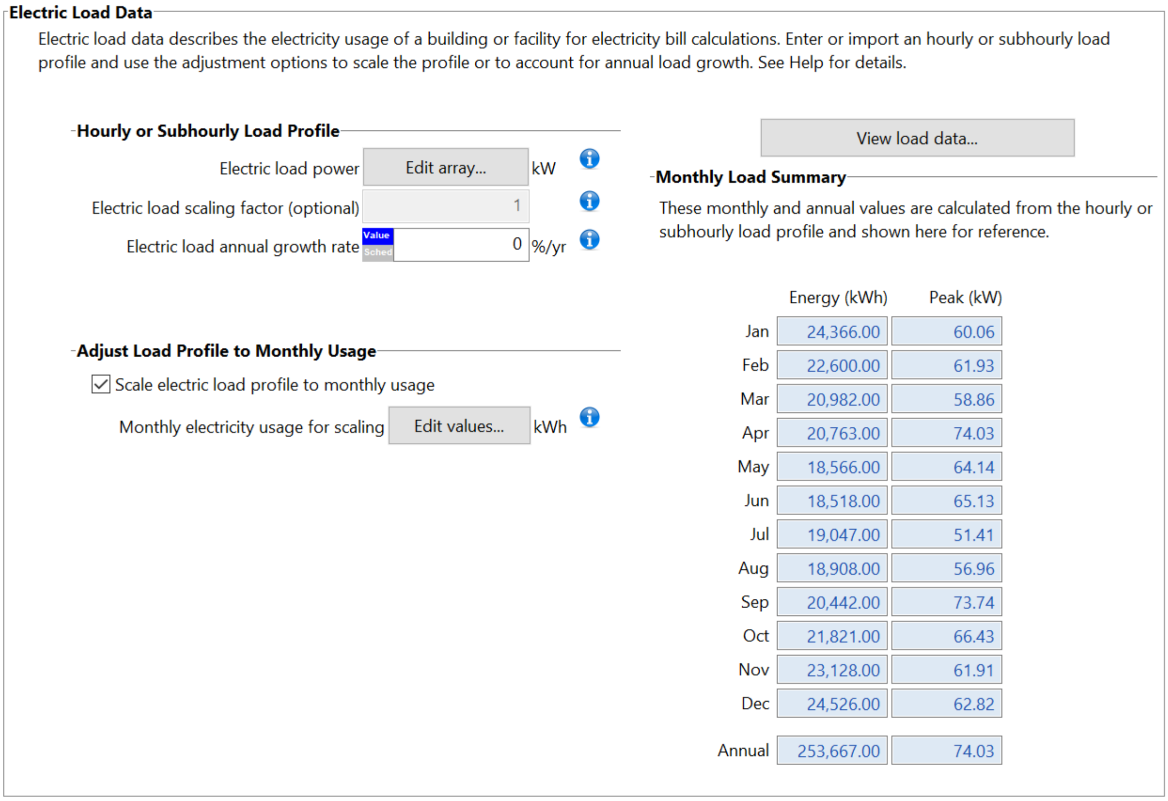

	Energy (kWh)	Peak (kW)
Jan	24,366.00	60.06
Feb	22,600.00	61.93
Mar	20,982.00	58.86
Apr	20,763.00	74.03
May	18,566.00	64.14
Jun	18,518.00	65.13
Jul	19,047.00	51.41
Aug	18,908.00	56.96
Sep	20,442.00	73.74
Oct	21,821.00	66.43
Nov	23,128.00	61.91
Dec	24,526.00	62.82
Annual	253,667.00	74.03

2. Biomass financial

This section explains the different input sections required by the SAM to simulate the financial analysis of the biomass system. As discussed in section 5.2, they are Lifetime and Degradation (Appendix VI.2.1), Installation Costs (Appendix VI.2.2), Operating Costs (Appendix VI.2.3), Feedstock Cost (Appendix VI.2.4), Financial Parameters (Appendix VI.2.5), Revenue (Appendix VI.2.6), Incentives (Appendix VI.2.7), Depreciation (Appendix VI.2.8), Electricity Rates (Appendix VI.2.9). Remark that to perform the simulation, the Single Owner model was chosen.

2.1 Life Time and degradation

As explained in the solar financial model, the annual degradation rate must be indicated. In this case, there is no data sheet with a set value. For this reason, and since the combustion system of the SAM libraries is chosen, the default values (1%) are selected.

2.2 Installation Costs

In this menu, the cost values of the boiler are indicated. It is supposed to cost approximately €170,000. This value has been established given that in the current market, a biomass boiler with the characteristics requested by our project ranges from €150,000 to €200,000 (Hargassner, 2018). Moreover for its installation, it has been estimated that the value will increase by 10% of the total cost of the boiler.

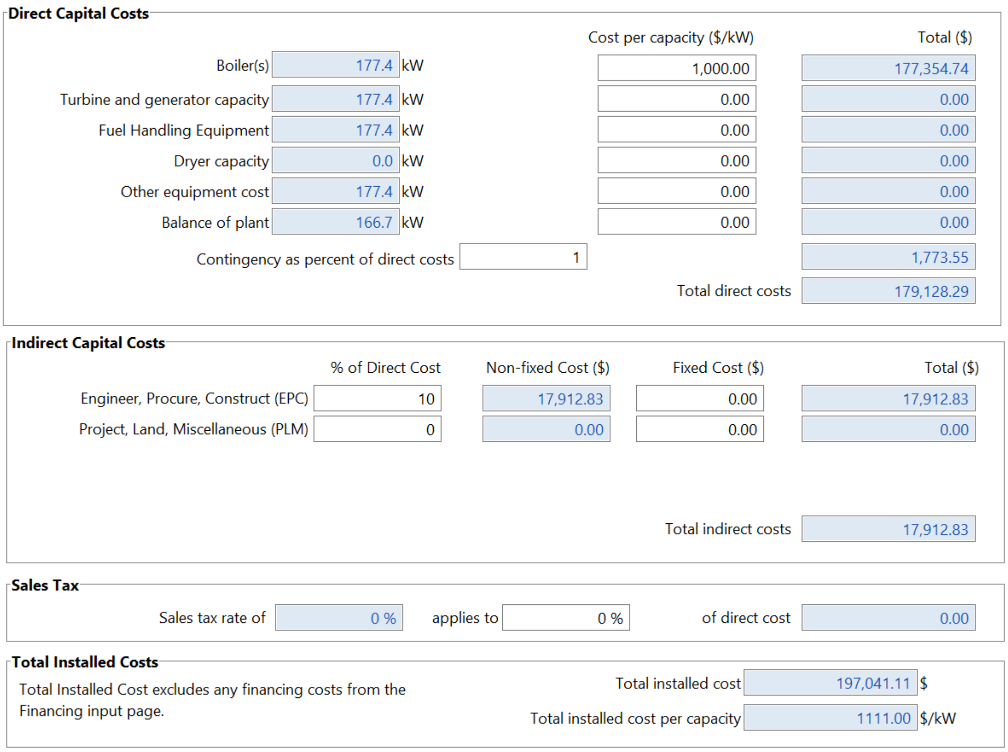

Direct Capital Costs

	Capacity	Cost per capacity ($/kW)	Total ($)
Boiler(s)	177.4 kW	1,000.00	177,354.74
Turbine and generator capacity	177.4 kW	0.00	0.00
Fuel Handling Equipment	177.4 kW	0.00	0.00
Dryer capacity	0.0 kW	0.00	0.00
Other equipment cost	177.4 kW	0.00	0.00
Balance of plant	166.7 kW	0.00	0.00
Contingency as percent of direct costs	1		1,773.55
Total direct costs			179,128.29

Indirect Capital Costs

	% of Direct Cost	Non-fixed Cost ($)	Fixed Cost ($)	Total ($)
Engineer, Procure, Construct (EPC)	10	17,912.83	0.00	17,912.83
Project, Land, Miscellaneous (PLM)	0	0.00	0.00	0.00
Total indirect costs				17,912.83

Sales Tax

Sales tax rate of 0 % applies to 0 % of direct cost 0.00

Total Installed Costs

Total Installed Cost excludes any financing costs from the Financing input page.

Total installed cost 197,041.11 $

Total installed cost per capacity 1111.00 $/kW

2.3 Operating Costs

In the operating costs section, the annual hiring of a worker by the renewable energy centre is defined since a person in charge of supervising the biomass, the drying process, etc. will be needed. An annual salary of €17,100 has been estimated.

Operation and Maintenance Costs

	First year cost		Escalation rate
Fixed annual cost	18000	$/yr	0 %
Fixed cost by capacity	0	$/kW-yr	0 %
Variable cost by generation	0	$/MWh	0 %

In Value mode, SAM applies both inflation and escalation to the first year cost to calculate out-year costs. In Schedule mode, neither inflation nor escalation applies. See Help for details.

2.4 Feedstock Costs

As previously discussed in section 6.2.2, two simulations are discussed. On the first one, it is supposed that the feedstock is completely free.

Annual Biomass Fuel Costs

Distance-fixed delivery cost	$ 0.00	$/dry ton
Distance-variable delivery cost	$ 0.00	$/dry ton - mile

Traditional Residues

			Feedstock Price
Bagasse	0	dry tons/year	0.00 $/dt
Barley Straw	0.170800000000(	dry tons/year	0.00 $/dt
Corn Stover	0	dry tons/year	0.00 $/dt
Rice Straw	0	dry tons/year	0.00 $/dt
Wheat Straw	0	dry tons/year	0.00 $/dt
Forest Residues	0	dry tons/year	0.00 $/dt
Primary Mill Residues	59.5	dry tons/year	0.00 $/dt
Urban Wood Residues	0	dry tons/year	0.00 $/dt

Dedicated Energy Crops

Woody Energy Crops	0	dry tons/year	0.00 $/dt
Herbaceous Energy Crops	0	dry tons/year	0.00 $/dt
Additional Feedstock 1	49.97	dry tons/year	0.00 $/dt
Additional Feedstock 2	892.5	dry tons/year	0.00 $/dt

Total biomass fuel usage	1002.1408	dry tons/year	Biomass Fuel Cost	0.00 $/dry ton	$/dt	0.00 $/green ton
Biomass cost escalation rate	0 %	%/year		0.00 $/MMBtu		"Green" ton includes moisture

Through the parametric analysis offered by the software, a range of different prices for the raw material is studied. In order for the project to be profitable in approximately 15 years, it turns out that the biomass could be paid at 40 euros per tonne. Therefore, this value is entered to perform the simulation.

Total biomass fuel usage	1002.1408	dry tons/year	Biomass Fuel Cost	42.00 $/dry ton	$/dt	34.06 $/green ton
Biomass cost escalation rate	0 %	%/year		2.52 $/MMBtu		"Green" ton includes moisture

2.5 Financial Parameters

As already detailed in the financial parameters of the solar energy simulation, a period of analysis of 25 years is defined. All other configurations relating to the type of debt and financing of the project are cancelled as it is considered that it will be paid in a single initial payment.

2.6 Revenue

As the name of the menu indicates, the electricity revenue is defined. It is important to note that will have a constant and balanced distribution throughout the year.

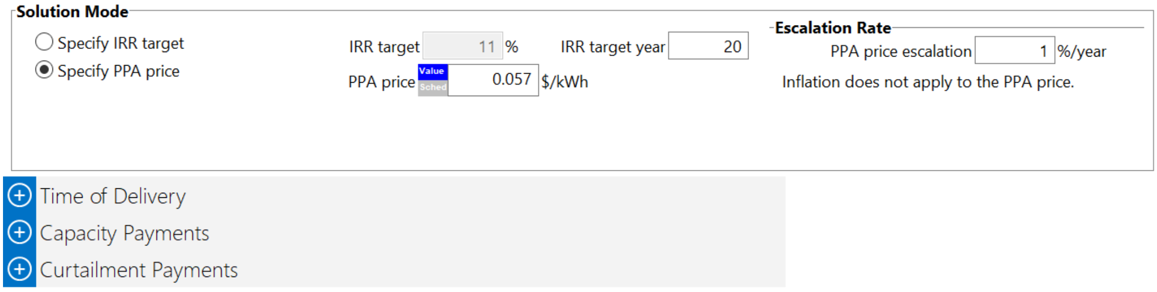

2.7 Incentives

As we have defined in the simulation of the financial model of solar energy, this section is cancelled.

2.8 Depreciation

This section discusses depreciation over its estimated useful life. All parameters are set to 0, therefore, it is as if this menu were not taken into account.

2.9 Electricity Purchases

For the analysis of electricity purchases, it is defined that the option "Use PPA or market prices" will be used. Precisely, it applies to the purchase and sale of energy at a pre-defined price in the revenue section.

It should be noted that PPA is the acronym for the power purchase agreement.

3. General system financial

In this final section on SAM inputs, the different input sections required by the software to simulate the general financial analysis of the system are explained. It should be noted that the sections are the same as those used in the financial analysis of the photovoltaic system since the same type of analysis is used (Residential/Commercial). As discussed in section 6.2.3, when simulating two different types of economic analysis, SAM shows errors when automatically joining the cases. For this reason, only energy analysis can be combined. Consequently, the economic analysis must be entered manually. To do this, the different costs of both systems are added and entered as if they were a joint system.

3.1 Power Plant

First, in the power plant menu, the option "Generate production and nameplates from open cases" is selected. Next, through the "Select cases" option, the software permits choosing the simulations to include. Finally, SAM automatically performs the automatic energy calculations of the combined system.

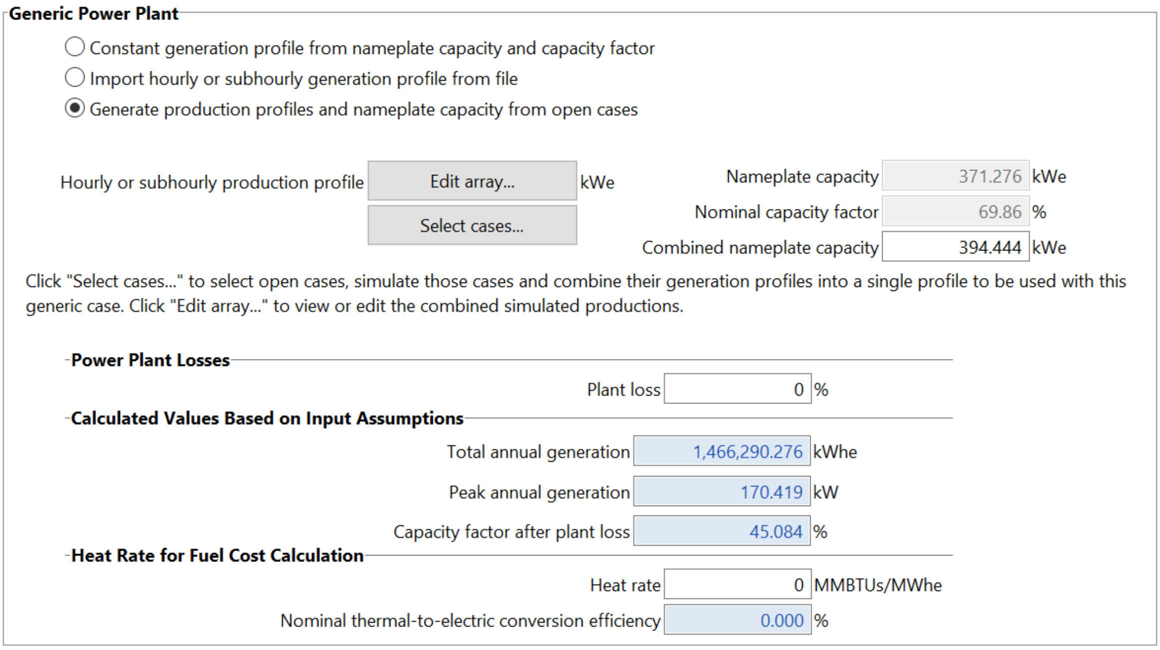

3.2 Grid Limits

As already detailed in the previous cases (biomass and solar), grid limits are not defined.

3.3 Life Time and Degradation

In this section, the annual degradation rate must be specified. SAM default lifetime degradation is used (1%).

3.4 Installing Costs and Operating Costs

This section details installation and operating costs. As already mentioned in the introduction, the prices of both cases are manually added. Thus, counting the values of each simulation independently, we obtain:

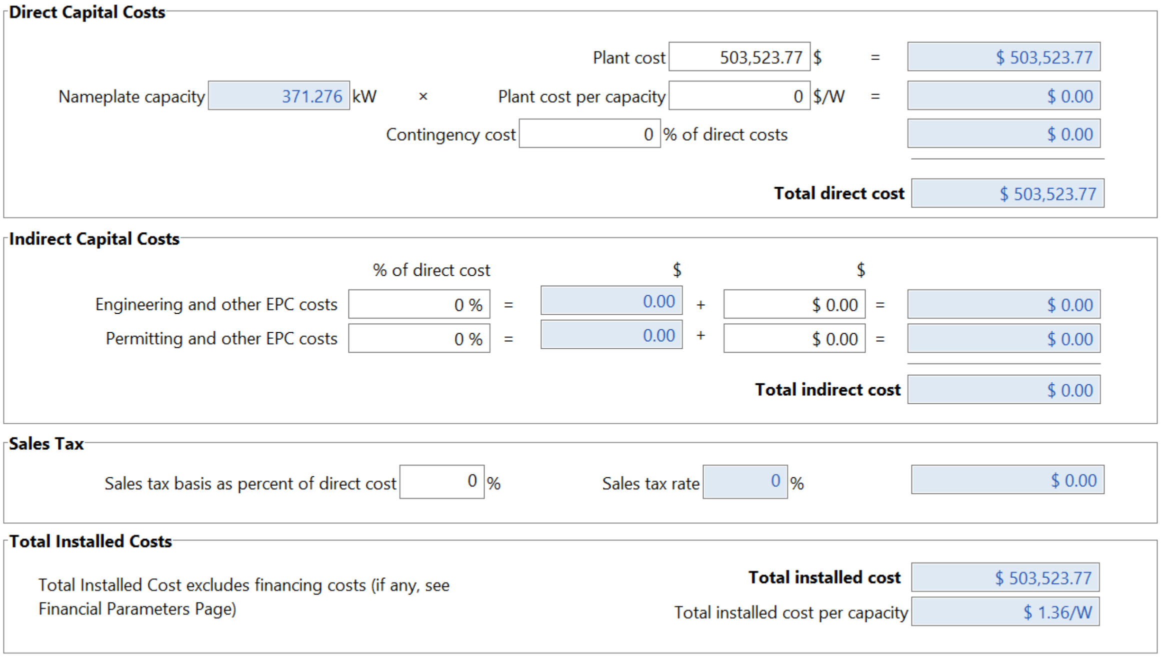

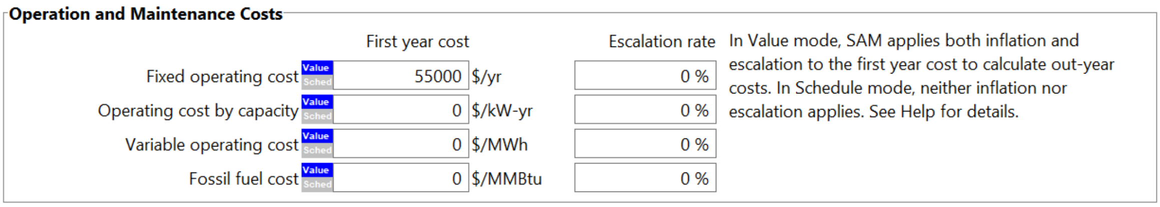

3.5 Financial Parameters, Incentives, Electricity Rates and Electricity Load sections.

For the Financial Parameters, Incentives, Electricity Rates and Electricity Load menus, values must also be entered manually. Because they were only considered in the solar simulation, the data entered are identical to those of the PV system's financial simulation. For this reason, they are not attached and are not detailed.

Appendix VII. SAM's generated cash flows

Attached to this appendix are the cash flows generated by SAM for each of the simulated financial models. The PV system cash flow result is included in section 1. In section 2, the biomass system is attached considering free feedstock, whereas, in section 3, it is considered that it is paid at 40 €/tonne. Finally, in section 4, the cash flow derived from the general system is connected.

1. PV system's cash flow

	Year												
	0	**1**	**2**	**3**	**4**	**5**	**6**	**7**	**8**	**9**	**10**	**11**	**12**
Electricity net generation [kWh]	0	332479	331929	331377	330822	330265	329704	329141	328574	328004	327429	326851	326269
Electricity bill without system [€/yr]	0	21469	21469	21469	21469	21469	21469	21469	21469	21469	21469	21469	21469
Electricity bill with system [€/yr]	0	-29	2	34	67	98	130	162	196	228	261	295	328
Value of electricity savings [€]	0	21499	21467	21435	21403	21371	21339	21307	21273	21241	21208	21175	21141
Total operating expense [€]	0	1000	1000	1000	1000	1000	1000	1000	1000	1000	1000	1000	1000
After-tax annual costs [€]	-266707	-1000	-1000	-1000	-1000	-1000	-1000	-1000	-1000	-1000	-1000	-1000	-1000
After-tax cash flow [€]	-266707	20499	20468	20435	20403	20372	20340	20307	20274	20242	20208	20175	20142
Cumulative payback [€]	-266707	-246208	-225740	-205305	-184901	-164530	-144190	-123883	-103609	-83367	-63159	-42984	-22842

	Year												
	13	**14**	**15**	**16**	**17**	**18**	**19**	**20**	**21**	**22**	**23**	**24**	**25**
Electricity net generation [kWh]	325682	325092	324499	323903	323303	322700	322094	321483	320869	320251	319628	319001	318372
Electricity bill without system [€/yr]	21469	21469	21469	21469	21469	21469	21469	21469	21469	21469	21469	21469	21469
Electricity bill with system [€/yr]	362	396	430	465	499	533	568	603	638	674	710	746	782
Value of electricity savings [€]	21107	21073	21040	21005	20970	20936	20901	20866	20831	20796	20759	20723	20687
Total operating expense [€]	1000	1000	1000	1000	1000	1000	1000	1000	1000	1000	1000	1000	1000
After-tax annual costs [€]	-1000	-1000	-1000	-1000	-1000	-1000	-1000	-1000	-1000	-1000	-1000	-1000	-1000
After-tax cash flow [€]	20108	20074	20040	20005	19971	19937	19902	19866	19831	19796	19760	19724	19688
Cumulative payback [€]	-2734	17339	37380	57385	77356	97292	117194	137060	156892	176688	196448	216172	235859

(Author's own, adapted with SAM).

2. Biomass system's cash flow (free feedstock)

	Year												
	0	**1**	**2**	**3**	**4**	**5**	**6**	**7**	**8**	**9**	**10**	**11**	**12**
Electricity to grid [kWh]	0	1292791	1279863	1267064	1254393	1241850	1229431	1217137	1204965	1192916	1180986	1169177	1157485
PPA price [€/kWh]	0.000	0.055	0.056	0.056	0.057	0.057	0.058	0.058	0.059	0.060	0.060	0.061	0.061
PPA revenue [€]	0	71103	71096	71089	71082	71075	71068	71061	71054	71047	71040	71032	71025
Total operating expenses [€]	0	17100	17100	17100	17100	17100	17100	17100	17100	17100	17100	17100	17100
After-tax annual costs [€]	-187189	-17100	-17100	-17100	-17100	-17100	-17100	-17100	-17100	-17100	-17100	-17100	-17100
Cash flow from operating activities[€]	-187189	54003	50441	50435	50428	50421	50415	50408	50401	50395	50388	50380	50374
Cumulative payback [€]	-187189	54003	53292	52588	51891	51202	50519	49843	49173	48511	47854	47205	46561

	Year												
	13	**14**	**15**	**16**	**17**	**18**	**19**	**20**	**21**	**22**	**23**	**24**	**25**
Electricity to grid [kWh]	1145910	1134451	1123106	1111875	1100757	1089749	1078852	1068063	1057382	1046809	1036340	1025977	0
PPA price [€/kWh]	0.062	0.063	0.063	0.064	0.064	0.065	0.066	0.066	0.067	0.068	0.068	0.069	0.000
PPA revenue [€]	71018	71011	71004	70997	70990	70983	70976	70969	70961	70954	70947	70940	0
Total operating expenses [€]	17100	17100	17100	17100	17100	17100	17100	17100	17100	17100	17100	17100	0
After-tax annual costs [€]	-17100	-17100	-17100	-17100	-17100	-17100	-17100	-17100	-17100	-17100	-17100	-17100	0
Cash flow from operating activities [€]	50367	50360	50354	50347	50341	50334	50327	50321	50313	50306	50300	50293	0
Cumulative payback [€]	45925	45295	44671	44053	43442	42836	42237	41643	41056	40475	39899	39329	38765

(Author's own, adapted with SAM).

3. Biomass system's cash flow (assuming 40€/tonne)

	Year												
	1	2	3	4	5	6	7	8	9	10	11	12	13
Electricity to grid [kWh]	0	1292791	1279863	1267064	1254393	1241850	1229431	1217137	1204965	1192916	1180986	1169177	1157485
PPA price [€/kWh]	0	0	0	0	0	0	0	0	0	0	0	0	0
PPA revenue [€]	0	71103	71096	71089	71082	71075	71068	71061	71054	71047	71040	71032	71025
Total operating expenses [€]	0	51373	51373	51373	51373	51373	51373	51373	51373	51373	51373	51373	51373
After-tax annual costs [€]	-187189	-51373	-51373	-51373	-51373	-51373	-51373	-51373	-51373	-51373	-51373	-51373	-51373
Cash flow from operating activities[€]	-187189	19730	19019	18315	17618	16929	16245	15569	14900	14237	13581	12932	12288
Cumulative payback [€]	-187189	-167459	-148440	-130125	-112506	-95578	-79333	-63763	-48863	-34626	-21044	-8113	4175

	Year												
	14	15	16	17	18	19	20	21	22	23	24	25	26
Electricity to grid [kWh]	1145910	1134451	1123106	1111875	1100757	1089749	1078852	1068063	1057382	1046809	1036340	1025977	0
PPA price [€/kWh]	0	0	0	0	0	0	0	0	0	0	0	0	0
PPA revenue [€]	71018	71011	71004	70997	70990	70983	70976	70969	70961	70954	70947	70940	0
Total operating expenses [€]	51373	51373	51373	51373	51373	51373	51373	51373	51373	51373	51373	51373	51373
After-tax annual costs [€]	-51373	-51373	-51373	-51373	-51373	-51373	-51373	-51373	-51373	-51373	-51373	-51373	-51373
Cash flow from operating activities [€]	11652	11022	10398	9780	9169	8563	7964	7370	6783	6201	5625	5056	4491
Cumulative payback [€]	15827	26849	37247	47027	56195	64758	72722	80092	86874	93076	98701	103757	108248

(Author's own, adapted with SAM).

4. Generic system's cash flow

	Year												
	1	**2**	**3**	**4**	**5**	**6**	**7**	**8**	**9**	**10**	**11**	**12**	**13**
Electricity net generation [kWh]	0	1392976	1392976	1392976	1392976	1392976	1392976	1392976	1392976	1392976	1392976	1392976	1392976
Electricity bill without system [€/yr]	0	21803	21803	21803	21803	21803	21803	21803	21803	21803	21803	21803	21803
Electricity bill with system [€/yr]	0	-63245	-63245	-63245	-63245	-63245	-63245	-63245	-63245	-63245	-63245	-63245	-63245
Value of electricity savings [€]	0	85048	85048	85048	85048	85048	85048	85048	85048	85048	85048	85048	85048
Total operating expense [€]	0	51373	51373	51373	51373	51373	51373	51373	51373	51373	51373	51373	51373
After-tax annual costs [€]	-187189	-51373	-51373	-51373	-51373	-51373	-51373	-51373	-51373	-51373	-51373	-51373	-51373
After-tax cash flow [€]	-503524	34524	34524	34524	34524	34524	34524	34524	34524	34524	34524	34524	34524
Cumulative payback [€]	-503524	-468999	-434475	-399951	-365427	-330902	-296378	-261854	-227329	-192805	-158281	-123756	-89232

	Year												
	14	**15**	**16**	**17**	**18**	**19**	**20**	**21**	**22**	**23**	**24**	**25**	**26**
Electricity net generation [kWh]	1392976	1392976	1392976	1392976	1392976	1392976	1392976	1392976	1392976	1392976	1392976	1392976	1392976
Electricity bill without system [€/yr]	21803	21803	21803	21803	21803	21803	21803	21803	21803	21803	21803	21803	21803
Electricity bill with system [€/yr]	-63245	-63245	-63245	-63245	-63245	-63245	-63245	-63245	-63245	-63245	-63245	-63245	-63245
Value of electricity savings [€]	85048	85048	85048	85048	85048	85048	85048	85048	85048	85048	85048	85048	85048
Total operating expense [€]	51373	51373	51373	51373	51373	51373	51373	51373	51373	51373	51373	51373	51373
After-tax annual costs [€]	-51373	-51373	-51373	-51373	-51373	-51373	-51373	-51373	-51373	-51373	-51373	-51373	-51373
After-tax cash flow [€]	34524	34524	34524	34524	34524	34524	34524	34524	34524	34524	34524	34524	34524
Cumulative payback [€]	-54708	-20183	14341	48865	83390	117914	152438	186962	221487	256011	290535	325060	359584

(Author's own, adapted with SAM).